DISSERTATION

FROM TREES TO STANDS: PRODUCTION ECOLOGY, GROWTH DOMINANCE AND CARBON PARTITIONING

Submitted by

Ezequiel Fernandez Tschieder

Graduate Degree Program in Ecology

In partial fulfillment of the requirements

For the Degree of Doctor of Philosophy

Colorado State University

Fort Collins, Colorado

Fall 2021

Doctoral Committee:

Advisor: Daniel E. Binkley

Michael G. Ryan
Nicholas T. Hobbs
William L. Bauerle

ABSTRACT

FROM TREES TO STANDS: PRODUCTION ECOLOGY, GROWTH DOMINANCE AND CARBON PARTITIONING

Growth of a stand is the sum of the growth of individual trees, and it can be distributed among trees proportional to their size or a group of trees may produce a disproportional share of the stand's growth. Large trees within a stand usually have higher growth rates than smaller trees. The production ecology of trees shows that this is the result of large trees' greater resource acquisition, and greater efficiency of wood production per unit of resource used. However, the fact that large trees grow faster than small trees does not necessarily imply that these trees produce a disproportional share of the stand growth. The distribution of a stand's growth among trees is influenced by how trees compete for resources (symmetric or asymmetric competition) and by the efficiency with which trees used those resources to grow. This dissertation had two main questions: (1) how growth distribution relates to patterns of competition and patterns of resource use efficiency with tree size (Chapter I, II and III), and (2) why large trees have greater resource use efficiency for wood production than small trees within a stand (Chapter IV).

In the first chapter, I proposed a specific connection between production ecology of trees and growth dominance patterns. Growth dominance is a measure of how the growth of a stand is distributed among trees. It can be negative or positive whether small or large trees account for a greater proportion of stand growth than its contribution to stand biomass, or null if all trees contribute a similar proportion to the growth and biomass of a stand (Fig. 1). Specifically, positive growth dominance should relate to asymmetric competition for resources and (or) to

increasing resource use efficiency with tree size in a stand. Null growth dominance should result from symmetric competition for resources and similar resource use efficiency among trees in a stand. Reverse growth dominance should arise from symmetric competition for resources and (or) from a decreasing resource use efficiency with tree size in a stand.

In the second chapter, I used a *Pinus ponderosa* stand undergoing strong negative growth dominance (growth dominance negative = −0.22) to test the corresponding pattern proposed in Chapter I. Dominant trees were 5-times larger than suppressed trees but captured a less-than-proportional amount of light relative to their size compared with suppressed trees (90.4 vs. 20.9 GJ $year^{-1}$ $tree^{-1}$) and light use efficiency declined with tree size. Suppressed trees were twice as efficient as dominant trees (0.11 vs. 0.05 kg[wood] GJ $[PAR]^{-1}$).

In the third chapter, I studied the relationship between growth dominance and production ecology across species including conifer and broadleaf. Both light competition and patterns of resource use efficiency with tree size explained a large portion of the variation in the distribution of growth across tree sizes. Growth dominance increased with the asymmetry of competition for light (i.e., growth dominance increased as larger trees increased their share of light interception) and as light use efficiency increased with tree size.

In the fourth chapter, I analyzed the pattern of water use efficiency across trees in eucalyptus experimental plots. I hypothesized that differences in water use efficiency related to changes in carbon partitioning between trees. Specifically, dominant trees should partition less photosynthate belowground than smaller trees, resulting in greater wood growth per unit of resource used. I combined tree transpiration and integrated crown water use efficiency to estimate tree-scale gross primary production, and belowground fluxes were estimated by subtracting aboveground production and respiration from gross primary production. Dominant

trees produced 2.3-times more wood per unit of water transpired (0.87 vs. 0.38 gC LH_2O^{-1}), fixed 1.1-more carbon per unit of water transpired (3.4 vs. 3 gC LH_2O^{-1}) and partitioned 2.2-times more carbon to wood production than suppressed trees (0.26 vs 0.12). Belowground partitioning decreased with tree size; however, the uncertainty in transpiration measurements showed that this pattern might be the result of the underestimation of gross primary production in dominant trees.

Overall, this study indicated that growth distribution (growth dominance) and production ecology patterns were related, but in variable ways. Stands with asymmetric distributions of growth are likely to have greater asymmetries in resource interception and resource use efficiency among trees. Variation in resource use efficiency related to both photosynthetic efficiency of trees and carbon partitioning to wood. However, the evidence supporting lower belowground carbon partitioning by dominant trees needs to be corroborated with future tests.

Tree	1	2	3	...	14	15
Tree mass (kg)	20	40	60	...	280	300
Tree growth (kg)	45	62	72	...	111	113
Cumulative mass (kg)	20	60	120	...	2100	2400
Cumulative growth (kg)	45	107	179	...	1259	1372
Cum. prop. mass	0.01	0.03	0.05	...	0.88	1
Cum. prop. growth	0.03	0.08	0.13	...	0.92	1

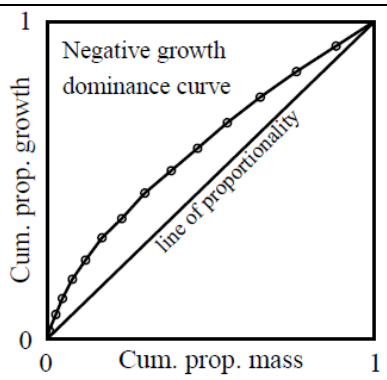

Tree growth (kg)	8	16	24	...	112	120
Cumulative growth (kg)	8	24	48	...	840	960
Cum. prop. growth	0.01	0.03	0.05	...	0.88	1

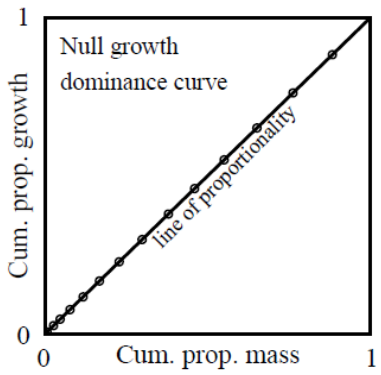

Tree growth (kg)	1	3	7	...	142	162
Cumulative growth (kg)	1	4	11	...	747	909
Cum. prop. growth	0.001	0.004	0.01	...	0.82	1

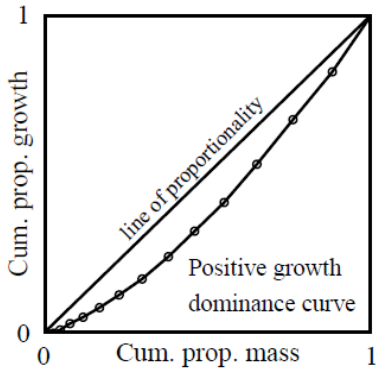

Figure 1. Growth dominance describes how the growth of a stand is distributed among trees. It is calculated by ordering the trees by size and plotting the proportional cumulative size on the x-axis and the proportional cumulative growth on the y-axis. Growth dominance is negative if small trees produce disproportional share of stand growth relative to their contribution to stand biomass (top). Growth dominance is null if all trees in a stand produce a proportional share of growth relative to their contribution to stand biomass (middle). Finally, growth dominance is positive if large trees produce a disproportional share of stand growth relative to their contribution to the stand biomass (bottom).

ACKNOWLEDGEMENTS

Different institutions and many people were involved during the development of this dissertation. The support of all of them was essential to accomplish my PhD.

First, I would like to acknowledge my advisor, Dan Binkley. His guidance, critical thinking and questioning were invaluable in formulating the research questions and methodology. Also, his friendship helped to cope through these years. I thank my committee members Mike Ryan, Tom Hobbs and Bill Bauerle for their valuable comments and suggestions. The insights of them all are beyond this dissertation.

The INTA -Instituto Nacional de Tecnología Agropecuaria- provided the scholarship to pursue my PhD. The IPEF -Instituto de Pesquisas e Estudos Florestais- and the TECHS Project (Tolerance of Eucalyptus Clones to Hydric, Thermal and Biotic Stresses) financed part of the research and provided data that were fundamental for my dissertation. I would like to recognize the Graduate Degree Program in Ecology and Natural Resource Ecology Laboratory for providing a friendly and supportive environment to accomplish my goals.

I am grateful for the fieldwork and data provision from Rob Hubbard, Rafaela Carneiro, Otavio Campoe, and Jose Luis Stape. Further contributions of original data from prior research projects was kindly provided by David Forrester, Jean-Paul Laclau, Guerric le Maire, Otavio Campoe, Rachel Cook, Hubert Sterba, and Martin Gspaltl.

I very much appreciate and value my colleagues and friends at CSU and INTA for their friendship and support throughout these years.

Finally, thanks to my family. Their unconditional support and companionship were essential and an inspiration throughout these years.

DEDICATION

To my parents

To my wife, son, and daughter

TABLE OF CONTENTS

INTRODUCTION

Productivity of stands and trees have been a core subject of forestry (Assmann 1970). In the early stages of forestry, productivity of stands was described by age, a measure of density and a representation of the potential productivity of the site - usually the height of dominant trees at a specific age (site index). Later, Oliver and Larson (1990) developed the concept of growing space. Growing space refers to the amount of resources available for a stand or tree that can be used for photosynthesis. The main idea behind growing space is that the larger the growing space the greater the amount of resources available to grow. However, this concept has the disadvantage that is not quantifiable, limiting the opportunities for hypothesis testing.

An alternative to the study of the productivity of stand and trees is the production ecology equation (Monteith and Moss 1977). According to this equation the productivity of a tree or a stand depends on supply of resources (light, water, nutrients) in the environment, the amount of resources captured by a tree or stand, the efficiency of converting the resources into photosynthates, and the partitioning of photosynthates into the various tree compartments. This approach allows for quantitative tests of hypothesis (Ryan et al. 1997, Binkley et al. 2004, 2010, Stape et al. 2008) and modelling (Landsberg and Waring 1997).

In tree populations, productivity of trees increases with tree size (Stephenson et al. 2014) as a result of greater resource acquisition and resource use efficiency to produce wood of large trees (Binkley et al. 2002, 2010, Campoe et al. 2013b, 2013a, Otto et al. 2014). Within a stand, trees compete among each other for resources, and large trees have the potential to preempt resources - especially light (Weiner 1990, Schwinning and Weiner 1998). On the other hand, mechanisms explaining differences in resource use efficiency to produce wood might be related

to differences in rates of photosynthesis per unit of resource and differences in carbon partitioning patterns to wood production among trees. Evidence at the stand level showed that increasing carbon partitioning to wood production was associated with a decreasing carbon partitioning to belowground carbon fluxes (Giardina et al. 2003, Litton et al. 2007, Epron et al. 2012).

Growth dominance (Binkley 2004, Binkley et al. 2006) described how growth is distributed among trees within a stand. Growth dominance provides a quantitative description of the relative contribution of individual trees -ranked in increasing order of size- to stand growth and biomass. If all trees in a stand grow in proportion to their biomass the stand shows null growth dominance. If large trees account for a greater proportion of stand growth than its contribution to stand biomass, the stand shows positive growth dominance. Conversely, if small trees account for a greater proportion of growth than biomass, the stand shows negative or reverse growth dominance (Binkley 2004, Binkley et al. 2006).

The magnitude and pattern of growth dominance varies between species. Withing a broad range of patterns, usually eucalyptus stands tend to have high-positive growth dominance (Binkley et al. 2003, Binkley 2004, Doi et al. 2010) whereas pine stands tend to have high-negative or low-positive growth dominance (Martin and Jokela 2004, Binkley et al. 2006, Fernández and Gyenge 2009, Bradford et al. 2010, Fernández Tschieder et al. 2012). It remains the question if growth dominance patterns are related to patterns of resource acquisition and resource use efficiency with tree size.

This dissertation was divided in four chapters. In the first chapter, I analyzed how competition can be examined with two stand metrics: the Gini coefficient and growth dominance and proposed a relationship between these metrics and the production ecology equation. This

chapter is a conceptual chapter and I only used data together with simulated stands to illustrate some points. In the second chapter, I studied an old-growth stand of ponderosa pine (*Pinus ponderosa*) in Colorado undergoing strong negative growth dominance. I used this stand as case of study to evaluate the relationships between growth dominance and production ecology proposed in the first Chapter for a stand with negative growth dominance. In the third chapter, I studied the relationship between growth dominance and production ecology across species including conifers and broadleaf species. I used two indices to assess competition and differences in resource use efficiency between trees within a stand and correlated these indices with growth dominance. In the last chapter, I evaluated in eucalyptus trees if greater resource use efficiency for wood production in large trees was related to greater rate of photosynthesis per unit of resource (photosynthetic efficiency) or changes in the carbon partitioning pattern between trees.

CHAPTER 1: LINKING COMPETITION WITH GROWTH DOMINANCE AND PRODUCTION ECOLOGY[1]

Introduction

Competition occurs between neighboring individuals and involves the effect on the partitioning of environmental resources (light, water and nutrients) among individuals, and the efficiency with which these resources are used to support growth. Competition may be defined as the difference in growth between an individual growing in a crowded stand and a same-size individual growing under isolated conditions (Hara 1993). Competition is difficult to study as a process, and it has been often assessed as a pattern. Most work on competition has concentrated on studying the size structure of populations. Some degree of size hierarchy is common in forests, and even homogeneous clonal plantations often have coefficients of variation in tree size of more than 15% (Binkley et al. 2010).

In this paper, we analyze how competition can be examined with two stand metrics: the Gini coefficient and Growth dominance coefficient. We also explore how these indices relate to the production ecology equation (Monteith and Moss 1977). Patterns of Gini and growth dominance coefficients derive from the combined influence of resource use (resource uptake) and resource use efficiency distribution among trees within a population. We use case studies and simulated stands to illustrate some points. This focus on size and growth of individuals is not identical to reproductive success, but if competitive dominance and genotype are correlated, size and growth will relate to evolutionary fitness (Weiner 1990). This paper concerns processes that

[1] Fernández-Tschieder, E., Binkley, D., 2018. Linking competition with Growth Dominance and production ecology. For. Ecol. Manage. 414, 99-107. doi:https://doi.org/10.1016/j.foreco.2018.01.052

lead to differences in growth rate of tress, without analyzing the effect of competition on fitness of individuals trees (see Table 1.1 for definition of terms used in this paper).

Table 1.1. A glossary of terms used in forest competition and forest production ecology.

Term	Definition	Source
Complete size asymmetric competition	One individual, the largest, captures all the contested resources (also called absolute size asymmetric competition).	Schwinning and Weiner (1998)
Complete symmetric competition	All individuals capture the same amount of resources irrespective of their sizes (also called absolute size symmetric competition).	Schwinning and Weiner (1998)
Growth dominance	Growth dominance describes the growth distribution of trees in relation to size distribution of trees in a stand.	Binkley (2004)
Partial size symmetric competition	Capture of contested resources increases with size but less than proportionally.	Schwinning and Weiner (1998)
Partial size asymmetric competition	Capture of contested resources increases with size and larger individuals obtain a disproportionate share of resources.	Schwinning and Weiner (1998)
Perfect size symmetric competition	Capture of contested resources is proportional to size (also called relative size symmetric competition).	Schwinning and Weiner (1998)
Resource	An element or form of energy used by plants in direct or indirect processes of production; light (energy form), water (lost in transpiration), and nutrients (catalysts for biochemical reactions, and components of cells) are the resources of interest.	Binkley et al. (2004)
Resource use	The quantity of resources used by a plant at a defined scale of space and time (= resource capture, resource uptake, resource acquisition).	Binkley et al. (2004)
Resource use efficiency	Production per unit of resource used. It needs to be defined clearly for any particular plant component (e.g., stem production).	Binkley et al. (2004)
Size hierarchy	Size hierarchy described the degree to which biomass is concentrated among a few individuals.	Weiner and Solbrig (1984)
Size-growth relationship	Functions relating growth to size of individuals plants in a population at a point in time (also called distribution modifying functions).	Westoby (1982)

Competition and stand structure

Competition is usually considered as a continuum between absolute symmetric competition and absolute asymmetric competition. Asymmetric competition develops when larger individuals have a disproportional competitive advantage over small individuals, resulting from greater proportional preemption of resources (Weiner 1990, Schwinning and Weiner 1998). A crown of a large tree intercepts light, preempting the supply to a smaller tree with little or no influence of a smaller tree's light capture on the larger tree. Symmetric competition implies that the competitive effects of larger and smaller individuals are similar, with either equal resource use (absolute symmetry), or resource use that scales less than proportional with tree size (partial size symmetry) or proportionally with tree size (perfect or relative size symmetry) (Weiner 1990, Schwinning and Weiner 1998). For example, equal use of soil water by all plants would be symmetric competition, and water use in constant proportion to tree size would be relative-size symmetric.

Size hierarchy described the degree to which biomass is concentrated among a few individuals, and refers to a concept of size inequality or concentration in the size distribution of a population (Weiner and Solbrig 1984). Scientists have assumed size hierarchy as the outcome of competition, and various characteristics of size distribution have been used to evaluate size hierarchy. These include: skewness, bimodality, size inequality or size variation, and growth distribution (Ford 1975, Westoby 1982, Weiner and Solbrig 1984, Bendel et al. 1989, Damgaard and Weiner 2000). The Gini coefficient has been recommended as a statistic to measure size hierarchy in plant populations (Weiner and Solbrig 1984).

The effect of competition on size hierarchy varies according to the mode of competition. While asymmetric competition increases size hierarchy over time (in a stand without intense

mortality), symmetric competition sustains the current size hierarchy over time (Westoby 1982, Weiner 1990).

The size distribution of a forest results in part from the distribution of growth of the stand among trees, with feedback effects on subsequent growth among trees. The "distribution modifying functions" (Westoby 1982) (also called size-growth relationships) are functions relating growth to size of individuals plants in a population at a point in time. The shape of these functions influences the development of size distributions, and relates to the mode of competition (Weiner 1990). Using the relationship between growth and size, competition is considered size-symmetric if individuals grow proportional to their size (all individuals experience similar relative growth rate), and competition is considered size-asymmetric if large individuals grow more than proportionally to size (larger individuals experience higher relative growth rate). Finally, competition is considered inverse size-asymmetric (also called partial size-symmetric) when small individuals grow disproportionately more relative to their size (Weiner 1990, Weiner and Damgaard 2006, Metsaranta and Lieffers 2010, Pretzsch and Biber 2010). Asymmetric competition is the most likely explanation for those cases with size-asymmetric growth, however, size-asymmetric growth is not a good measure of the strength of asymmetric competition (Weiner and Damgaard 2006).

Another representation of the relationship between growth and stand structure is growth dominance (Binkley 2004, Binkley et al. 2006). Growth dominance describes the distribution of a stand's growth among individual trees in relation to tree size and has been used as a quantitative method to evaluate stand structure. Growth dominance varies across species and forest stands. For example, stands of *Eucalyptus* species often show high positive Growth Dominance at young ages (Binkley et al. 2003), declining but remaining positive with age (Doi

et al. 2010). In contrast, stands of *Pinus* species show a relatively small positive growth dominance or null growth dominance (Fernández and Gyenge 2009, Bradford et al. 2010, Fernández Tschieder et al. 2012). Fernandez et al. (2011) proposed that differences in Growth Dominance patterns could be related to species traits as leaf physiological plasticity. Explicitly or implicitly, Growth dominance has been related to symmetric or asymmetric competition (Fernández and Gyenge 2009, Bradford et al. 2010, Doi et al. 2010, Keyser 2012, Fernández Tschieder et al. 2012, Pothier 2017). Positive Growth Dominance has been related to asymmetric competition, null Growth Dominance to perfect symmetric competition, and reverse Growth Dominance to absolute or partial symmetric competition (Doi et al. 2010, Fernández Tschieder et al. 2012, Pothier 2017).

Size hierarchy and competition: the Gini coefficient

Weiner and Solbrig (1984) introduced the Lorenz Curve (Lorenz 1905) and the Gini coefficient (Gini 1912, see Ceriani and Verme 2012 for a futher discussion) into the ecological literature. Both concepts come from economics and can be used as a metric to characterize the degree of hierarchy or inequality in a size distribution of a tree population. The Lorenz curve graphically represents the degree of hierarchy in the distribution of biomass, and the Gini coefficient condenses the information of the Lorentz curve into a single coefficient (Fig. 1.1). The degree to which the observed curve departs from the line of equality describes the degree of size hierarchy in the size distribution (Weiner and Solbrig 1984). The Gini coefficient represents the area between the line of equality and the Lorenz curve as a proportion of the total area under the diagonal. The Gini coefficient (GC) can be calculated as the mean of the difference between every possible pair of individuals $GC = \sum_i^n \sum_j^n |x_i - x_j| / 2n^2 \bar{x}$, where x_i is the size of tree i, x_j is the size of tree j, n is the number of individual trees in the sample, and $\overline{x}$ is the mean tree size

(Damgaard and Weiner 2000). The Gini coefficient has a minimum value of 0, when all plants in a population have exactly the same biomass and approaches a maximum of 1 as the population moves toward mostly very small trees with one large tree.

The Gini coefficient has been used to infer the process of competition (Weiner 1990, Cordonnier and Kunstler 2015). Weiner and Thomas (1986) found that inequality increased in most of the plant populations they analyzed, and concluded that asymmetric competition was the prevailing mode of competition (at least for light). The results from Weiner and Thomas (1986) have been used to assume asymmetric competition in plant populations, supporting the use of the Gini coefficient to evaluate competition. A larger Gini coefficient implies a higher degree of asymmetric competition, assuming that competition is asymmetric. Before the onset of self-thinning and assuming that density-dependent mortality affects small individuals more than large ones, asymmetric competition accentuates size hierarchy over time (increasing the Gini coefficient) as larger individuals grow disproportionally more than the smaller individuals (large individuals have higher relative growth compared to smaller individuals).

However, asymmetric competition is not always the dominant mode of competition (Stoll et al. 1994, see for example Binkley et al. 2006, Pretzsch and Biber 2010, Castagneri et al. 2012). The correspondence between Gini coefficient and degree of competition is not always simple, and inferences about the degree of competition may be wrong. A stand undergoing symmetric competition would develop a size hierarchy that remained relatively constant, and inversely asymmetric competition would lead to a declining Gini coefficient over time. In these cases, accurate inferences about competition could be gained only if the pattern of the Gini coefficient was followed over time.

Stands could also have the same Gini coefficient and stand structures but could have developed from different modes of competition. For example, three stands with the same Gini coefficient at time *t* will develop different Gini coefficients at time *t+1* depending on the type of competition among trees (Fig. 1.1). Stand *A* experiencing size-asymmetric competition developed to a more hierarchical stand at time *t+1* (higher Gini coefficient). On the other hand, Stand *B* under size-symmetric competition maintained the same degree of hierarchy between time *t* and *t+1* (identical Gini coefficient). Stand *C* under inverse size-asymmetric competition developed to a more uniform stand at time *t+1* (lower Gini coefficient). A comparison of the stands only at time *t* would lead to an erroneous conclusion that the three stands were experiencing the same degree of competition. In addition, a high degree of size variability could or could not be related to size-asymmetric competition. For example, an age chronosequence of lodgepole pine (*Pinus contorta*) stands in Yellowstone National Park never showed size-asymmetric competition despite high size variability among trees within stands (Kashian et al. 2005, Binkley et al. 2006). This pattern resulted from a of declining growth per unit of leaf area (a *proxy* of light use efficiency) with tree size and age (Binkley and Kashian 2015).

The same reasoning could be applied for two stands with different Gini coefficient but undergoing the same type of competition. We calculated the Gini coefficient for two poplar stands with different densities (Fernandez-Tschieder, unpublished data). The denser stand showed a higher Gini coefficient (0.19 *vs.* 0.12) at time *t*. After 6 years, the denser stand was still showing higher size hierarchy, but both stands had experienced a decrease in the Gini coefficient (0.17 *vs*. 0.09). Using solely the Gini coefficient at time *t* as a measure of competition would have implied that the denser stand was experiencing a more intense asymmetric competition, missing the fact that both stands were experiencing inverse asymmetric competition. The results

from Castagneri et al. (2012) for long-term data on three Norway spruce plots showed a similar limitation of the information conveyed by Gini coefficient. One plot had the lowest Gini coefficient yet showed a trend from inverse asymmetric to asymmetric competition and the greatest asymmetric competition index.

Stand hierarchy structure develops from growth distribution among individuals composing the population (Westoby 1982, Weiner 1990), and the Gini coefficient can be used to characterize the size hierarchy of a stand. However, inferences about competition using the Gini coefficient at a single point in time are robust only when the mode of competition is asymmetric. Stand development needs to be followed over time to be sure about the mode of competition using the Gini coefficient.

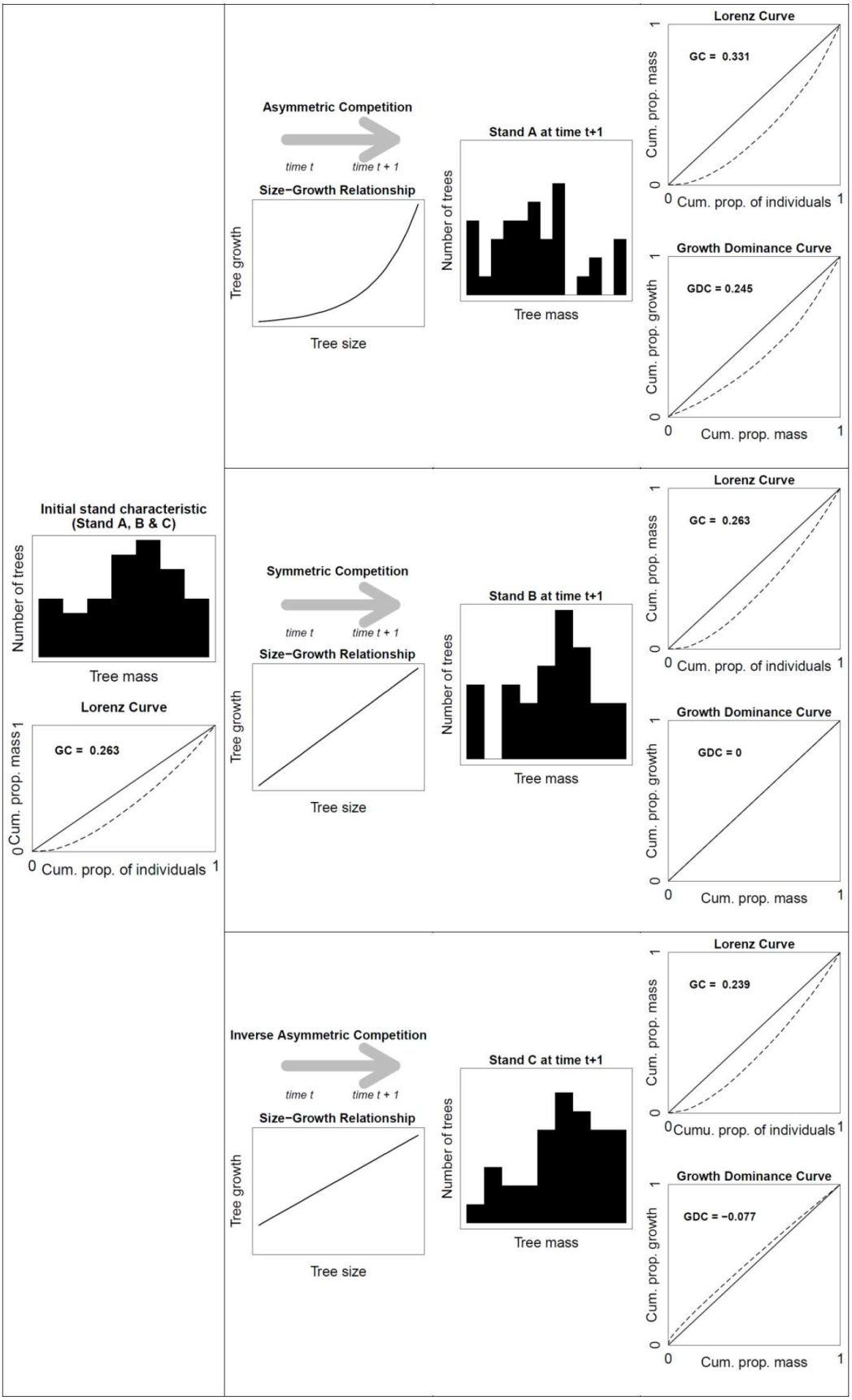
Initial stand characteristic
(Stand A, B & C)
Number of trees
Tree mass
Lorenz Curve
GC = 0.263
Cum. prop. mass
Cum. prop. of individuals
Asymmetric Competition
time t
time t + 1
Size−Growth Relationship
Tree growth
Tree size
Stand A at time t+1
Number of trees
Tree mass
Lorenz Curve
GC = 0.331
Cum. prop. mass
Cum. prop. of individuals
Growth Dominance Curve
GDC = 0.245
Cum. prop. growth
Cum. prop. mass
Symmetric Competition
time t
time t + 1
Size−Growth Relationship
Tree growth
Tree size
Stand B at time t+1
Number of trees
Tree mass
Lorenz Curve
GC = 0.263
Cum. prop. mass
Cum. prop. of individuals
Growth Dominance Curve
GDC = 0
Cum. prop. growth
Cum. prop. mass
Inverse Asymmetric Competition
time t
time t + 1
Size−Growth Relationship
Tree growth
Tree size
Stand C at time t+1
Number of trees
Tree mass
Lorenz Curve
GC = 0.239
Cum. prop. mass
Cumu. prop. of individuals
Growth Dominance Curve
GDC = −0.077
Cum. prop. growth
Cum. prop. mass

Figure 1.1. A set of hypothetical stands with the same size distribution and Gini coefficient (GC) at time *t* but experiencing distinct types of competition. Stand *A* is under size-asymmetric competition, while stand *B* is under size-symmetric competition. As a result of size-asymmetric competition size inequality increases in stand *A* as reflected by the Gini coefficient. On the other hand, size inequality in stand *B* remains relative constant trough time; the Gini coefficient at time *t* is similar to Gini coefficient at time *t+1*. This figure shows that a single Lorenz curve (and Gini coefficient) represents one point in time and can be paired with more than one sort of Growth dominance curve, and Growth dominance coefficient (GDC, see next section), depending on the nature of competition. We simulated tree biomass development in each plot as stem biomass at time *t* plus growth between *t* and *t+1*. For stand *A*, growth of each tree was estimated with an exponential relationship, and for stand *B* with a linear relationship with intercept equal zero. The exponential size-growth relationship represents a stand undergoing size-asymmetric competition, whereas the linear relationship represents a stand undergoing size-symmetric competition. Tree biomass distribution at time *t* and *t+1* was used to estimate the Gini coefficient (GC) using the *ineq* function (Zeileis 2014) from the *ineq* R package (R Core Team 2018). $GC = \frac{\sum_{i=1}^{n}(2i-n-1)x_i}{n^2\mu}$ where n = sample of trees ordered by increasing size plant, x_i = size of tree *i*, μ = average tree size (Damgaard and Weiner 2000).

Growth dominance and competition

The starting point of the analysis of size hierarchy in size distributions can be expanded by assessing the relationship between biomass distribution and growth distribution. In practice, this requires following a stand over at least two points in time during the stand development.

The relationship between tree sizes and growth rates can be examined simultaneously with the growth dominance approach (Binkley 2004, Binkley et al. 2006). This approach relates the relative contribution of individual trees, ranked in increasing order of size, to stand growth and biomass (Binkley 2004). Similar to the Gini coefficient, the growth dominance coefficient represents the departure from a line of equality (the null growth dominance line) and can be graphically represented by the growth dominance curve. The degree of departure from the line of null growth dominance can be measured by the growth dominance coefficient (GDC) as $GDC = 1 - \sum_{i=1\ldots n}(s_i - s_{i-1}) \cdot (d_i + d_{i-1})$, where s_i is the cumulative proportional size, d_i is the cumulative proportional growth, and *n* is the sample size (Binkley et al. 2006, West 2014). The growth dominance coefficient can take theoretical values between -1 and 1 (unlike Gini

coefficients which cannot be negative). The growth dominance curve considers the growth of each tree (even though the y-axis is cumulative) in relation to the tree's position in the size hierarchy of a stand. A stand might experience null growth dominance (GDC = 0; all individuals in a stand grow in proportion to their biomass), positive growth dominance (GDC > 0; larger individuals account for a greater proportion of stand growth than their contribution to stand biomass), and reverse growth dominance (GDC < 0; smaller trees account for a greater proportion of growth than to stand biomass).

As with the Gini coefficient, the growth dominance coefficient can be related to the mode of competition. Mathematically, the growth dominance concept is related to the relative growth of trees (Ducey 2010). Positive growth dominance in stands should reflect asymmetric competition, with larger trees showing larger relative growth rate. Null growth dominance should reflect symmetric competition, with all trees having similar relative growth rate. Reverse growth dominance entails smaller trees showing greater relative growth rates, reflecting inverse asymmetric competition (Table 1.2). However, these simple inferences about modes of competition may be confounded if growth differences among trees within stands includes differences in the efficiency of resource use (see section Production ecology and competition and Table 1.2).

Both the growth dominance and the Gini coefficient represent characteristics at the stand level and are based on similar concepts. However, there are some distinctive differences in the ecological processes these inequality indices express. The Gini coefficient summarizes the size hierarchy of the size structure of a population at time *t* and does not entail any information on growth distribution. The growth dominance coefficient summarizes the inequality in growth distribution in relation to size structure between time *t* and *t+1*. Growth dominance does not

represent the size structure: a stand could have a high degree of size hierarchy (high Gini coefficient) and a still have null growth dominance if all trees were growing proportionally to their size (as the lodgepole stand described in Binkley et al. 2006). These two indices are directly related only if the prevailing competition mode is size-asymmetric. In such situation, both coefficients are positively correlated: a higher size hierarchy should reflect a higher growth dominance. Under size-symmetric or inverse size-asymmetric competition (stands B and C, respectively, in Fig. 1.1) a single Lorenz curve at time *t*) could be paired with more than one growth dominance curve depending on the mode of competition (see the resulting growth dominance curves at time *t+1* for Stand B and C in Fig. 1.1). The Gini coefficient and the growth dominance coefficient provide complementary (but not identical) information.

Unlike the Gini coefficient, size-growth relationships and growth dominance hold the same information: growth distribution among trees in a stand. The basic difference between these two approaches is how they express the information (see section Competition and stand structure). However, each size-growth relationship (Metsaranta and Lieffers 2010, Pretzsch and Biber 2010) can be associated with a particular pattern of growth dominance (Table 1.2). The symmetric size-growth relationship is equivalent to the concept of null growth dominance, the asymmetric size-growth relationship is equivalent to the concept of positive growth dominance, and the inversely asymmetric size-growth relationship is equivalent to the concept of reverse growth dominance.

The growth dominance approach may offer some advantages over size-growth relationships. First, the information contained in the growth dominance curve can be summarized in a unitless coefficient, and this coefficient would be sufficient to evaluate the mode of competition and the degree of growth dominance. Such a coefficient is particularly useful to

compare stands across ages or productivity gradients. For example, to compare across stand ages on sites of similar quality, differences in growth and stand biomass among stands ages are removed and brought into a common scale between -1 and 1 (see Binkley et al. 2006). A single condensed coefficient loses some detailed information that is embodied in the growth dominance curve. Thus, in some cases comparisons may be useful with only the growth dominance coefficient, and others may require evaluation of the full growth dominance curve (Damgaard and Weiner 2000, Pommerening et al. 2016).

Production ecology and competition

Explanations about competition have typically focused on resource partitioning (light, water and nutrients) among neighboring individuals. As mentioned in the Introduction section, growth of individual trees also depends on how efficiently these resources are being used to fix carbon to produce biomass, and any substantial differences in resource use efficiency could confound competition inferences that rely only on resource partitioning. These components comprise the production ecology equation (Monteith and Moss 1977, Binkley et al. 2010). According to the production ecology equation the growth of a tree based on the supply of photosynthetically active radiation (PAR) can be expressed as:

$$\begin{aligned} &Net\ Primary\ Production\ (kgC\ tree^{-1}\ year^{-1}) = \\ &\quad Resource\ supply\ (MJ\ tree^{-1}\ year^{-1}) \\ &\quad x\ Proportion\ of\ resource\ supply\ acquired \\ &\quad x\ Efficiency\ of\ resource\ use\ (kgC\ MJ^{-1}) \quad [1] \end{aligned}$$

When the focus is on a particular tissue, such as stemwood, growth is also influenced by carbon partitioning within individual trees (Landsberg and Waring 1997, Ryan et al. 1997, Binkley et al. 2010).

Competition can be quantified with the production ecology equation. The production ecology equation shows that growth differences between trees could result from differences in resource use (resource supply x proportion of resource supply acquired) and from differences in resource use efficiency for producing growth. Therefore, any disproportionality in growth in relation to size among trees should be related to size patterns in resource use and (or) resource use efficiency. Simultaneously, this disproportionality in growth is reflected in the growth dominance pattern. According to this description, growth dominance should result from differences in resource use and (or) resource use efficiency among trees within a stand. In the next section, we developed an analytical approach between growth dominance and production ecology. As it was shown (section 1.2), size hierarchy may be related to more than one mode of competition (Fig. 1.1). In addition, size hierarchy – as measured with the Gini coefficient- does not include any information on growth. For these reasons, we did not develop a link between size hierarchy and the production ecology concept.

Analytical approach: Growth dominance and the production ecology equation

The patterns of growth dominance (Binkley 2004) and production ecology (Monteith and Moss 1977) provide the context for partitioning of growth among trees within stands. Growth dominance expresses the growth partitioning in relation to biomass partitioning in a stand. In a stand with null growth dominance, trees grow proportionally to their size (i.e., if a tree contributes with 2% of the stand biomass, it also contributes with 2% of stand growth):

$$growth_i(kg_{wood}\ year^{-1})/growth_{stand}\ (kg_{wood}\ year^{-1}) =$$

$$biomass_i(kg_{wood})/biomass_{stand}\ (kg_{wood}) \qquad [2]$$

Null growth dominance means that the ratio between growth and biomass of each tree is the same among all trees and equal to the ratio at stand level. With some rearrangement from equation 2:

$$growth_i(kg_{wood}\ year^{-1})/biomass_i(kg_{wood}) =$$

$$growth_{stand}(kg_{wood}\ year^{-1})/biomass_{stand}(kg_{wood}) \qquad [3]$$

Where $growth_i$ is the stem growth of the tree *i* defined as mass accumulation per unit of time, $biomass_i$ is the stem biomass of the tree *i*, $growth_{stand}$ is the stem growth of the stand and $biomass_{stand}$ is the stem biomass of the stand. The equality in equation 3 is true for all trees in the stand (1, 2, ...*n*):

$$growth_1/biomass_1 = growth_2/biomass_2 = \cdots\cdots\cdots = growth_n/biomass_n \qquad [4]$$

Stem growth of an individual tree can be regarded as NPP_{sw} (kg_{wood} $year^{-1}$), and by equation 1, growth of tree *i* is the product of its resource use (RU_i, MJ_{PAR} $year^{-1}$) and its resource use efficiency for producing stemwood (RUE_{sw}, kg_{wood} MJ_{PAR}^{-1}). Substituting for $growth_i$ in equation 4 results in:

$$RU_1(MJ_{PAR}\ year^{-1})/biomass_1(kg_{wood}) \times RUE_1(kg_{wood}\ MJ_{PAR}^{-1}) = RU_2/biomass_2 \times$$

$$RUE_2 = \cdots\cdots\cdots = RU_n/biomass_n \times RUE_n \qquad [5]$$

By definition, any change in this equality must derive from differences in the amount of resource captured per unit of biomass and time (symmetric or asymmetric competition concept) and (or) differences in the resource use efficiency for stem wood production among trees in the stand.

Depending on the shape of the relation between resource use and resource use efficiency with tree size, growth dominance patterns may be reverse, null or positive. Stands with reverse growth dominance have smaller trees growing proportionally more than larger trees because smaller trees capture either obtain resources beyond their proportional size (Table 1.2. a) or smaller trees capture size-proportional amounts of resources and use them more efficiently than larger trees (Table 1.2. e). Stands with null growth dominance have all trees either obtaining resources in proportion to their sizes and similar efficiency of use or have offsetting patterns of resource acquisition and efficiency of use (Table 1.2. b). In stands with positive growth dominance, larger trees grow disproportionally faster than smaller trees because they acquire a disproportionate amount of resources and use those resources equally efficiently (Table 1.2. c and Table 1.2. d) or more efficiently (Table 1.2. f). A positive growth dominance pattern also would be compatible with symmetric competition for resources and a higher resource use efficiency by larger trees (Table 1.2. f).

Given the multiplicative nature of the definition of growth and the ratios between variables involved, other patterns may arise. For example, larger trees could capture a disproportionate amount of resources but using those resources with a lower efficiency and still show some degree of growth dominance. The same pattern of resource use and resource use efficiency could lead to null growth dominance if the higher resource use efficiency of smaller trees could offset the disproportionate amount of resources captures by larger trees. Dominating the use of resources is not enough to show growth dominance, the higher proportions of resource acquisition should translate into a proportional increase of stem growth.

Do the various types of growth dominance patterns reflect consistently different processes, or does a given pattern often develop from various trends in resource use and

efficiency of resource use? If a given pattern of growth dominance always has a given production ecology distribution among tree sizes, then the growth dominance could indicate both pattern and process. However, if a given growth dominance pattern results from more than one pattern of resource use and resource use efficiency among tree sizes, or varies according to the relative effect of each other, then growth dominance alone cannot support simple inferences.

Table 1.2. Patterns in growth dominance, and hypothetical patterns in resource use and resource use efficiency. We suggest that growth dominance reflects different patterns in resource use and resource use efficiency with tree size. Part A of the table describes patterns where only resource use (RU, MJ_{PAR} $tree^{-1}$ $time^{-1}$) changes with tree size (stem mass, kg), whereas Part B of describes patterns where resource use and resource use efficiency (RUE, productivity/resource use = kg_{wood} MJ_{PAR}^{-1}) change with tree size. When possible, each growth dominance pattern was linked to a size-growth relationship proposed by Pretzsch and Biber (2010) and to a type of competition proposed by Schwinning and Weiner (1998). GDC stands for growth dominance coefficient. We only differentiated between negative, null and positive growth dominance coefficients. Cum. prop. mass stands for Cumulative proportional mass, and Cum. prop. growth stands for cumulative proportional growth.

	Part A. Only resource use varies with tree size. Resource use efficiency remains constant.			
	Growth dominance	Resource use	Resource use efficiency	Expected size-growth relationship and Resource competition
1.2.a. Reverse growth dominance	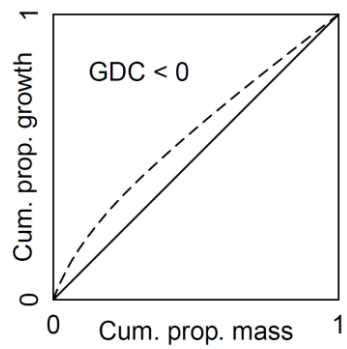	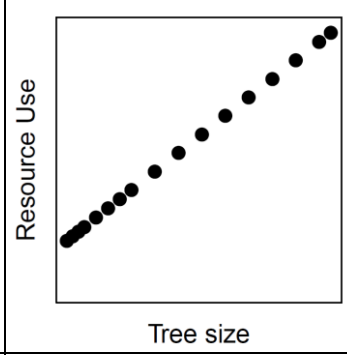	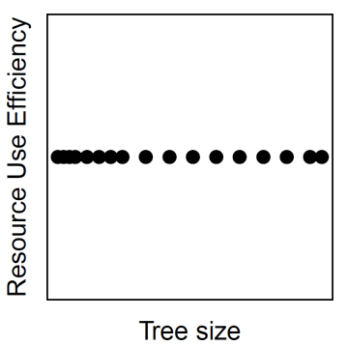	Size-growth relationship: partial size-symmetric. Growth increases less than proportionally with tree size (Pretzsch and Biber 2010). Y-intercept of RU = *f* (stem mass) is positive, and competition is partial size-symmetric (Schwinning and Weiner 1998). Resource use increases less than proportionally with tree size.
1.2.b. Null growth dominance	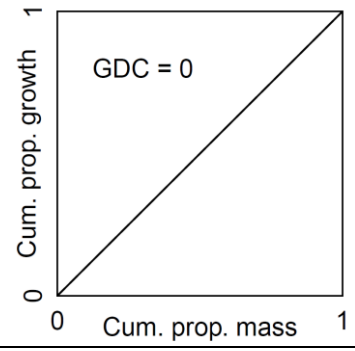	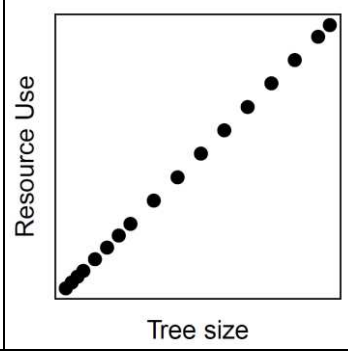	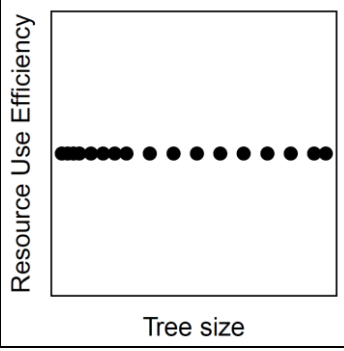	Size-growth relationship: perfect size-symmetric. Growth increases proportionally with tree size (Pretzsch and Biber 2010). Y-intercept of RU = f (stem mass) equals 0, and competition is perfect size symmetric. Resource use increases proportionally with tree size (Schwinning and Weiner 1998).

Table 1.2. Continued.

	Part A. Only resource use varies with tree size. Resource use efficiency remains constant.			
	Growth dominance	Resource use	Resource use efficiency	Expected size-growth relationship and Resource competition
1.2.c. Positive growth dominance	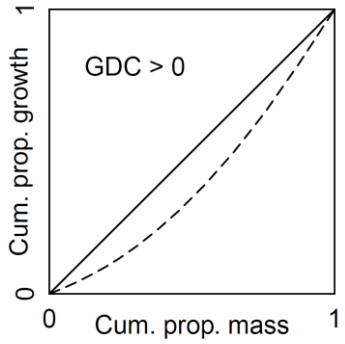		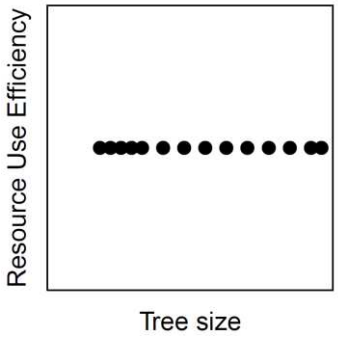	Size-growth relationship: size-asymmetric. Growth increases more than proportionally with tree size (Pretzsch and Biber 2010). Y-intercept of RU = *f* (stem mass) is negative, and competition is partial size asymmetric (Schwinning and Weiner 1998). Resource use increases more than proportionally with tree size. Larger trees account for a disproportionate share of resources.
1.2.d Positive growth dominance	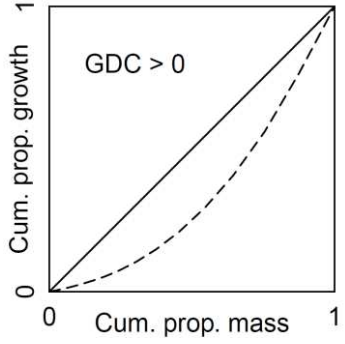		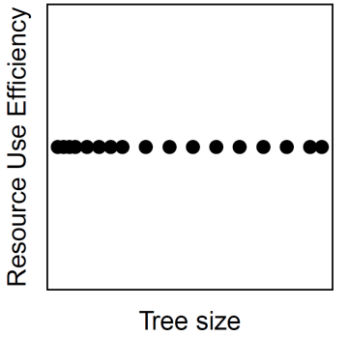	Size-growth relationship: convex size-asymmetric. Growth increases progressively with tree size (Pretzsch and Biber 2010). Y-intercept of RU = *f* (stem mass) is 0 or greater than 0 and the curve is convex. Competition is partial size asymmetric (Schwinning and Weiner 1998). Resource use increases more than proportionally with tree size at an increasing rate.

Table 1.2. Continued.

	Part B. Both resource use and resource use efficiency vary with tree size			
	Growth dominance	Resource use	Resource use efficiency	Expected size-growth relationship and Resource competition
1.2.e Reverse growth dominance	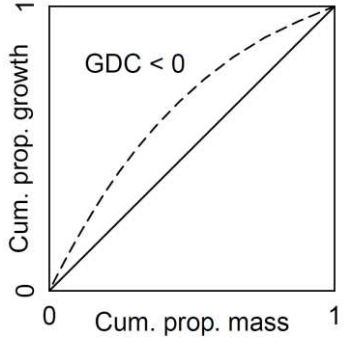	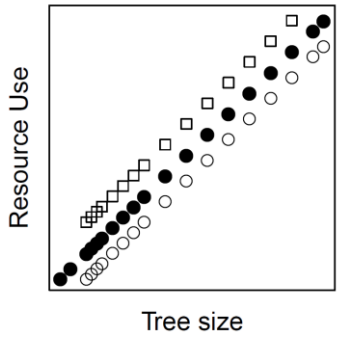	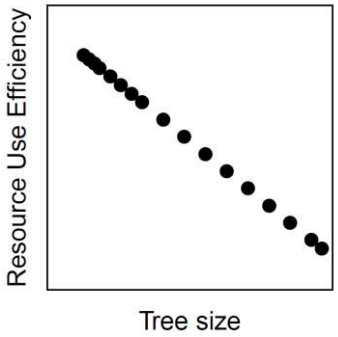	Size-growth relationship: depending on the combination of RU and RUE many size-growth relationships can be expected. For example: perfect symmetric, partial size-symmetric and concave size-symmetric (Pretzsch and Biber 2010). In all cases growth increases with tree size, but less than proportionally. Y-intercept of RU = *f* (stem mass) is 0, negative or positive. Any combination of increasing resource use and decreasing resource use efficiency with stem mass, where the RUE effect offsets the RU effect, leads to a competition where smaller trees growth proportionally more than larger trees. There is not a definition for this situation in the literature, but we can use an analogy with the inverse asymmetric size growth relationship (Metsaranta and Lieffers 2010).

Table 1.2. Continued.

	Part B. Both resource use and resource use efficiency vary with tree size			
	Growth dominance	Resource use	Resource use efficiency	Expected size-growth relationship and Resource competition
1.2.f. Positive growth dominance	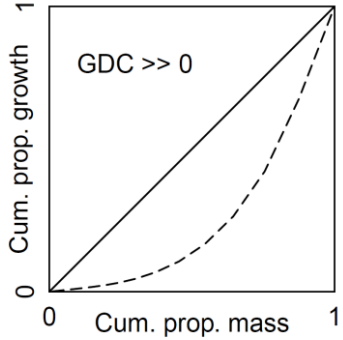		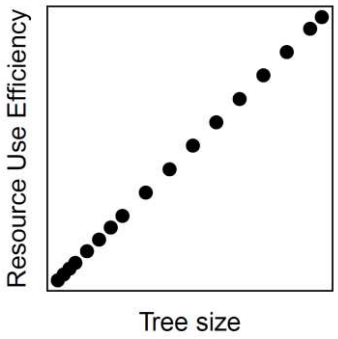	Size-growth relationship: convex size-asymmetric. Growth increases progressively with tree size (Pretzsch and Biber 2010). Any combination of increasing resource use and increasing resource use efficiency with stem mass leads to competition that is partial size asymmetric (Schwinning and Weiner 1998). We exemplified this idea with an exponential x linear combination, but it could be also an exponential x exponential or linear x linear combination.
		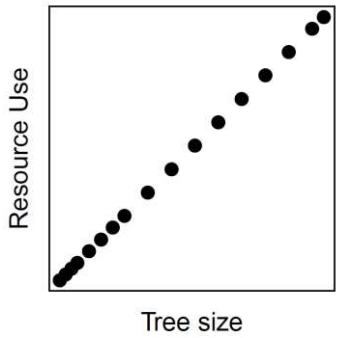	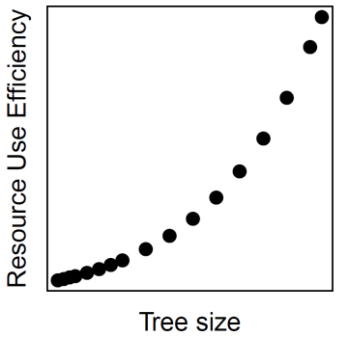	

Ultimately, growth dominance expresses the partitioning of environmental resources and the efficiency with which these resources are used among individuals within a stand in relation to their size. The proposed relation between growth dominance patterns and production ecology (Table 1.2) should be empirically explored and can be evaluated with information about growth dominance at the plot scale combined with information about resource use and resource use efficiency at individual tree scale. To illustrate these ideas, we re-analyzed two plots with contrasting growth dominance patterns (Fig. 1.2). We compared a six-year-old *Eucalyptus grandis* (W. Hill ex Maiden) plot with a relative strong positive growth dominance (GDC = 0.233) (Campoe et al. 2012, 2013b), and an eight-year-old *Pinus taeda* L. plot with a relative low reverse growth dominance (GDC = -0.027) (Campoe et al. 2013a). Absorbed photosynthetically active radiation at tree scale was estimated using the MAESTRA model (Campoe et al. 2012, 2013b, 2013a), and growth dominance was estimated for this manuscript from growth inventory data following West (2014). The Eucalyptus plot displayed asymmetric competition for light (exponential increase in the use of light with tree size) and a linear increase in the light use efficiency for stem growth (Fig. 1.2) (Table 1.2. f). The loblolly pine plot showed a partial size-symmetric competition in the use of light (light use increased with tree size, but less than proportionally), and a similar light use efficiency among trees (Fig. 1.2) (Table 1.2. a). Other plots might show different combinations of factors in the production ecology equation that could lead to other patterns of growth dominance. The application of this approach to a wide variety of forests will provide two valuable outcomes: a clearer characterization of how competition influences stand development, and how growth dominance patterns are explained by quantifiable resource use and efficiency of use patterns. The analysis of two plots showed that positive growth dominance was related to asymmetric competition for light and an increase in light use

efficiency with tree size. On the other hand, a relatively low negative growth dominance was related to a symmetric competition for light and a similar light use efficiency among trees.

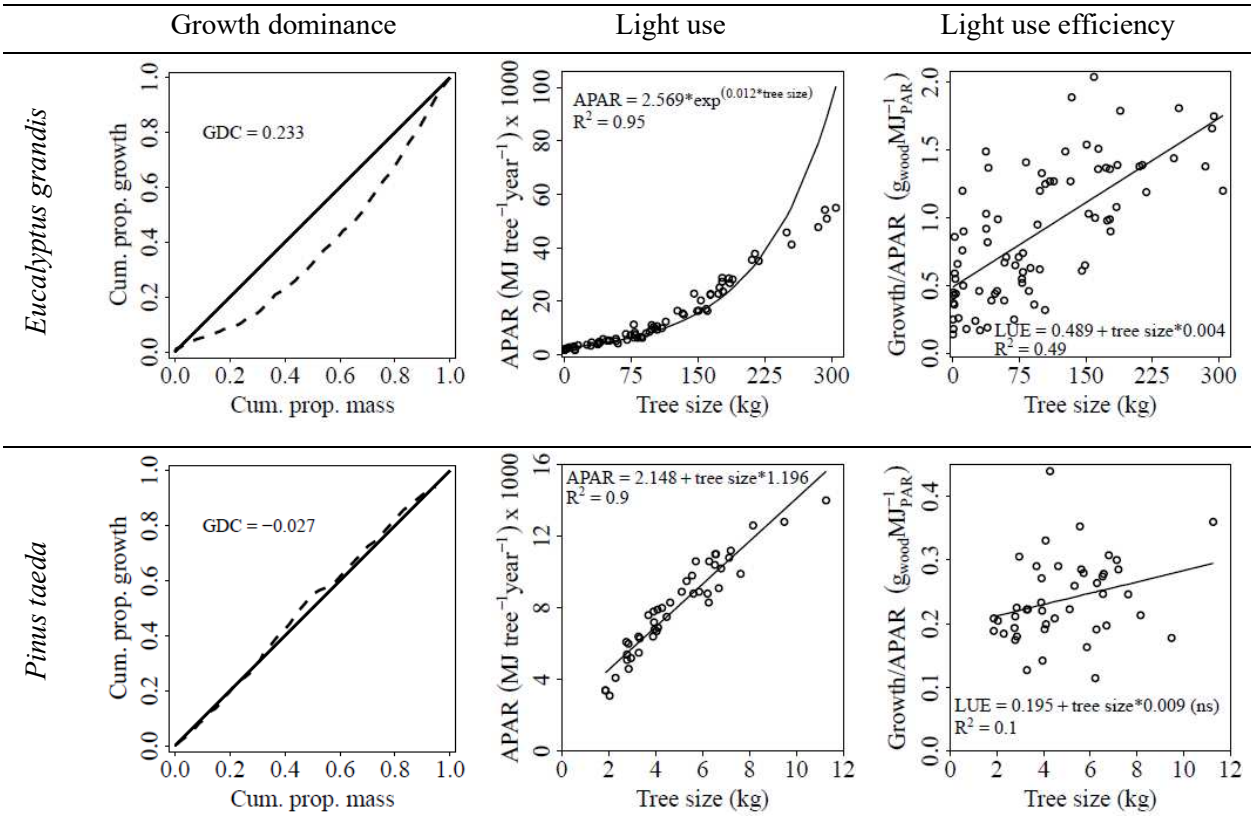

Figure 1.2. Patterns in growth dominance and its relationship with patterns in resource use and resource use efficiency. Positive growth dominance in *Eucalyptus grandis* plot related to asymmetric competition for light (large trees used light more than proportionally to their size) and a higher light use efficiency by large trees. Reverse growth dominance in *Pinus taeda* plot related to size-symmetric competition for light (large trees used more light than small trees, but less than proportionally to their size), and a similar light use efficiency among trees. APAR: absorbed photosynthetically active radiation; GDC: growth dominance coefficient; LUE: light use efficiency; ns: slope of the regression is non-significant (p-value > 0.05), R^2: multiple R-squared. Growth dominance coefficient was estimated following West (2014). Regressions lines were fit with *lm* function in R (R Core Team 2018). The original values of APAR and light use efficiency correspond to a re-analysis of data in Campoe et al. (Campoe et al. 2012, 2013b, 2013a).

CHAPTER 2: PRODUCTION ECOLOGY AND REVERSE GROWTH DOMINANCE IN AN OLD-GROWTH PONDEROSA PINE FOREST[2]

Introduction

The rate of tree growth can be described as a function of the amount of available resources captured by an individual tree and how efficiently the resources are converted into biomass (usually referred as the production ecology equation) (Monteith and Moss 1977, Binkley et al. 2010). Typically, large trees in a stand grow faster than small trees because large trees capture a greater amount of light and use the light more efficiently (see the special issue Light interception and growth of trees and stands in Forest Ecology and Management 2013). The amount of light captured by a tree depends in part on the competition with other neighboring trees. Competition can be symmetric, if all trees intercept light proportional to their size or asymmetric if a group of trees intercepts light more than proportional to their size (Schwinning and Weiner 1998). Competition for light has been described as strictly asymmetric (Weiner and Thomas 1986, Weiner 1990, Onoda et al. 2014). However, light interception has also been found to increase proportional or less than proportional with tree leaf area, indicating that symmetric competition for light is possible (Binkley et al. 2010, 2013, Campoe et al. 2013a, Gspaltl et al. 2013). In this article, we explored the growth dominance-production ecology connection in an old-growth ponderosa pine stand. Specifically, we explored if negative growth dominance could be explained by symmetric competition for light and a declining light use efficiency with tree size.

[2] Fernández-Tschieder, E., Binkley, D., Bauerle, W., 2020. Production ecology and reverse growth dominance in an old-growth ponderosa pine forest. For. Ecol. Manage. 460, 117891. doi:https://doi.org/10.1016/j.foreco.2020.117891

The growth dominance concept merges the distribution of individual growth and the distribution of individual size as a function of population percentile in a single curve; the "Growth dominance curve" (Binkley 2004, Binkley et al. 2006). If all trees in a stand grow proportionally to their size, growth dominance is neutral. Growth dominance is negative (also called reverse growth dominance) when small trees grow more than proportionally to their size, and growth dominance is positive when large trees grow more than proportionally to their size. The patterns of growth dominance appear to differ among genera, though too few studies are available to provide robust generalizations. For example, eucalyptus species (*Eucalyptus* spp.) tend to show positive growth dominance even at advanced age and high stand biomass (Binkley et al. 2003, Doi et al. 2010), whereas pines (*Pinus* spp.) typically show slightly positive, null or negative growth dominance during stand development (Binkley et al. 2003, 2006, Martin and Jokela 2004, Fernández and Gyenge 2009, Bradford et al. 2010, Doi et al. 2010, Fernández Tschieder et al. 2012).

Do differences in growth dominance patterns emerge from consistent, predictable interactions between resource use and resource use efficiency patterns at the individual-tree scale? Fernández-Tschieder and Binkley (2018) developed a theoretical framework relating patterns of growth dominance to particular trends in the production ecology of trees. Some evidence for this question can be found in eucalyptus and pine studies. Both large eucalyptus and pine trees intercept more light than small trees, but the differences in light use efficiency between large and small trees are larger in eucalyptus stands (Binkley et al. 2002, 2010, Campoe et al. 2013b, 2013a). Moreover, in eucalyptus stands large trees capture proportionally more light than small trees, whereas the opposite may be true in pine stands (Binkley et al. 2013, Campoe et al. 2013a, 2013b). More evidence for the connection between growth dominance and production

ecology came from two pine species studies that used growth efficiency (growth/leaf area or leaf biomass) as a *proxy* for light use efficiency. Fernandez-Tschieder et al. (2012) found that on average large loblolly pine (*Pinus taeda*) trees had 1.4-fold greater growth efficiency than small trees, and that differences in growth efficiency were positively correlated with growth dominance. A similar correlation was found in lodgepole pine stands (*Pinus contorta*) with growth dominance ranging from strongly negative to slightly positive (from -0.5 to 0.1) (Binkley and Kashian 2015). In these stands, small trees had greater growth efficiency than large trees for growth dominance values lower than -0.1 (Binkley and Kashian 2015).

We examined the production ecology of growth dominance in an old-growth stand of ponderosa pine (*Pinus ponderosa*) in Colorado. This stand had strong negative (reverse) growth dominanace (Binkley et al. 2006), implying that small trees are growing proportionally more than large trees. Negative growth dominance may result from the following combinations between light interception and light use efficiency as a function of tree size (from Fernández-Tschieder and Binkley 2018)

- light interception by individual trees increases proportionally with tree size but light use efficiency decreases with tree size,
- light interception by individual trees increases more than proportionally with tree size but light use efficiency decreases with tree size counterbalancing the effect of light competition,
- light interception by individual trees increases but less than proportional to tree size and light use efficiency decreases with tree size (or remains constant),
- light interception by individual trees increases but less than proportional to tree size and light use efficiency does not change with tree size.

In this paper, we combined the analysis of growth dominance and production ecology to evaluate which combination between light competition and light use efficiency was responsible for the observed negative growth dominance in the old-growth ponderosa pine stand. This ponderosa pine stand represents the statistical population of inference in our study. However, this analysis has broader interest beyond this single site because results could be extrapolated to other stands under reverse growth dominance based on the production ecology mechanisms behind reverse growth dominance.

Methods

Site description and data preparation

We used an existing data set from a 9.3 ha plot of monospecific old-growth ponderosa pine established by the USDA Forest Service in 1974 (Fig. 2.1). The plot is located in the Manitou Experimental Forest close to Colorado Spring, Colorado, USA. All trees in the plot taller than 1.4 m were tagged and mapped using an x-y-coordinate system. Diameters of all trees were measured (dbh, diameter at 1.4-m height) in 1974, 1983, 1991, 2001 and 2010. A sample of trees in the plot was measured for total height during 1974, 1991, 2001 (n = 3423), for height to the base of crown during 1974 and 1991 (n = 1061), and for right-angled crown radius during 2011 (n = 99). A sample of trees (n = 27) located close to the plot were destructively sampled for needle biomass during September and October 2016. All samples, except the needle biomass sample, included trees representing the size range of trees in the plot. Trees in the needle biomass sample ranged between 16.7 and 60.8 cm in dbh.

Figure 2.1. The old-growth ponderosa pine stand in the Manitou Experimental Forest was dominated by a cohort of large trees (>150 years old) with patchy smaller cohorts. Tree density was approximately 400 trees per hectare in 2010. Minor selective harvesting occurred in the late 1880s. See Boyden et al. (2005) for a further description of the stand structure.

A complete description of the plot's structure and characteristics can be found in Boyden et al. (2005) and Boyden and Binkley (2016). Briefly, the plot has an uneven-aged structure with major cohorts of trees dating to periods around 1780, 1880, and 1960, with a few trees remaining from the early 1600s. About 30 trees ha^{-1} (15% of the estimated stand density at the time) were removed during the last selective logging of large tree between 1880 and 1886. Plot density increased from 270 trees ha^{-1} (basal area ≈ 19 m^2 ha^{-1}) in 1974 to 420 trees ha^{-1} in 2001 (basal area ≈ 21 m^2 ha^{-1}). Density of small trees (< 6 cm dbh) increased from 20 trees ha^{-1} in 1974 to 150 trees ha^{-1} in 2001. Overall, trees in the plot were clustered, except for large trees (dbh > 40 cm) that were regularly dispersed. Mortality in the stand was less than 1% per year (Boyden et al. 2005).

For the purpose of this study, we analyzed the period between years 2001 and 2010. Because the equation used to estimate needle biomass included only trees larger than 16 cm in dbh, trees smaller than 10 cm in dbh were omitted from the analysis. This included a group of 401 trees from the subplot (see below) mostly regenerated after year 2001with 75% of trees

smaller than 4.1 cm in dbh, that represented 0.2% and 5% of the subplot biomass and growth, respectively. We considered the uncertainty of estimating needle biomass in this group of trees, where error in the estimation could have large effects. We assumed that the crown structure of a tree 10 cm in dbh is similar to the structure of a tree 16 cm in dbh. We evaluated if trends in growth dominance and production ecology (see section 2.3) would substantially change by the presence/absence of trees smaller than 10 cm in dbh. We found no considerable change in the patterns (data not shown).

Any tree present at time *t* that did not survive to time *t+1* (mortality) or any tree present at time *t+1* that was not present at time *t* (recruitment) was omitted from the analysis. We checked for missing values, extremely large growth values and negative growth values in dbh. When possible, errors were corrected by interpolation between time *t* and time *t+2* to obtain time *t+1* dbh. When it was not possible to interpolate, trees were deleted from the data set. We assigned a stem biomass growth value equal to 0.001 kg period^{-1} to growth values of zero to avoid model fitting problems.

Because the number of trees in the plot exceeded the maximum number of plot trees the MAESTRA model (Wang and Jarvis 1990, Medlyn 2004. See section Light interception and light use efficiency for a description of the MAESTRA model) can accommodate, we used a subplot of the 9.3 ha-original plot for our analysis (Fig. 2.2). The MAESTRA model simulates the light absorption by individual trees. A 2.6 ha subplot in the middle of the plot contained 28% the total tree count (1044 out of 3767 live trees). For the simulations we included a 15 m border surrounding the 2.6 ha subplot. Trees included in the border were used only as neighboring trees during the MAESTRA simulation (Fig. 2.2).

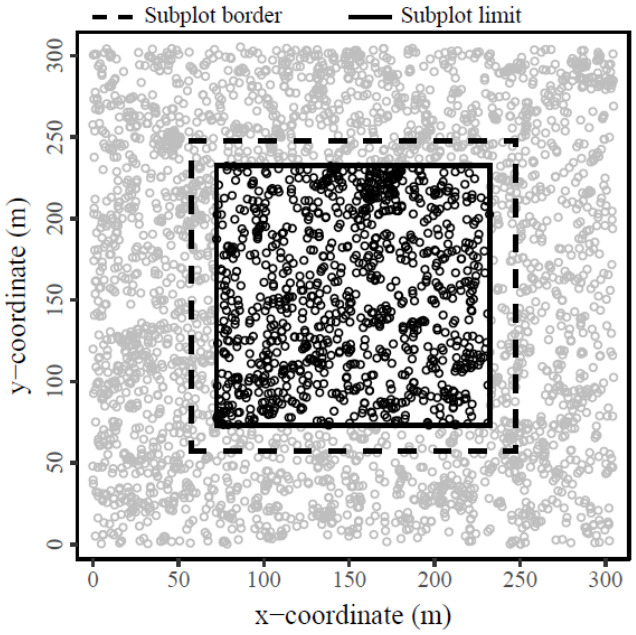

	Plot	Subplot
Area (ha)	9.3	2.6
Density (trees ha^{-1})	405	402
dbh (cm)	21.7 (1.0 – 68.6)	21.8 (1.3-65)
height (m)	11.7 (1.9 – 22.1)	11.9 (2.0-22.0)
Basal area (m^2 ha^{-1})	23.0	23.1
Stem biomass (Mg ha^{-1})	97.3	97.5
Growth (Mg ha^{-1} $year^{-1}$)	0.7	0.6
Leaf area index (m^2 m^{-2})	1.8	1.8

Figure 2.2. Spatial distribution of trees during year 2010 across a 9.3 ha old-growth ponderosa pine plot located at the Manitou Experimental Forest. For our analysis we selected a 2.6 ha subplot surrounded by a 15-meter border (delimited by dashed line) that had a similar structure to the main plot. Trees (denoted by open black circles) inside the subplot limit were used for the analysis. Values within parenthesis are the minimum and maximum.

Variables estimation

We estimated three principal variables: stand growth dominance, absorbed photosynthetically active radiation, and individual tree light use efficiency. For general comparisons, we classified trees based on their biomass distribution rather than their crown position in the canopy. Suppressed trees were defined as the lower 40% tile of the stem biomass distribution, intermediate trees were defined as trees between the 40% tile and the 80% tile of the stem biomass distribution, and dominant trees were defined as the upper 20% tile of the stem biomass distribution. The subplot contained 48 dominant trees, 146 intermediate trees and 449 suppressed trees (after removing trees smaller than 10 cm in dbh). Average diameter was 52 cm (range: 47-64 cm), 41 cm (range: 37-47 cm) and 25 cm (range: 10-37 cm) for dominant, intermediate and suppressed trees, respectively. Average height was 22 m (range: 21-22 m), 20

m (range: 20-21 m) and 15 m (range: 6-20 m) for dominant, intermediate and suppressed trees, respectively. A positive relationship between tree size and age was found for this stand (Boyden et al. 2005).

Stem biomass and growth

Stem biomass (without bark) was estimated using a volume equation developed from trees along the Colorado Front Range (Edminster et al. 1980) and wood density:

stem biomass (kg dry mass) = $(0.0000325 \times dbh^2 \times height) \times wd$,

where dbh is diameter in cm at 1.4 meters, *height* is tree height in meters, and *wd* is wood density (537 kg/m^3; Hall et al., unpublished data cf. Boyden and Binkley (2016)). Stem growth (kg tree^{-1} year^{-1}) was calculated as the difference between stem biomass at time *t+1* (2010) and time *t* (2001) divided by the numbers of years between *t* and *t+1*.

Height of trees was estimated using a Gompertz model fit with the *height* - *dbh* data pairs from this stand:

height (m) = 1.4 + 20.8372 *exp (-3.9936 *exp (-0.0934 **dbh* (cm))) [1] (R^2= 0.96; *s* = 1.5 m, n= 3423, where *s* is the residual standard deviation).

Growth dominance

Growth dominance coefficient (GD) was estimated following West (2014) as GD = 1 - $\sum_{i=1....n}$ (x[i]-x[i-1])*(z[i]+z[i-1]) where *x* is the cumulative proportional size and *z* is the cumulative proportional growth. Individual stem biomass was used as the "size" variable and stem biomass growth as the "growth" variable. A coefficient smaller than zero indicates a negative growth dominance, a coefficient equal to zero indicates null growth dominance, and a coefficient bigger than zero indicates positive growth dominance.

Light interception and light use efficiency

Absorbed photosynthetically active radiation (APAR) by individual trees during a whole year (GJ[APAR] tree^{-1} year^{-1}), was simulated using the MAESPA model (Duursma and Medlyn 2012) set in the MAESTRA mode which runs the original MAESTRA code (Wang and Jarvis 1990, Medlyn 2004). MAESPA is a model of an array of trees in a stand that uses radiative transfer calculations and leaf physiology to calculate radiation absorption, photosynthesis and transpiration of individual trees (Duursma and Medlyn 2012). In MAESTRA, light absorption by individual trees is modeled based on the x-y co-coordinates of each tree, shape of the crown, length and radii of the crown in x and y directions, height to the crown base, and leaf area and distribution within each crown. Factors considered within the model include shading within the crown as well as shading by neighboring tree, the location of the sun, and both direct and diffuse radiation (Wang and Jarvis 1990, Duursma and Medlyn 2012).

Light use efficiency for each tree (LUE; kg[wood] GJ[APAR]$^{-1}$) was calculated as the ratio of mean annual stem biomass growth between 2001-2010 to APAR during a complete year. Absorbed photosynthetically active radiation by individual trees and light use efficiency of trees were used as independent in the analysis of production ecology (Table 2.1).

Maestra parametrization

MAESTRA simulations were run hourly for a complete year using air temperature (ºC), percent relative humidity (%), photosynthetically active radiation (PAR, μmol m^{-2} s^{-1}) and wind speed (m s^{-1}). Annual meteorological data was obtained as the average values from years 2001 to 2010 (except year 2004 since this year had incomplete data) to represent the mean climatic conditions during the growth period. Meteorological data was obtained from Manitou Experimental Forest meteorology data (Asherin 2016).

Parameterization of the model was performed by estimation of tree attributes using regression models and parameters obtained from the literature. All parameters related to photosynthesis and transpiration of individual trees and tree dimensions remained constant during simulations.

Radii of crown in the *x*- and *y*-direction was estimated using an exponential model:

crown radius (m) = 0.5976*exp (0.0298**dbh* (cm)) [2] (R^2 = 0.76, *s* = 0.5 m, n = 99).

Height to crown base was estimated with an S-shape model:

height to crown base (m) = 8.0273/(1+16.8877*exp(-0.1598**dbh*(cm)) [3] (R^2 = 0.74, *s* =1.8 m, n = 1061).

Individual leaf area was estimated by multiplying needle mass by specific leaf area. We used a specific leaf area value of 2.58 (m^2 kg^{-1}) (Marshall and Monserud 2003) and needle mass was estimated using a power model:

needle mass (kg) = 0.1269**dbh*(cm)$^{1.5238}$ [4] (R^2= 0.70; *s* = 9.7 kg, n = 27).

Light interception validation

We compared the average light interception from the MAESTRA simulation for all trees with plot-scale measurements of light interception measured in the field. The MAESTRA average light interception was estimated as the ratio of total absorbed PAR by trees (GJ day^{-1}) and total incoming PAR in the plot (GJ day^{-1}) on June 21 using the average values between years 2001 and 2010. Field measurements of PAR were taken with a ceptometer at 15 m x 15 m grid points across the 9.3-ha plot in June 2012. For this study we used 159 points inside the 2.6-ha subplot. At each point, ceptometer readings were averaged from samples taken in each of 4 cardinal directions, so light interception estimates represented a footprint of about 6-8 m^2. We

compared the MAESTRA average light interception with the bootstrap 95% confidence interval of field light interception.

Production ecology analysis

The continuum between symmetric and asymmetric competition can be described by a set of simple models (Weiner and Damgaard 2006, Pretzsch and Biber 2010, Fernández-Tschieder and Binkley 2018). Symmetric competition is related to a proportional or less than proportional increase in growth rate or light interception with tree size, while asymmetric competition involves a more than proportional increase in growth or light interception with tree size. A proportional increase in the *y* variable can be described with a linear model with intercept zero, while an increase in the *y* variable at a decreasing rate can be described by a linear model with positive intercept or a non-linear model with concave shape. On the other hand, an increase in the *y* variable at an increasing rate can be described by a linear model with negative intercept or a non-linear model with convex shape (Table 2.1). To assess the mode of competition we fit a simple linear model with and without intercept, power and exponential functions to growth *vs*. tree size data, light interception *vs*. tree size data and light use efficiency *vs*. tree size data (where stem biomass was used as the measure of tree size) (Table 2.1). To facilitate comparisons with other stands all models were also fit with tree rank as the *x*-variable; where tree rank represents the i^{th}-position of the i^{th}-tree with respect to the total number of trees sorted by size from smallest to largest in the plot. For example, a tree with a tree rank of 0.2 in the subplot represents a tree that occupies the position 129 in the rank of trees sorted from smallest to largest.

Regressions were fit using the *lm* and *nls* function in R for linear and non-linear models, respectively (R Core Team 2018) and compared using the Akaike's information criterion (AIC). To obtain the maximum likelihood estimation of the variance (σ^2) AIC was corrected by *n*-

(p+1))/n, where n is the sample size and p is the number of parameters in the model (Burnham and Anderson 1998).

Table 2.1. Models representing the continuum between symmetric and asymmetric competition. These models were used to fit regressions between tree growth *vs.* tree size, tree light interception *vs.* tree size and tree light use efficiency *vs.* tree size. In the first two cases the models were associated to a specific mode of competition, in the last case the models only describe the light use efficiency pattern with tree size. Light interception by trees were the output of the MAESTRA simulation.

Model Type	Mathematical expression	Mode of Competition represented by the Model* and light use efficiency pattern
Linear model	$y = a + b\,x$ ($a < 0$)	Size-asymmetric competition *Decreasing light use efficiency pattern*
	$y = a + b\,x$ ($a = 0$)	Perfect size-symmetric competition *Increasing light use efficiency pattern*
	$y = a + b\,x$ ($a > 0$)	Partial size-symmetric competition *Increasing light use efficiency pattern*
Power model	$y = a\,x^b$ ($0 < b < 1$) (concave shape)	Partial size-symmetric competition *Increasing light use efficiency pattern*
	$y = a\,x^b$ ($b > 1$) (convex shape)	Size-asymmetric competition *Increasing light use efficiency pattern*
	$y = a\,x^b$ ($b < 1$)	*Decreasing light use efficiency pattern*
Exponential model	$y = a\,e^{bx}$ ($b > 0$)	Size-asymmetric competition *Exponential increasing light use efficiency pattern*
	$y = a\,e^{bx}$ ($b < 0$)	*Exponential decreasing light use efficiency pattern*

*Perfect size-symmetric competition: capture of contested resources or growth is proportional to size, partial size-symmetric competition: capture of contested resources or growth increases with size but less than proportionally, size-asymmetric competition: capture of contested resources or growth increases more than proportional with size (large individuals obtain a disproportionate share of resources).

Results

MAESTRA evaluation

MAESTRA estimated an average light interception of 45% for all trees, matching the 45% stand-level value estimated from the ceptometer measurements (sd = 33%, n = 159, with a 95% bootstrap confidence interval between 40 – 50%). Since ceptometer measurements included

light interception by leaves and branches, whereas MAESTRA does not, an underestimation of light interception by MAESTRA would have been expected but was not observed.

Growth dominance pattern

Growth dominance was negative during the period 2001-2010 in the old growth ponderosa pine plot, with a growth dominance coefficient of -0.22. Suppressed trees (lower 40% tile of the stem biomass distribution) accounted for 56% of stand growth, whereas dominant trees (upper 20% tile of the stem biomass distribution) contributed only 13% of stand growth (Fig. 2.3). Suppressed trees represented 70% of the tree population in the subplot, while dominant trees only 7%. Intermediate trees (trees comprised between the lower 40% tile and the upper 20% tile of the stem biomass distribution) accounted for 31% of stand growth and represented 23% of the tree population.

Tree growth pattern

Mean growth of all trees was 2.4 kg $year^{-1}$ $tree^{-1}$ (range = 0.0 - 23.1 kg $year^{-1}$ $tree^{-1}$) and tree productivity increased with tree size but at a decreasing rate (Fig. 2.4). On average, dominant trees were 5 times larger than suppressed trees (1024 vs. 211 kg $tree^{-1}$) but grew only at about twice the rate of suppressed trees (4.3 kg $year^{-1}$ $tree^{-1}$ vs. 1.9 kg $year^{-1}$ $tree^{-1}$) (Table 2.2). The growth-size relationship was best described by the power model with concave shape (parameter *b* confidence $interval_{95\%}$: 0.373 - 0.552), explaining about 20% of the variation in growth with tree size. The AIC difference (Δ_i) with the linear zero intercept (a = 0) model was 85 units as compared to 17 with the exponential model (Table 2.3). The pattern of tree growth in relation to tree rank was best described by a linear positive intercept model (Table 2.3). The median dominant tree (974 kg) in the subplot, that represented approximately a 96th percentile

tree, grew 3.5 times more than the median suppress tree (187 kg), that represented approximately a 35th percentile tree (Fig. 2.4).

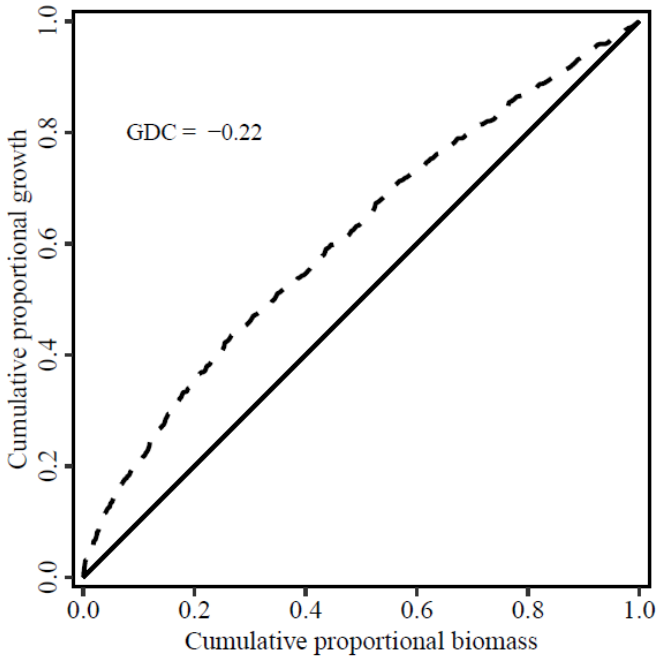

Figure 2.3. Negative growth dominance in an old-growth ponderosa pine stand. Negative growth dominance shows that smaller trees represent a larger proportion of stand growth than stand biomass. The largest trees comprised in the upper 20%-tile of stem mass distribution accounted for about 13% of stand growth while the smallest trees comprised in the lower 20%-tile of stem mass distribution contributed 35% of stand growth. This larger proportional growth in small trees corresponded with size-growth relationships where growth increased with tree size but less than of equal proportion (see Fig. 2.4.A and Table 2.2).

Table 2.2. Production ecology parameters for dominant, intermediate and suppressed trees in an old-growth ponderosa pine stand. Dominant trees were almost 5 times larger than suppressed trees and captured nearly 4 times more light but grew only slightly more than 2 times faster than suppressed trees (a result of a declining light use efficiency with tree size).

Tree class[a]	Average size (kg tree^{-1})	Average growth (kg year^{-1} tree^{-1})	Average light interception (GJ year^{-1} tree^{-1})	Average Light use efficiency (kg[wood] GJ[PAR]$^{-1}$)
Dominant	1024 (817-1548)	4.3 (0-9.2)	90.4 (62.5-132.9)	0.05 (0-0.11)
Intermediate	604 (473-807)	3.3 (0-23.1)	53.4 (20.4-82.1)	0.06 (0-0.36)
Suppressed	211 (11-473)	1.9 (0-12.4)	20.9 (1.5-56.3)	0.11 (0-0.78)
Dominant vs. suppressed	4.8	2.3	4.3	0.5

[a] suppressed trees: trees comprised in the lower 40% tile of the stem biomass distribution (n = 449), intermediate trees: trees comprised between the 40% tile and the 80% tile of the stem biomass distribution (n = 146), dominant trees: trees comprised in the upper 20% tile of the stem biomass distribution (n = 48). In parenthesis are the minimum and maximum values for each variable.

Light interception by individual trees

Mean light interception across all trees was 33.4 GJ year^{-1} tree^{-1} (range = 1.5 – 132.9 GJ year^{-1} tree^{-1}). Similar to tree productivity, the amount of light intercepted by trees increased with tree size but less than proportionally (Fig. 2.4). On average, dominant trees captured more than 4 times as much light as suppressed trees (90.4 *vs*. 20.9 GJ year^{-1} tree^{-1}) but they were 5 times larger than suppressed trees (Table 2.2). The relationship between light interception and tree size was best described by a linear model with a positive intercept. The linear model explained almost 95% of the variation present in light interception by trees and had a Δ_i of 49 units with the linear model with a zero intercept (a = 0) and 686 with the exponential model (Table 2.3). The pattern of light interception with tree rank was best characterized by a positive exponential function (Table 2.3). The median dominant tree in the subplot, approximately a 96th percentile tree,

intercepted 2.9 times more than the median suppress tree, approximately a 35th percentile tree (Fig. 2.4).

Light use efficiency of trees

Light use efficiency for stem wood production averaged 0.09 kg[wood] GJ[PAR]$^{-1}$ across all trees (range = 0 – 0.78 kg[wood] GJ[PAR]$^{-1}$), decreasing with tree size (Fig. 2.4). Light use efficiency of dominant trees was half the efficiency of suppressed trees (0.05 *vs*. 0.11 kg[wood] GJ[PAR]$^{-1}$) (Table 2.2). The light use efficiency pattern with tree size was best described by a negative exponential model (Table 2.3). The exponential model explained about 10% of the variation in light use efficiency and the AIC difference with the power model and linear model were 5 and 10 units, respectively (Table 2.3). Because of the relatively low variation explained by the tested models, we explored other models such as logarithmic, hyperbolic, rational and generalized additive models. All of the models confirmed the same declining pattern in light use efficiency and the exponential model resulted in the best AIC value (the maximum Δ_i was 1.9; data not shown). The pattern of light use efficiency with tree rank was described equally well by a negative exponential model or a negative linear model (Table 2.3).

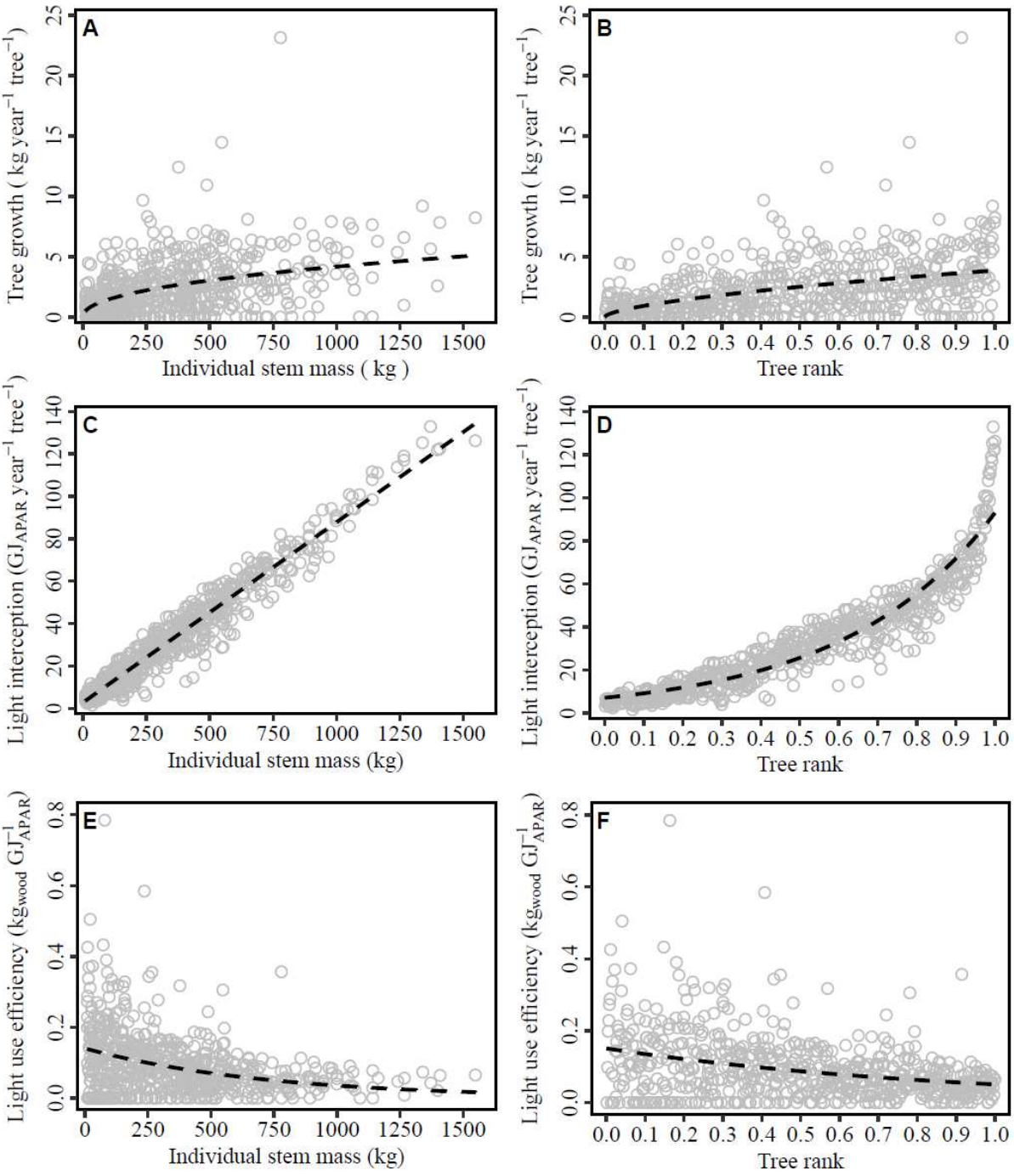

Figure 2.4. Growth pattern as a function of tree size (A) or tree rank (B) can be combined with light interception (C, D) and light use efficiency patterns (E, F) to explain growth dynamics. Growth increased with tree size but less than proportional as the result of a less than proportional light interception increase with tree size and a declining light use efficiency pattern. The less than proportional increase in growth with tree size results in a negative growth dominance in the stand (see Fig. 2.3). Dashed lines correspond to the best fit model representing each relationship (see Table 2.3). Light interception points are the output from MAESTRA simulations. Light use efficiency was estimated as growth/light interception.

Table 2.3. Regressions between tree growth *vs.* tree size, tree light interception *vs.* tree size, and tree light use efficiency *vs.* tree size. Tree growth and tree light interception increased with tree size but less than proportional. In contrast, light use efficiency decreased with tree size. Patterns where the *y*-variable increased with the *x*-variable but less than proportional, were best described by concave models and linear models with a positive intercept. Patterns where the *y*-variable decreased with the *x*-variable are best described by a negative linear or negative exponential model. Unless noted otherwise, model parameters were significant (p-value < 0.001). Number of observations $n = 643$.

	Models for tree size (kg)				Models for tree rank (percentile)			
Model	Param		*AIC*	R^2	Param		*AIC*	R^2
	a	*b*			*a*	*b*		
Growth (kg year^{-1} tree^{-1})								
Linear (a = 0)	-----	0.0054	2798	0.07	-----	-----	-----	-----
Linear	1.194	0.0033	2717	0.18	0.761	3.2690	2717	0.18
Power	0.176	0.4586	2713	0.19	3.853	0.6232	2721	0.18
Exponential	1.586	0.0011	2730	0.17	1.141	1.3416	2720	0.18
Light interception (GJ[APAR] tree^{-1} year^{-1})								
Linear (a = 0)	-----	0.0897	4162	0.94	-----	-----	-----	-----
Linear	2.768	0.0850	4113	0.94	-5.617	77.993	4829	0.83
Power	0.130	0.9429	4142	0.94	82.561	1.5710	4649	0.87
Exponential	17.65	0.0016	4799	0.84	7.062	2.5771	4450	0.90
Light use efficiency (kg[wood] GJ[APAR]$^{-1}$)								
Linear	0.126	-0.0001	-1384	0.10	0.142	-0.0100	-1393	0.11
Power	0.338	-0.2450	-1389	0.11	0.074	-0.1959	-1369	0.08
Exponential	0.140	-0.0014	-1394	0.11	0.151	-1.0907	-1393	0.11

R^2 is the coefficient of determination estimated as $R^2 = (sst - sse)/sst$ where *sst* is the total sum of squares and *sse* is the error sum of squares.

Discussion

Previous studies in ponderosa pine stands suggest that growth dominance ranges from negative to zero (Biondi 1996, Fernández and Gyenge 2009, Ex and Smith 2013, McGown et al. 2016). The old-growth ponderosa pine stand analyzed here showed a strong negative growth dominance (growth dominance coefficient: -0.22), similar to the -0.25 growth dominance coefficient estimated for the stand during the previous decade (Binkley et al. 2006). Growth dominance of a stand expresses patterns of tree growth as a function of tree size (the so called size-growth relationship) (Pothier 2017, Fernández-Tschieder and Binkley 2018) and these

patterns are defined by competitive interactions among individual trees (Weiner and Damgaard 2006, Pretzsch and Biber 2010). Consequently, the interaction between resource competition and size-related differences in resource use efficiency across trees account for differences in the degree of growth dominance (Fernández-Tschieder and Binkley 2018).

Growth of ponderosa pine trees increased monotonically with trees size, but in accordance with negative growth dominance, the difference in growth between larger and smaller trees was less than the difference in tree sizes (Fig. 2.4. A and Table 2.2). This growth pattern, defined as partial size-symmetric competition (Pretzsch and Biber 2010), was described by a concave power function with a *b* parameter between 0 and 1 (Table 2.1 and Table 2.3). A similar concave size-growth relationship was found in the same stand during the previous decade (Boyden and Binkley 2016). The increase in growth with tree size has been well documented (Stephenson et al. 2014), however the specific shape of the size-growth relationship can vary among species, age, management and environmental conditions (Metsaranta and Lieffers 2010, Pretzsch and Dieler 2011, Castagneri et al. 2012, Trouvé et al. 2014, Dye et al. 2019). A few studies suggest that species with negative growth dominance showed either concave size-growth relationships or positive intercepts in linear size-growth relationships (Binkley et al. 2006, Binkley and Kashian 2015, Macinnis-Ng et al. 2017, Pothier 2017). On the contrary, species with positive growth dominance showed convex size-growth curves or negative intercepts in linear size-growth relationships (Campoe et al. 2013b, Pothier 2017). However, the degree of growth dominance not only depends on the size-growth relationships but also on the size distribution of the stand (Forrester 2019).

In this old-growth ponderosa pine stand, negative growth dominance was supported by an increasing light interception with tree size, but it was less than proportional (Fig. 2.4. C and

Table 2.2). This pattern, defined as partial size-symmetric competition (Schwinning and Weiner 1998), was described by a linear model with positive intercept (Table 2.1 and Table 2.3). Similar to our findings, Forrester (2019) found a strong positive correlation between growth dominance and the partitioning of light (i.e. the mode of competition) in some species (*Picea abies*, *Fagus sylvatica*, *Abies alba*, *Larix decidua* and *L. kaempferi*) in central Europe and one eucalyptus species in Australia. This implies that growth dominance changes from negative to positive as competition moves from partial size-symmetric to asymmetric competition. However, other species either lacked (*Pinus sylvestris*) or showed a weak correlation (*Pseudotsuga menziesii*) (Forrester 2019) suggesting that the effect of light competition on the degree of growth dominance might be species-specific. Other studies analyzed the relationship between light interception and trees size. For example, large loblolly pine trees captured proportionally less light than small trees (a concave model to describe this pattern using tree rank as the independent variable) (Campoe et al. 2013a) suggesting negative or low growth dominance. Contrary, large eucalyptus and Norway spruce (*Picea abies*) trees captured a disproportionate amount of light relative to their wood biomass or leaf area (size asymmetric competition) suggesting positive growth dominance (Binkley et al. 2010, Campoe et al. 2013b, Gspaltl et al. 2013). Different from the relationship between light interception and tree size, tree light interception across tree rank was supported by a positive exponential model (Table 2.3), showing that light interception increased more than proportionally with tree rank (*see below*).

Our results agree with a positive correlation between growth dominance and size-related differences in resource use efficiency. Light use efficiency followed the expected declining pattern with tree size for stands with negative growth dominance (Table 2.2 and Fig. 2.4. E). The same was true when light use efficiency was analyzed as a function of tree rank (Fig. 2.4. F).

Similar to our results, most lodgepole pine stands with negative growth dominance were associated with greater growth efficiency of small trees relative to large trees (Binkley and Kashian 2015) and growth dominance increased in loblolly pine stands under positive growth dominance as large trees became more efficient relative to small trees (Fernández Tschieder et al. 2012). Forrester (2019) also found a positive correlation between size-related differences in the resource use efficiency between trees and the degree of growth dominance. However, some species showed no trend between the variables. The light use efficiency pattern in ponderosa pine contrasts with most studies carried out with MAESTRA, where light use efficiency increased with tree size (Binkley et al. 2010, Campoe et al. 2013a, 2013b, Gspaltl et al. 2013, le Maire et al. 2013) or was relatively similar among trees (Forrester et al. 2013, le Maire et al. 2013). The exception being juvenile white spruce (*Picea glauca*) trees where light use efficiency showed a slight decline with tree size (Nelson et al. 2016). However, it is not possible to evaluate the correlation between size-related differences in resource use efficiency and growth dominance in these studies.

Contrary to our results, Ex and Smith (2013) found that large trees had about 20% greater growth efficiency (growth/leaf area) than small trees in a stand undergoing negative growth dominance. The growth efficiency approach does not consider shading by neighbors or self-shading. Shading by neighbors can be important when considering light competition (Gspaltl et al. 2013) and have a larger impact on small trees (Binkley et al. 2013). As with light use efficiency dominant trees had lower growth efficiency than suppressed trees, but relative differences based on growth efficiency were smaller than differences based on light use efficiency. On average light use efficiency was 1.5 greater than growth efficiency on dominant trees, and 2.8 times on suppressed trees. Differences in stand structure and spatial distribution of

trees might be part of the reason explaining the different patterns between these two ponderosa stands. Neither study considered the spatial distribution of the trees in the stand, but leaf area index and stand density index were lower in our stand, indicating a lower competition for light between trees and potentially less shading in small trees.

The trend of light interception depended on the explanatory variable: tree size or tree rank. In both cases light interception increased, but when tree size was used as the explanatory variable light interception increased less than proportionally. In contrast, when tree rank was used as the explanatory variable light interception increased more than proportionally. This difference can be explained by the highly hierarchical size structure of the stand (Gini coefficient = 0.43, coefficient of variation = 0.78). High hierarchy in the size structure implies that a large number of trees that are relatively similar size account for a small proportion of biomass and a small number of large trees account for a large proportion of the biomass. When plotted as a percentile in the x-axis, trees are "spread" across the axis as compared to when trees are plotted with size as the x-axis. The spread of the trees in the x-axis implies relatively small changes in light interception among the lower percentiles because changes in tree size are also relatively small. On the contrary, in the upper percentiles changes in light interception are relatively large because changes in tree size are large. For example, an 80th percentile tree is 1.5 times larger than a 60th tree, but the largest tree in the plot is almost three times larger than an 80th percentile tree.

Because of the unidirectional nature of light, competition for light has been defined as asymmetric (Weiner 1990, Onoda et al. 2014). However, the results in this and other studies show symmetric competition. Differences in mode of competition for light among studies can be explained by tree allometry (especially the relationship between leaf area and stem biomass), tree

plasticity (either morphological and/or physiological) and the spatial patterns of competitors (Schwinning and Weiner 1998, Berntson and Wayne 2000). The symmetry or asymmetry notion of competition is conditioned to a "measure of size", on what Schwinning and Weiner (1998) called the "allometry of resource uptake". Depending on which "measure of size" is used, the interpretation of the results can change. For example, Onoda et al. (2014) found a consistent pattern using leaf area and aboveground biomass as measures of size, but Berntson and Wayne (2000) observed that light competition was size asymmetric in relation to leaf area and size symmetric in relation to total plant biomass.

The mechanisms driving the observed decline in light use efficiency with tree size remain elusive. Light use efficiency for stem wood production is the result of the combination of the amount of carbon fixed (gross primary production) per unit of light captured and carbon partitioning. Hydraulic conductance was suggested to limit photosynthesis in large (old) ponderosa pine trees (Ryan and Yoder 1997, Hubbard et al. 1999). Hubbard et al. (1999) found that assimilation ($\mu mol[CO_2]\ m^{-2}$[Leaf area] s^{-1}) was 21% lower for older large ponderosa pine trees as compared to young short trees, despite similar photosynthetic capacity between tree classes. Belowground partitioning remains challenging at the individual tree level. Nevertheless, if this mechanism was involved in the explanation of the declining light use efficiency as a function of tree size, dominant trees should be partitioning a larger amount of carbon to sinks other than stem growth. In this sense, Vanninen and Mäkelä (2005) using a semi-empirical method found that dominant Scots pine trees (*Pinus silvestris*) allocated less carbon to stem growth.

In this study we focused on light and light use efficiency as major drivers of tree growth and patterns of growth dominance. However, water and nutrients are also likely to influence the

pattern of tree growth and therefore growth dominance. Tree growth of ponderosa pine was strongly influenced by nitrogen supply on this same stand (Boyden and Binkley 2016) and by nitrogen efficiency in plantations of ponderosa pine (Gyenge and Fernández 2014). Considering the variation between locations and treatments, a multiple resource use approach (Han et al. 2016) might prove useful in untangling the interactions among the supply of resources and the use efficiency of those resources.

Conclusions

We combined the pattern-focused approach of growth dominance with the process-focused approach of production ecology in an old-growth ponderosa pine stand undergoing a relatively strong negative growth dominance to test the link between growth dominance and production ecology. Light interception of individual trees increased with tree size but less than proportional and light use efficiency declined as a function of tree size. These patterns matched the expected trends in the production ecology for negative growth dominance (Fernández-Tschieder and Binkley 2018) and add evidence to the correlation between growth dominance and production ecology obtained in lodgepole pine (Binkley and Kashian 2015) and conifer and broadleaves in central Europe (Forrester 2019). However, these studies represent too few assessments to establish a strong connection between production ecology and growth dominance patterns.

CHAPTER 3: CONNECTING PRODUCTION ECOLOGY AND GROWTH DOMINANCE ACROSS FOREST TYPES

Introduction

Growth of a stand is the summation of individual tree growth. Within a stand, growth is distributed non-uniformly among trees. Growth dominance quantifies how growth is apportioned between trees in relation to size within a stand (Binkley 2004, Binkley et al. 2006). The distribution of growth across tree sizes varies with species, age, management, the competitive environment and climate (Binkley et al. 2006, Metsaranta and Lieffers 2010, Bradford et al. 2010, Fernández et al. 2011, Trouvé et al. 2014, Soares et al. 2017, 2020). Based on the production ecology of trees, growth distribution across trees would result from the patterns of production ecology among the trees, including resource acquisition, resource use efficiency, and allocation to stem growth (Schwinning and Weiner 1998, Pothier 2017, Fernández-Tschieder and Binkley 2018, Forrester 2019).

The production ecology of trees describes growth as the product of the supply of resources from the environment, the amount of resources captured by trees and the amount of wood produced per unit of resource (resource use efficiency) (Monteith and Moss 1977, Binkley et al. 2004). Within a stand, environmental resources are distributed between individual trees depending on the mode and degree of competition. Competition ranges along a continuum from symmetric -if all trees capture a proportional share of environmental resources- and asymmetric competition -if a group of trees capture a disproportional share of resources (Weiner 1990, Schwinning and Weiner 1998). Studies at the tree level showed that large trees obtained a greater amount of resources and that the amount of wood produced per unit of resource can increase with tree size (Binkley et al. 2002, 2010, Campoe et al. 2013b, 2013a, Otto et al. 2014), be

relatively similar among trees (Forrester et al. 2013, le Maire et al. 2013) or decline (Onoda et al. 2014, Fernández-Tschieder et al. 2020).

How do patterns of competition (symmetric or asymmetric) relate to growth distribution, and how do these interact with resource use efficiency patterns? Forrester (2019) found that growth distribution showed a wide range of relationships with resource partitioning and size-related difference in resource use efficiency in central European forests. In a similar study carried out in an old-growth *Pinus ponderosa* stand, negative growth dominance was associated to a slight size-symmetric competition for light and a greater use efficiency of light by small trees (Fernández-Tschieder et al. 2020).

In this study we explored this question further, using data from a variety of conifer and broadleaf forests around the world. We expected to find a positive correlation between growth dominance, the degree of asymmetric competition and the increasing light use efficiency with tree size. Species with positive growth dominance would show asymmetric competition for light and increasing light use efficiency with tree size. In species with null growth dominance all trees would capture light in proportion to their size and use these resources with similar efficiency. Lastly, species with reverse growth dominance would have a symmetric competition for light but light use efficiency would decrease with tree size.

Methods

Data

We explored data from conifer and deciduous species covering a wide range of ages, sites and management (Table 3.1). All data sets had tree-scale estimates for stem size (biomass or volume), growth, interception of photosynthetically active radiation (APAR) based on the

MAESTRA simulations (Wang and Jarvis 1990, Medlyn 2004) and light use efficiency of wood production (LUE = growth/APAR). Some of the data sets also have information about the leaf area of trees. Specific details of each data set can be found on the original papers (Table 3.1).

Before the analysis, we performed an error checking for each data set. For each plot and age, trees with negative or zero growth value, and extreme values for any of the variables (values larger than 3 times the interquartile range of the data) were removed from the data sets.

Table 3.1. Characteristics of the data sets used to evaluate the link between production ecology and growth dominance.

ID	Source	Species	Location	Management	n	Age (year)[a]	Density (trees ha^{-1})	Trees per plot[b]
1.A	Binkley et al. (2010)	*Eucalyptus grandis* x *urophylla* (hybrid A)	Brazil (4 sites)	Homogeneous & heterogenous stand structures	11	1.4 - 5.5	1100	34
1.B		*Eucalyptus grandis* x *urophylla* (hybrid B)			6	1.4		34
1.C		*Eucalyptus grandis* x *urophylla* (hybrid C)			6	5.5		33
1.D		*Eucalyptus grandis* x *urophylla* (hybrid D)			6	1.4		36
2	Campoe et al. (2012, 2013b)	*Eucalyptus grandis*	Brazil	Productivity gradient	12	6	1600	77
3	Campoe et al. (2013a)	*Pinus taeda*	USA	Fertilization & irrigation	16	8	1200	40

Table 3.1. Continued.

ID	Source	Species	Location	Management	n	Age (year)[a]	Density (trees ha^{-1})	Trees per plot[b]
4	Fernández-Tschieder et al. (2020)	*Pinus ponderosa*	USA	Unmanaged uneven-aged forest	1	----	400	643
5	Forrester et al. (2013)[c]	*Eucalyptus nitens*	Australia	Thinning & fertilization	12	3.4 - 8.1	1000	39
6	Gspaltl et al. (2013)	*Picea abies*	Austria	Thinning & age classes	8	38 - 128	----	230
7	le Maire et al. (2013)[d]	*Acacia mangium*	Brazil	None	3	1 - 6	1100	34
8		*Eucalyptus grandis*	Brazil	Fertilization	6	1 - 6	1100	35

n = number of plots included in this study, [a] age indicates the range of age for each data set, [b] trees per plot is the mean number of trees in each plot included in this study, [c] data set included 4 remeasurements of plots, [d] data set included 5 remeasurements of plots. Density corresponds to an approximation of the density that would correspond with the planted tree distance.

Growth distribution, resource competition and resource use efficiency asymmetry

We quantified the distribution of growth, light interception, and light use efficiency in relation to tree sizes within plots. The distributions were condensed into coefficients, analogous to the Gini coefficient, but ranging between -1 and 1.

Growth distribution was assessed using the growth dominance coefficients (D_{GROWTH}) following West (2014). The growth dominance coefficient quantifies both the degree of growth distribution (the absolute value of the coefficient) and whether larger trees (positive growth dominance), smaller trees (negative growth dominance) or any tree (nil dominance) in the stand

are producing a disproportional amount of growth with respect to their share of the stand biomass.

Resource distribution was assessed the same way, but with light interception rather than stem growth. Light interception was estimated using the MAESTRA. The light dominance coefficient (D_{LIGHT}) was estimated with stem biomass or volume of trees as the size variable for all data sets and with leaf area of trees as the size variable for 5 of the data sets. A negative light dominance coefficient indicates that small trees intercept light more than proportional to their size, and positive light dominance indicates that large trees intercept light more than proportional to their size. Nil light dominance coefficient indicates that all trees acquire light proportional to the proportion they represent of stand biomass or leaf area. Negative values correspond to the concept partial size-symmetric (capture of contested resources increases with tree size but less than proportionally), nil values correspond to the concept of symmetric competition (capture of contested resources is proportional to size), and positive values to the concept of partial size asymmetric competition (capture of contested resources increases with size and dominant trees obtain a disproportionate share of resources) (Schwinning and Weiner 1998).

To assess difference in light use efficiency (LUE = growth/light interception) between trees we estimated a coefficient similar to growth dominance and light use dominance coefficients. We assessed the size-related differences in light use efficiency between trees using a modified formula of the growth dominance coefficient (West 2014). We replaced the cumulative proportional size in (the x-axis in the graphical description of growth dominance) by the cumulative proportion of trees. Then we estimated a dominance of light use efficiency (D_{LUE}) that indicated if light use efficiency increases with tree size ($0 > D_{LUE} \leq 1$), is the same for all trees ($D_{LUE} = 0$) or decreases with tree size ($-1 \leq D_{LUE} < 0$).

Statistical analysis

We performed our analysis at two levels: within and across species. Within species, we analyzed for each data set described in Table 3.1 how growth dominance (D_{GROWTH}) varied with light competition (D_{LIGHT}) and size-related differences in light use efficiency (D_{LUE}) using regression analysis. Sample size for each species corresponded to the number of plots included in this study (Table 3.1). The data sets used in this study had different experimental designs. Based on the experimental design of each data set, we used linear regression or linear mixed-effects models to fit regressions. For mixed-effects models we used age nested within plot, as the random effect. Multiple regressions were fitted using the *lm* function and mixed-effects models were fitted using *lme* function (Pinheiro et al. 2019) in R (R Core Team 2018).

For the analysis across species, we used the mean value of growth dominance, light competition, and size-related differences in light use efficiency of each species to fit the regression between growth dominance, light competition and size-related differences in light use efficiency. Sample size for this analysis was n = 11. We used the bootstrap technique to estimate the mean and the 95% confidence interval ($CI_{95\%}$) for each species.

Within and across species, we compared models including both D_{LIGHT} and D_{LUE} as predictor variables or only one of them using Akaike's information criterion (AIC). Akaike's information criterion was estimated as AIC = $2p$ - 2 ln $L(\hat{\theta})$, where $L(\hat{\theta})$ is the likelihood of the estimated model, p is the total number of parameters that were estimated in the model. For regression fit with ordinary least squares AIC was corrected by n-(p+1))/n, where n is the sample size and p is the number of parameters in the model (Burnham and Anderson 1998).

Results

Across all data points (study x species x treatment x age x plot, n = 159) growth dominance averaged 0.01 and ranged between -0.22 and 0.23 (Fig. 3.1). The maximum D_{GROWTH} was observed in a plot corresponding to *E. grandis* (data set #2), whereas the minimum D_{GROWTH} corresponded to *P. ponderosa* (data set #4).

Mean growth dominance of across species (n = 11) averaged -0.01 ($CI_{95\%}$: -0.05, 0.04) and ranged between -0.22 for *P. ponderosa* (single plot) and 0.15 ($CI_{95\%}$: 0.13, 0.18) for *E. grandis* in the data set #2 (Table 3.2). Overall D_{GROWTH} was relatively close to zero for all data sets, except for *E. grandis* (data set #2) and *E. grandis* x *urophylla* (hybrid A, data set #1.A) that showed some degree of positive growth dominance, and for *P. ponderosa* that showed a relatively strong negative growth dominance (Fig. 3.1 and Table 3.2).

Growth dominance (D_{GROWTH}) related strongly with light partitioning (D_{LIGHT}) and differences in light use efficiency between trees (D_{LUE}) (Fig. 3.2). Across species and within each species, D_{GROWTH} increased with D_{LIGHT} and D_{LUE} (Table 3.2, Fig. 3.2). D_{LIGHT} and D_{LUE} together explained approximately 90% of the variability in D_{GROWTH} (Table 3.2). For *E. grandis* x *urophylla* hybrid D, D_{GROWTH} did not show a relationship with D_{LIGHT} or D_{LUE}, and for hybrid C D_{LIGHT} was unrelated to D_{GROWTH} (Table 3.2). Within each data set, age and treatments did not modify the relationship of D_{GROWTH} with D_{LIGHT} and D_{LUE} except for hybrid A (Table 3.2).

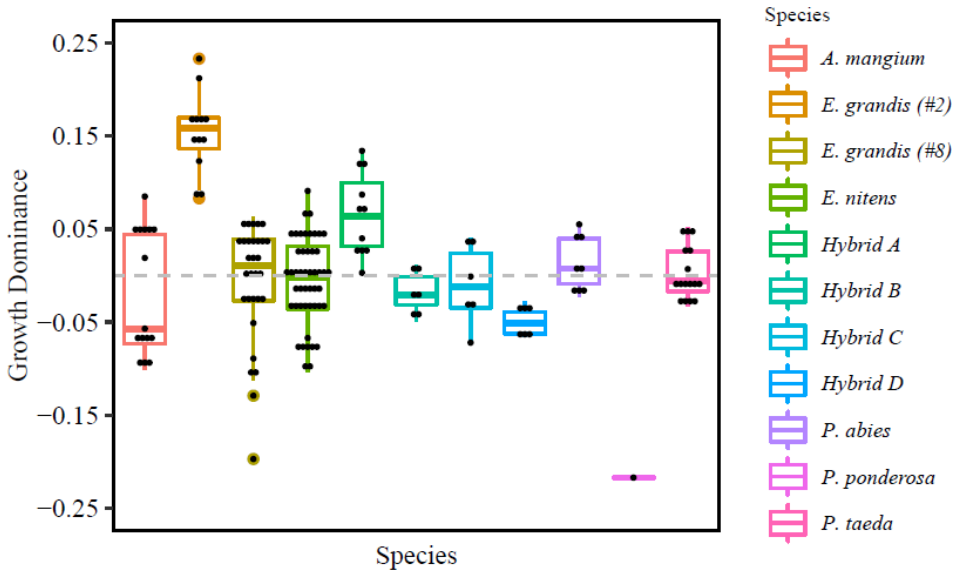

Figure 3.1. Distribution of growth dominance across species. Growth dominance within species ranged approximately between -0.05 negative growth dominance and 0.05 positive growth dominance except for *E. grandis* from data set #2 and one hybrid of *E. grandis* x *urophylla* (hybrid A) that showed a positive growth dominance, and *P. ponderosa* that showed a strong negative growth dominance. Numbers between parenthesis in the legend indicate the data set identification on Table 3.1. Grey dashed line indicates null growth dominance. Each box shows the median (horizontal line), first and third quartile (hinges), maximin and minimum values (vertical lines) and outliers (point beyond vertical lines) of growth dominance for each species.

To evaluate the influence of the point with strong positive D_{GROWTH} (*E. grandis*) and the point with strong negative D_{GROWTH} (*P. ponderosa*) we fit the same model without these two points. The general pattern of the model fit without the two extreme points (n = 9) was similar to the pattern including all points (n = 11).

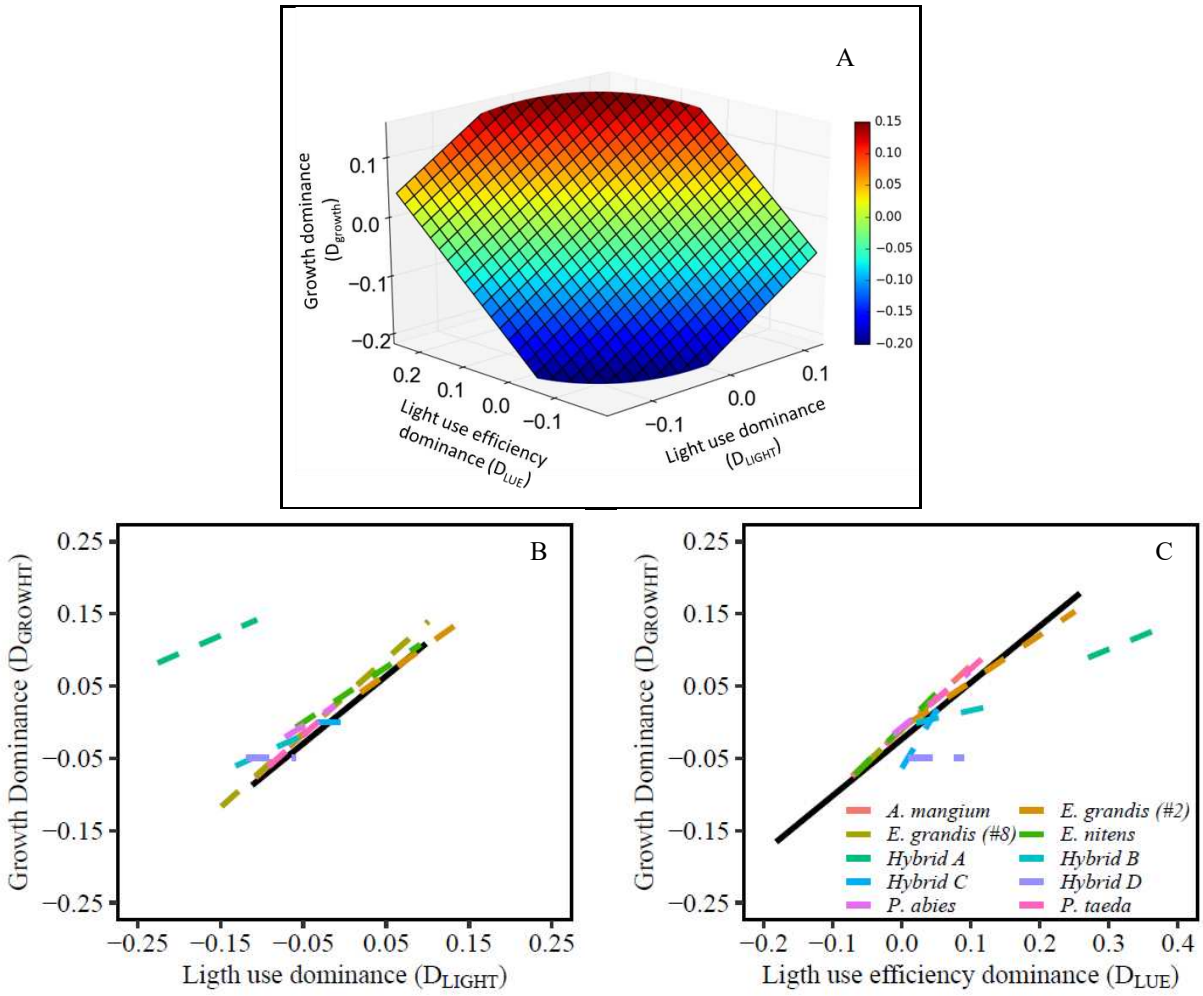

Figure 3.2. Growth dominance (D_{GROWHT}) increased as the result of both light dominance (D_{LIGHT}) and increasing size-related differences in light use efficiency with trees size (D_{LUE}) (A). Plots B and C show the patterns for individual species; the solid black line is the overall average across species. Plots B and C used species-specific models in Table 3.2 and mean values of D_{LUE} for each species for lines in plot B and mean values of D_{LIGHT} for each species for lines in plot C. Negative values of D_{LIGHT} indicates that small trees are intercepting light more than proportional to their size, whereas positive values of D_{LIGHT} indicates that large trees are intercepting light more than proportional to their size. Similarly, negative values of D_{LUE} indicates that light use efficiency decrease with tree size, whereas positive values indicates that light use efficiency increase with tree size. See Table 3.1 for characteristics of each species.

Table 3.2. Coefficients and statistics of the regressions of growth dominance (D_{GROWTH}) as a function of light competition (D_{LIGHT}) and size-related difference in light use efficiency between trees (D_{LUE}). Within species and across species growth dominance of large trees increased with asymmetric competition and with increasing difference in light use efficiency with tree size. Fitted model correspond to the form $D_{GROWTH} = a + b \times D_{LIGHT} + c \times D_{LUE} + d \times age + e \times treatment$. Values in parenthesis are the 95% confidence interval for the mean of D_{GROWTH} estimated using the bootstrap technic.

ID	Species	D_{GROWTH}	Coefficients					R^2	rse	df
			a	b	c	d	e			
	Across species	-0.01 (-0.05, 0.04)	-0.0141	0.9336	0.7818	---	---	0.97	0.02	8
1.A	Hybrid A (*E. grandis* x *urophylla)*[a]	0.07 (0.04, 0.09)	-0.0308	0.4990	0.3913	0.0604	0.0414	0.94	0.02	6
1.B	Hybrid B (*E. grandis* x *urophylla)*	-0.02 (-0.03, -0.00)	ns	0.5239	0.2141	---	ns	0.94	0.01	4
1.C	Hybrid C (*E. grandis* x *urophylla)*	-0.01 (-0.04, 0.02)	-0.0635	ns	1.5871	---	ns	0.84	0.02	4
1.D	Hybrid D (*E. grandis* x *urophylla)*	-0.05 (-0.06, -0.04)	-0.0495	ns	ns	---	ns	---	0.02	5
2	*E. grandis*	0.15 (0.13, 0.18)	ns	0.8129	0.6432	---	---	0.98	0.03	10
3	*P. taeda**	0.00 (-0.01, 0.02)	ns	1.0300	0.8425	---	ns	---	---	11
4	*P. ponderosa*	-0.22	---	---	---	---	---	---	---	---
5	*E. nitens**	-0.01 (-0.02, 0.01)	ns	0.7634	0.9493	ns	ns	---	---	35
6	*P. abies*	0.01 (-0.01, 0.03)	ns	0.7203	0.7777	---	ns	0.93	0.01	6
7	*A. mangium**	-0.02 (-0.05, 0.01)	ns	1.0368	0.8897	ns	---	---	---	11
8	*E. grandis**	-0.01 (-0.03, 0.02)	ns	1.0252	0.9023	ns	ns	---	---	23

ID refers to the identification of each data set on Table 3.1, R^2 = coefficient of determination ($R^2 = (sst - sse)/sst$ where sst is the total sum of squares and sse is the error sum of squares); rse = residual standard error ($rse = \sqrt{sse/df}$); df = residual degree of freedom. *Regressions fit with

mixed-effects models. [a] where age is 0 for the reference level of age 1.4 and 1 for level of age 5.5, and treatment is 0 for the reference level of heterogenous structure and 1 for uniform structure. ns = no significant with a probability alpha of 0.05.

Discussion

According to the production ecology of trees, patterns of growth dominance within stands should be driven by the combined effect of competition for resources and size-related differences in resource use efficiency between trees in the stand (Schwinning and Weiner 1998, Pothier 2017, Fernández-Tschieder and Binkley 2018, Forrester 2019). Resource use efficiency results from either greater photosynthetic efficiency (carbon fixed per unit of resource used) or greater carbon partitioning of carbon to wood growth. Our results showed that light competition and size-related difference in light use efficiency strongly correlated with the variation in growth dominance, and that growth dominance increase with increasing competition for light and increasing light use efficiency with tree size. Forrester (2019) analyzed the relationship between growth dominance and light competition, and growth dominance and sized-related difference in light use efficiency separately for central European forests. Most species showed a strong positive correlation for both variables; however, some species showed a low or no correlation with either competition for light or sized-related difference in light use efficiency.

For most species, we observed that small trees captured a greater proportion of light relative to their size. We used stem mass or volume as the measure of tree size, however, using leaf area as the measure of size to estimate competition can modify this pattern (Berntson and Wayne 2000, Onoda et al. 2014). Using leaf area as the size variable might indicate that large trees capture a greater proportion of light relative to size if light interception of trees is relatively proportional to leaf area, and the loss of light interception due to shading by neighbors is greater for small trees (Binkley et al. 2013). However, the estimation of competition using stem mass

and the estimation of competition using leaf area as the measure of size have been shown to be positively correlated, showing the same pattern with growth dominance (Onoda et al. 2014, Forrester 2019). This suggested that the overall pattern found in our analysis is unlikely to change using tree leaf area as the measure of size.

The pattern between growth dominance and light use efficiency of trees could emerge because both variables have growth as their numerator. We explored whether autocorrelation could explain the pattern between growth dominance and light use efficiency of trees. For this purpose, we compared a "null pattern" explained by autocorrelation with the "current pattern" between the variables. The "null pattern" was defined as growth/mean size (mean of size of all trees in a plot) as a function of growth/mean APAR (mean of APAR of all trees in a plot). If the "current pattern" matches the "null pattern" autocorrelation could be the responsible of the pattern between growth dominance and light use efficiency. If both patterns differ substantially, then autocorrelation is at most responsible for only part of the correlation between variables. We found that for most plots the "current pattern" differed from the "null patten" showing that light use efficiency explained some of the variation in the growth dominance pattern.

Most of the forests we examined showed values closed to null growth dominance. Only two data sets of eucalyptus showed a relatively strong positive growth dominance, and the data set of *P. ponderosa* showed a strong negative growth dominance. This contrast particularly with the strong positive growth dominance above 0.4 reported for a 11 years old seed-origin stand of *E. saligna* (Binkley et al. 2003, 2006). However, Soares et al. (2020) analyzed monoclonal plots of a variety of eucalyptus clones and sites up to five years old and found that growth dominance varied mostly between -0.1 and 0.1. Greater or lower values of growth dominance were rather unusual (Soares et al. 2020). Similarly to previous studies, conifers showed low-positive to high-

negative growth dominance (Fernández and Gyenge 2009, Bradford et al. 2010, Fernández Tschieder et al. 2012, e.g. Binkley and Kashian 2015). Since growth dominance can increases with age (Binkley et al. 2006, Fernández Tschieder et al. 2012, Soares et al. 2020), low growth dominance in some broadleaf species could be partially explained by young ages included in these species. For example, *A. mangium* showed an increase of growth dominance with age. However, some of the eucalyptus plots with low growth dominance had their canopy was fully closed, and tree interaction should be well stablished.

Growth dominance combined with size distributions functions is important to understand and predict the response of stand growth to changes in stand structure or management practices (Forrester 2019). For example, Soares et al. (2020) found that stand growth decreases with negative and positive growth dominance (i.e. stand growth was greater with null growth dominance). This pattern was related to the bell-shaped distributions of tree diameter in eucalyptus mono-clonal plantations (Soares et al. 2020). In this paper we showed that changes in growth dominance were related to changes in light competition and changes in the pattern of light use efficiency with tree size. The information about the patterns of light competition and light use efficiency provided by growth dominance could be helpful to plan management interventions. However, the outcome of these intervention depends on the size distribution of the stand (Forrester 2019). For example, in a stand undergoing negative growth dominance improving the growing conditions of small trees might or might not increase stand productivity. If size distribution of a stand is right side skewed, releasing resources for small trees (the most efficient) by thinning large trees might increase stand productivity. On the contrary, if size distribution is left side skewed thinning large trees might decrease productivity because the proportion of small trees is low compare with the proportion of large trees. The increase in

resource supply for small trees might not be sufficient to offset the productivity loss of thinned trees.

Overall, we found that the growth distribution between trees within a stand reflects the patterns of competition for light and the pattern of light use efficiency between trees. Growth dominance increased as large trees intercepted an increasingly disproportional amount of light and as larger trees increased their light use efficiency compare with small trees. Differences in light use efficiency suggest that carbon partitioning or photosynthetic capacity changes among trees of different size. Despite the diversity of species included in our study, growth dominance was close to zero and relatively similar between species with a few exceptions. However, when growth dominance deviated from null growth dominance it was correlated with competition for light and differences in light use efficiency among trees. Growth dominance showed to be an effective link between processes at the tree scale (competition and resource use efficiency) and processes at the stand scale (growth distribution).

CHAPTER 4: A METHOD TO ESTIMATE GROSS PRIMARY PRODUCTION AT THE TREE LEVEL: DO DOMINANT EUCALYPTUS TREES PARTITION LESS CARBON BELOWGROUND?

Introduction

Wood productivity of individual trees depends on the supply of resources in the environment, the proportion of these resources captured by trees and how efficiently these resources are used to produce wood (Monteith and Moss 1977, Binkley et al. 2004). Within tree populations, wood productivity of trees increases with tree size (Stephenson et al. 2014) as a result of positive feedbacks between increasing size and resource capture. In some *Eucalyptus* plantations, large trees also have greater efficiency of wood production per unit of resource use (Binkley et al. 2002, 2010, Campoe et al. 2013b, Otto et al. 2014). Large trees can have as much as 1.8-times greater light use efficiency than small trees (Binkley et al. 2010). Higher wood growth per unit of resource use could result from either greater photosynthetic efficiency (carbon fixed per unit of light intercepted) or greater carbon partitioning of carbon to wood production.

Differences in photosynthetic efficiency of leaves would likely be too small to account for large differences in wood growth per unit of resource use. Photosynthetic capacity of dominant *Eucalyptus globulus* trees was greater than suppressed trees (O'Grady et al. 2008); however, greater photosynthetic capacity of dominant trees reflected acclimation to the improved light environment (Field 1983). However, no systematic differences in the photosynthetic capacity between size class of trees were observed because dominant and suppressed trees shared the same the relationship between height and saturated photosynthesis (O'Grady et al. 2008). Because light interception increases with tree height and trees intercept light proportional to tree

leaf area (Binkley et al. 2013, Campoe et al. 2013b), photosynthetic efficiency is expected to be similar between dominant and suppressed trees.

We expect that greater wood production per unit of resource use results primarily from differences in carbon partitioning between trees. Aboveground production is easy to measure, but belowground production on an individual-tree basis has not been feasible under field conditions. Belowground production by individual trees could be estimated from whole-tree photosynthesis, minus aboveground production and respiration. Hu et al. (2010b) proposed a method to estimate individual-tree gross primary production combining tree transpiration and integrated water use efficiency derived from carbon stable isotope in soluble sugars from leaves. This approach can be modified using carbon isotopes in phloem sap as an integration of the whole canopy (Rascher et al. 2010, Ubierna and Marshall 2011). The analysis of carbon isotopes in phloem sap (Pate and Arthur 1998) has been proposed is an integrative $\delta^{13}C$ signal of the short-term (in the scale of days) influence of environmental conditions over the whole plant canopy activity (Keitel et al. 2003, Gessler et al. 2004).

We explored the applicability of using carbon isotopic composition of phloem contents and canopy transpiration to estimate photosynthetic carbon flux of individual eucalyptus trees. By subtracting aboveground production and respiration, we tested the hypothesis that belowground partitioning for an individual tree decreased with increasing tree size in Eucalyptus plantations.

Methods

Study site and experiment description

Our study was conducted in a eucalyptus experiment on a tropical site located near Mogi Guaçu at an altitude of 633 m (SP, Brazil) (Lat −22.35 Long −46.97) on an Oxisol soil (Binkley et al. 2017). This experiment corresponded to site #20 in a larger project on the influence of climate, silviculture, and genetics on productivity (TECHS Project, Clonal Eucalyptus Tolerance to the Hydrous and Thermal Stresses, Binkley et al. 2020). For this study, we used a relatively drought tolerant *E. grandis* × *E. camaldulensis* hybrid clone, in treatments with and without rain reduction (Table 4.1). The rain reduction treatment removed 30% of rain, with the under-canopy troughs installed for the final four years of the six-year rotation. The experiment was planted on 16-February-2012 in a single plot of 0.2 ha at 3 × 3 m spacing. Rain reduction treatment was applied to half of the plot (rainfed subplot and rain reduction subplot). Plot was fertilized intensively during the first year to alleviate any nutrient limitation and weeds were controlled. Our analysis spanned an 18-months period from age 53 to 71 months.

We selected nine trees representing the diameter distribution from each sub-plot for carbon isotope analysis of stem phloem sap, sap flow density and growth measurements (Table 4.1). Three trees were selected from small (suppressed), medium (intermediate) and large (dominant) size classes in each plot, giving a total of 18 trees for the study.

Meteorological data was obtained from an automatic weather station located in the study site and meteorological variables were measured hourly. During our study period (July 2016-January 2018) mean annual temperature averaged 22.1°C, precipitation 1193 mm $year^{-1}$, relative humidity 70%, and vapor pressure deficit during daylight hours, 1.4 kPa. These meteorological

conditions were similar to the environmental characteristics for the entire period of the rotation (Binkley et al. 2020).

Table 4.1. Biometric characteristics (mean ± standard deviation) of plots and individual trees sampled from each treatment for phloem sap. Wood mass includes stem wood + bark + branch. Stem dry matter represented 89% of wood dry matter, stem bark 9% and branches 2%. Plot mean and standard deviation were based on approximately 80 trees.

		Plot level					Sample of trees		
Rain treatment	Age (month)	dbh (cm)	Height (m)	Basal area (m^2 ha^{-1})	Wood mass (Mg ha^{-1})	LAI	n	dbh (cm)	Height (m)
control	51	14.3 (1.5)	22.3 (1.3)	18	77	1.3 (0.2)	9	14.6 (2.3)	21.9 (1.3)
reduction	51	13.7 (1.2)	20.9 (1.1)	17	68	1.3 (0.2)	9	14.0 (1.8)	20.7 (1.3)

dbh = tree diameter at 1.3-m height, LAI = leaf area index corresponds to the mean LAI between ages 52 and 73 months old, n = number of trees sampled for carbon isotope, transpiration, and growth.

Phloem sap sampling and carbon isotope analysis

Samples of phloem sap were extracted following the phloem exudation technique (Schneider et al. 1996, Rennenberg et al. 1996) in pure distilled water (Gessler et al. 2004, Devaux et al. 2009). This method simply consists in the extraction of soluble sugars by osmosis in distilled water from phloem samples. Each tree was sampled at four dates between July 2016 and January 2018 (18-July-2016, 9 & 10-November-2016, 17-April-2017 and 19-January-2018). On each date two discs (phloem + bark) from every tree were extracted at approximately 1.3 m above ground from the main stem using a 10 mm diameter cork-borer. Samples were washed with distilled water and the set of two phloem discs placed in vials with 4 mL of distilled water for a minimum of 4-5 hours at ambient temperature (Schneider et al. 1996, Devaux et al. 2009). Discs were removed, and the sample solution dried at 65°C and stored at -28°C for transport to the laboratory. Samples were collected within the same day, or on two consecutive days for

November 2016 sampling. Samples were rehydrated and filtered in the laboratory. Aliquots of the solution were placed in tin cups, dried at 65°C, packed and processed for determination of carbon isotopic composition of phloem sap ($\delta^{13}C_{ph}$) at the EcoCore Analytical Facility laboratory (Natural Resource Ecology Laboratory, Colorado State University, USA). The $\delta^{13}C_{ph}$ values were expressed in delta notation (‰ units) relative to the Vienna Pee Dee Belemnite (VPDB).

Estimation of integrated water use efficiency

We estimated the average crown integrated water use efficiency for each of *i* trees ($^{c}iwue_i$) across the four sampling dates using $\delta^{13}C$ of sap phloem as an integration of the tree crowns ($\delta^{13}C_{ph}$). Integrated water use efficiency is defined as the molar ratio of net CO_2 assimilation rate to transpiration, and was estimated with the leaf-level formulation (Farquhar and Richards 1984, Farquhar et al. 1989) adapted for canopy averages as:

$$^{c}iwue_{id} = {}^{c}A:{}^{c}E = Ca\ (1-{}^{c}Ci/Ca)/1.6\ VPD_d,$$

where $^{c}iwue_{id}$ is the integrated water use efficiency for tree *i* at date *d* (μmol CO_2 μmol H_2O^{-1}), ^{c}A is the net carbon assimilation rate of tree crown (μmol CO_2 m^{-2} s^{-1}), ^{c}E is the transpiration rate of tree crown (μmol H_2O m^{-2} s^{-1}), ^{c}Ci is the tree crown photosynthesis-weighted average of partial pressure of CO_2 in leaf intercellular spaces, Ca is the partial pressure of CO_2 in the atmosphere (kPa), 1.6 is the ratio of the diffusivities of water vapor and CO_2 in air, and VPD_d is the water vapor pressure difference between the intercellular spaces of the leaf and the well-mixed atmosphere outside the leaf at date *d* (kPa). Previous studies have shown that $\delta^{13}C$ of stem phloem sap or needle sugars was highly correlated with weather dynamics during the few days before sample collection (Pate and Arthur 1998, Keitel et al. 2003, Gessler et al. 2004, Hu et al. 2010a). VPD was the average for four days prior to each phloem sap sampling, expecting that $\delta^{13}C$ of stem phloem sap was the integration of the tree crown over the prior four days. Weather

was generally consistent for the days before each sampling period. We used a Ca value of 0.041 kPa (406 ppm) corresponding to the average CO_2 concentration between 2016 and 2018 at Mauna Loa, Hawaii (Dlugokencky et al. 2019).

The average crown integrated water use efficiency for each of *i* trees was estimated as:

$^{c}iwue_i = {}^{c}iwue_{id} / 4$.

The tree crown average ratio between intercellular to atmospheric partial pressure of CO_2 ($^{c}Ci:{}^{C}Ca$) was estimated using a linear model (Farquhar et al. 1982b) that relates isotopic discrimination against ^{13}C linearly to the ratio of intercellular to atmospheric concentration:

$^{c}Ci:Ca = ({}^{c}\Delta - a)/(b-a)$,

where $^{c}\Delta$ is the tree crown average discrimination against ^{13}C during photosynthesis, *a* (4.4 ‰) is the ^{13}C fractionation caused by diffusion of CO_2 in air; and *b* (27 ‰) is the ^{13}C fractionation during carboxylation by ribulose 1·5-bisphosphate carboxylase/oxygenase (Rubisco) (Farquhar et al. 1982a).

Assuming that $\delta^{13}C$ of stem phloem sap contents integrates the recent activity of the entire tree crown, crown average discrimination during photosynthesis ($^{c}\Delta$) was calculated as (Farquhar et al. 1982b):

$^{c}\Delta = \delta^{13}C_a - \delta^{13}C_{ph} / 1 + \delta^{13}C_{ph}/1000$,

where $\delta^{13}C_a$ is the carbon isotopic composition of the ambient air and $\delta^{13}C_{ph}$ is the carbon isotopic composition of stem phloem sap contents. We used a $\delta^{13}C_a$ value of -8.4 ‰ corresponding to the average isotopic composition of the air for the year 2014, the last available record at Mauna Loa Observatory (White et al. 2015).

Water vapor pressure difference between the intercellular spaces of the leaf and the atmosphere

Integrated mean daily leaf-to-air water pressure deficit (VPD_{day}) was estimated as the average between hourly VPD (VPD_{hour}) using hours of the day with solar radiation greater than zero. The VPD_{hour} was estimated as the difference between the water vapor pressure in the intercellular spaces of the leaf (e_{leaf}) and water vapor pressure in the atmosphere (e_{atmos}). Water vapor pressure in the intercellular spaces of the leaf was estimated as the saturation partial pressure of water vapor (e_s) (where $e_{leaf} = e_s$) as a function of temperature of the air (T_{air}) using the equation:

e_s (kPa) = (6.1121 * exp (17.368 * T_{air} /(238.88 + T_{air}))) * f *0.1,

where T_{air} is the mean hourly temperature of the air (°C) estimated from the maximum and minimum temperature, *f* is an enhancement factor to account for small differences between pure water and moist air f = 1.0007 + (3.46*10^-6 * P) where P is the atmospheric pressure in mb (Buck 1981). The value 0.1 was used to convert mb in the original equation to kPa.

Water vapor pressure in the atmosphere (e_{atmos}) was estimated using daily average relative humidity (RH, estimated from the maximum and minimum hourly relative humidity) and saturation vapor pressure (e_s) for four days prior to each phloem sap sampling as:

$e_{atmos} = e_s * RH/100$.

Leaf temperature was assumed to match air temperature, with a constant temperature profile with crown depth. These assumptions are expected in a canopy well-coupled with the atmosphere, which is likely in Eucalyptus plantations for wind speeds of > 2.5 m s^{-1} (Barnard and Ryan 2003).

Estimation of tree transpiration

Sap flux density (v, g cm^{-2} s^{-1}) was measured on each tree between 18-July-2016 and 19-January-2018 using the Granier style heat dissipation method (Granier 1987) as described in Hubbard et al. (2010, 2020). Briefly, a single pair of 2-cm long thermal dissipation probes were installed in a randomly selected cardinal direction for each tree approximately 10 cm above breast height. Sensors were moved every three months to account for the variation in sap velocity with circumference and to prevent over-growth on probes. Temperature differences between the upper and lower needle were measured every minute and 15-minute averages recorded. Sap flux density was estimated using a modified Granier equation calibrated for Eucalyptus plantations (Hubbard et al. 2010) and tree transpiration as the product of sap flux density and sapwood area. Sapwood area was estimated using a regression model between diameter at the probe location and sapwood area developed from harvested trees (n = 9 trees for each plot) at the end of the study. For specific details on estimation of tree transpiration see Hubbard et al. (2020). Transpiration for each tree (E, L H_20 day^{-1} $tree^{-1}$) was estimated as the average of daily transpiration between 18-July-2016 and 19-January-2018. This long-term average of transpiration tended to underestimate transpiration compared to short-term average (using between 1 and 7 days prior to each phloem sampling date) by about 10%. However, the underestimation was similar for all trees irrespective of tree size and did not, therefore, would not modify the patterns we found. To reduce the effect of nighttime transpiration that leaves no isotopic trace, we only used transpiration measurements during day light hours (solar radiation values > 0).

Estimation of tree fluxes and carbon partitioning

Tree gross primary productivity (GPP, g C $tree^{-1}$ day^{-1}) was estimated as product of average integrated water use efficiency ($^{c}iwue_{i,}$ g C L H_2O^{-1}) and average daily transpiration (E, L H_20 $tree^{-1}$ day^{-1}). Wood (stem + branch + bark) net primary productivity (NPP_{wood}, g C $tree^{-1}$ day^{-1}) was calculated as the difference between wood dry matter at time *t* (18-July-2016) and time *t+1* (19-January-2018) divided by the number of days between *t* and *t+1* (551 days). Dry mass of wood was estimated from dbh of each tree at the beginning and at the end of the study period using allometric equations (Table 4.2). Water use efficiency of wood production was estimated as the ratio between NPP_{wood} and transpiration ($WUE_{wood} = NPP_{wood} / E$, g C /L H_2O).

Leaf net primary production of trees (NPP_{leaf}, g C $tree^{-1}$ day^{-1}) was estimated from leaf production in each sub-plot. First, we estimated leaf production of each sub-plot as leaf litterfall (kg C $year^{-1}$ $plot^{-1}$) plus changes in the stock of leaf between *t* and *t+1* (kg C $year^{-1}$ $plot^{-1}$). Then we broke down the sub-plot leaf production to an individual tree basis using the proportion of the sub-plot leaf area carried by each tree at *t+1* NPP_{leaf} = plot leaf productivity times the proportion of leaf aera of tree *i*. A tree that carried 5% of the plot's leaf mass would be assigned 5% of the plot's leaf production. This approach to estimate leaf production of each tree assumed that leaf lifespan of all trees was similar. Litterfall of leaves was collected monthly in 9 traps in the control sub-plot. We assumed that litterfall for the rain reduction treatment was similar to the control treatment since leaf area index (LAI) was very similar between treatments during the studied period (Table 4.1).We used a carbon content for leaf litterfall of 0.48 g g^{-1} (Stape et al. 2008). The proportion of plot's leaf area carried by each tree (tree leaf area/plot leaf area) was estimated at the end of the studied period. Leaf area of each tree was estimated using allometric equations with dbh as the independent variable (Table 4.2). Plot leaf area was computed by

summing the estimated leaf area of all trees within each plot. Change in the stock of leaf was estimated from LAI values at time *t* and time *t+1* and specific leaf area specific leaf area for each clone (9.4 m^2/kg) at 72 months of age. LAI was estimated from interception of photosynthetically active radiation following Mattos et al. (2020). We used this approach because the relationship between tree size and leaf area or biomass is affected by age (le Maire et al. 2019) and because after canopy closure litterfall is a large component of leaf production (Stape et al. 2008, Ryan et al. 2010, Epron et al. 2012). Destructive sampling of trees was carried out at the end of the rotation. Since the ratio leaf area:dbh decreased with age, using leaf area model fitted with data at the end of the rotation would likely underestimate leaf area at younger ages.

Leaf respiration of trees (R_f, gC $tree^{-1}$ day^{-1}) was estimated as R_f = tree leaf area x 0.66 μmol C $m^{-2}_{leaf\ area}$ s^{-1} at 20 °C x temperature correction (Ryan et al. 2009, 2010). Leaf area of trees was estimated using the mean LAI between age 52 and 73-months for each plot and the proportion of the plot leaf area carried by each tree at age 72-months. We assumed that the proportion of plot leaf area carried by each tree was constant through the study period. Foliar respiration was adjusted by mean temperature at night between *t* and *t+1* using a Q_{10} of 2. Wood respiration of trees (R_w, g C $tree^{-1}$ day^{-1}) was estimated as R_w = (0.7163 - 0.0579 x age (month) / 12) x (NPP_{wood}, gC $tree^{-1}$ day^{-1})) x temperature correction (Ryan et al. 2009, 2010). Wood respiration was estimated as the average between respiration at age 53-months (*t*) and 71-months (*t+1*). Wood respiration was corrected for mean temperature between *t* and *t+1* using a Q_{10} value of 2. Aboveground respiration (R_a, g C $tree^{-1}$ day^{-1}) was estimated as the sum between R_f and R_w. Total belowground carbon fluxes (TBCF) were estimated as the difference between gross

primary productivity of trees and aboveground fluxes (aboveground net primary production + aboveground respiration).

Mass estimation

Dry mass (kg) of wood (stem + bark + branch dry mass) and leaf area was estimated using the allometric model $\ln(W_i) = a + \ln(dbh) \times b$ where W_i is the wood dry mass (kg) or leaf area (m^2) of tree *i*, dbh is tree diameter at 1.3-m height, and *a* and *b* are the intercept and slope parameters to be estimated. We tested for differences in intercepts and slopes between rainfall treatments. We selected the minimum adequate model using Akaike's information criterion (AIC), analysis of variance between models (model A *vs*. model B, where model A included one term for different intercepts and one term for different slopes and the significance of the terms in the model (we used a significance level of $\alpha = 0.05$) (Table 4.2). Selected models were tested for normality, homogeneity of variance and error distribution. Regressions were fitted using ordinary least squares with *lm* function in R (R Core Team 2018). We used the correction factor proposed by Baskerville (1972) to account for the bias introduced during the back-transformation from logarithmic to arithmetic units.

Nine trees representing the diameter distribution of each treatment were selected for destructive sampling at 72 months of age (Table 4.2). Trees were harvested and divided into stem wood, stem bark, branch, and foliage compartments. Each tree was weighed in the field and representative subsamples of each compartment were collected for water content determination (dried at 65 °C until constant weight) to calculate dry matter. The crown of each tree was divided in lower, mid and upper crown, and a subsample of leaves from each third was used to determine specific leaf area ($m^2\ kg^{-1}$). Leaf area of trees was estimated as the sum of the product of leaf dry mass and specific leaf area of each third of the crowns. Leaf area of two trees (11.9 and 12.6 cm

in dbh) were excluded from model fitting. These trees had extremely high or low dry mass values for the size and were highly influential on parameters estimation.

We used a carbon concentration value of 0.451 g g^{-1} (n = 6; sd = 0.022) to convert wood mass to C mass and 0.503 g g^{-1} to convert leaves mass to C mass (n = 4; sd = 0.004) (Giardina et al. 2003, Stape et al. 2008, Campoe et al. 2012, Epron et al. 2012). Wood carbon concentration value represents the average among carbon concentration for stem wood, branch wood and bark.

Table 4.2. Coefficients and statistics of wood dry mass (kg) and leaf area (m^2) allometric equations for eucalyptus trees. Fitted model correspond to the form ln (dry mass, kg) = *a* + ln (dbh, cm) x *b*. Wood dry mass equation has a common slope and clone-specific intercept. Leaf area equation has a clone-specific slope and a clone-treatment-specific intercept.

Compartment	Rain treatment	coef a	coef b	R^2	rse	df	CF	dbh range (cm)
Wood (kg)	control	-2.736	2.614	0.99	0.06	33	0.002	11.8-18.7
	reduction							
Leaf area (m^2)	control	-3.631	2.036	0.87	0.30	29	0.046	11.9-18.7
	reduction	-3.250						11.8-16.7

R^2 = coefficient of determination (R^2 = (sst − sse)/sst where *sst* is the total sum of squares and *sse* is the error sum of squares); rse = residual standard error (rse = $\sqrt{sse}$/df); df = residual degree of freedom; CF = correction factor following Baskerville (1972). Control treatment refers to rainfed treatment and reduction treatment refers to rain reduction of about 30%.

Statistical analysis

Simple linear regressions were used to examine patterns of water use efficiency of wood production (WUE_{wood}), crown integrated water use efficiency ($^{c}iwue_i$), fluxes (wood net primary production, leaf net primary production, aboveground respiration and gross primary production) and carbon partitioning with tree size. Carbon partitioning was defined as the fraction of gross primary productivity allocated to a given flux (Litton et al. 2007). Wood mass (kg $tree^{-1}$) at the beginning of the studied period was used as the measure of tree size. For most variables, rainfall reduction did not have any effect on the slope or intercept of the regressions of fluxes or efficiencies with tree size. For simplicity, we pooled data from control and rainfall reduction

treatments. Models were tested for normality and homogeneity of variance. Regressions were fitted using ordinary least squares with *lm* function in R (R Core Team 2018).

To compare between dominant and suppressed trees we used the mean tree size (wood mass = stem + bark + branch dry mass) of dominant and suppressed trees (n = 6 for each size class) and models fitted for each variable. Mean size of suppressed trees and dominant trees was 42 and 94 kg $tree^{-1}$ respectively. Wood mass was estimated using the equations in Table 4.2.

Results

Isotopic composition of phloem sap ($\delta^{13}C_{ph}$) averaged 28.0 ‰ (sd = 0.42‰, n = 18) and increased (became less negative) with tree size and rainfall reduction (Table 4.3). Accordingly, crown discrimination during photosynthesis ($^{c}\Delta$) decreased with tree size.

Aboveground net primary production ($ANPP = NPP_{wood} + NPP_{leaf}$) and aboveground respiration (Ra) increased with tree size (Fig 4.1. A, B, C). Dominant trees produced approximately 2.2-times as much wood as suppressed trees (10.8 vs. 4.8 gC $tree^{-1}$ day^{-1}) and 1.8-times as much foliage as suppressed trees (9.9 vs. 5.5 gC $tree^{-1}$ day^{-1}). Dominant trees respired aboveground 2.2-times as much carbon as suppressed trees (10.2 vs. 4.6 gC $tree^{-1}$ day^{-1}).

Wood productivity increased with tree size as the result of both increasing transpiration (E) and water use efficiency for wood production (WUE_{wood}) (Fig. 4.1. F, G). Dominant trees transpired 1.2-times as much water as suppressed trees (12.9 vs. 11.1 L H_2O $tree^{-1}$ day^{-1}) and produced 2.3-times as much wood per unit of water transpired as suppressed trees (0.87 vs. 0.38 gC LH_2O^{-1}). WUE_{wood} correlated positively with integrated water use efficiency of the crown ($^{c}iwue_i$) (one tailed Pearson correlation coefficient $r = 0.44$, p-value = 0.03) and carbon partitioning to wood production ($r = 0.99$, p-value < 0.001).

Gross primary production (GPP) of individual trees increased with tree size as the result of increasing transpiration and water use efficiency of trees crown ($^{c}iwue_i$) with tree size (Fig. 4.1. E, F, H). Dominant trees fixed 1.3-times as much carbon as suppressed trees (44.6 vs. 33.7 gC $tree^{-1}$ day^{-1}) and their canopies fixed 1.1-times as much carbon per unit of water transpired as suppressed trees (3.4 vs. 3.0 gC LH_2O^{-1}).

Total belowground carbon fluxes of trees (TBCF) -estimated subtracting aboveground net primary production and aboveground respiration from GPP- did not vary with tree size (Fig 4.1. D). Belowground carbon flux of dominant trees was 90% of the belowground productivity of suppressed trees (16.3 vs. 18.3 gC $tree^{-1}$ day^{-1}). Tree size explained around 2% of the variation in TBCF (Table 4.3) and the slope of the relationship was not different from zero (p-value = 0.54).

Carbon partitioning to aboveground fluxes increased with tree size (Fig. 4.1. I, J, K). In contrast, belowground carbon partitioning decreased with tree size (Fig. 4.1. L). Dominant trees partitioned 2.2-times as much carbon to wood production (0.26 vs. 0.12), 1.4-times to leaf production (0.23 vs. 0.16) and 1.6-times to aboveground respiration (0.23 vs. 0.14) as suppressed trees, respectively. Belowground carbon partitioning for dominant trees was 60% of that by suppressed trees (0.34 vs. 0.55).

Table 4.3. Regressions models used to describe the production ecology patterns with tree size in eucalyptus plots with and without rainfall reduction. The model corresponds to the form y = *a* + *b* x tree size (kg).

	Coefficients				
Variable	a	b	R^2	rse	df
$\delta^{13}C_{ph}$	-28.9735	0.0136	0.60	0.27	16
NPP_{wood}	ns	0.1141	0.9	2.78	17
NPP_{leaf}	1.9873	0.0844	0.93	0.58	16
Ra	ns	0.1082	0.97	1.51	17
TBCF[a]	19.9133	-0.0385	0.03	5.69	15
Transpiration	9.5387	0.0359	0.25	1.51	16
WUE_{wood}	ns	0.0092	0.9	0.23	17
GPP	24.9228	0.2089	0.39	6.36	16
[c]$iwue_i$	2.7147	0.0078	0.66	0.13	16
NPP_{wood}:GPP	ns	0.0028	0.89	0.07	17
NPP_{leaf}:GPP	0.1124	0.0012	0.55	0.03	16
Ra:GPP	0.0654	0.0018	0.49	0.04	16
TBCF:GPP[a]	0.73	-0.0042	0.46	0.11	15

R^2 = coefficient of determination (R^2 = (sst − sse)/sst where *sst* is the total sum of squares and *sse* is the error sum of squares); rse = residual standard error (rse = √*sse*/df); df = residual degree of freedom. ns = no significant with a probability alpha = 0.05. [a]one tree with negative TBCF estimation was not considered for model fitting.

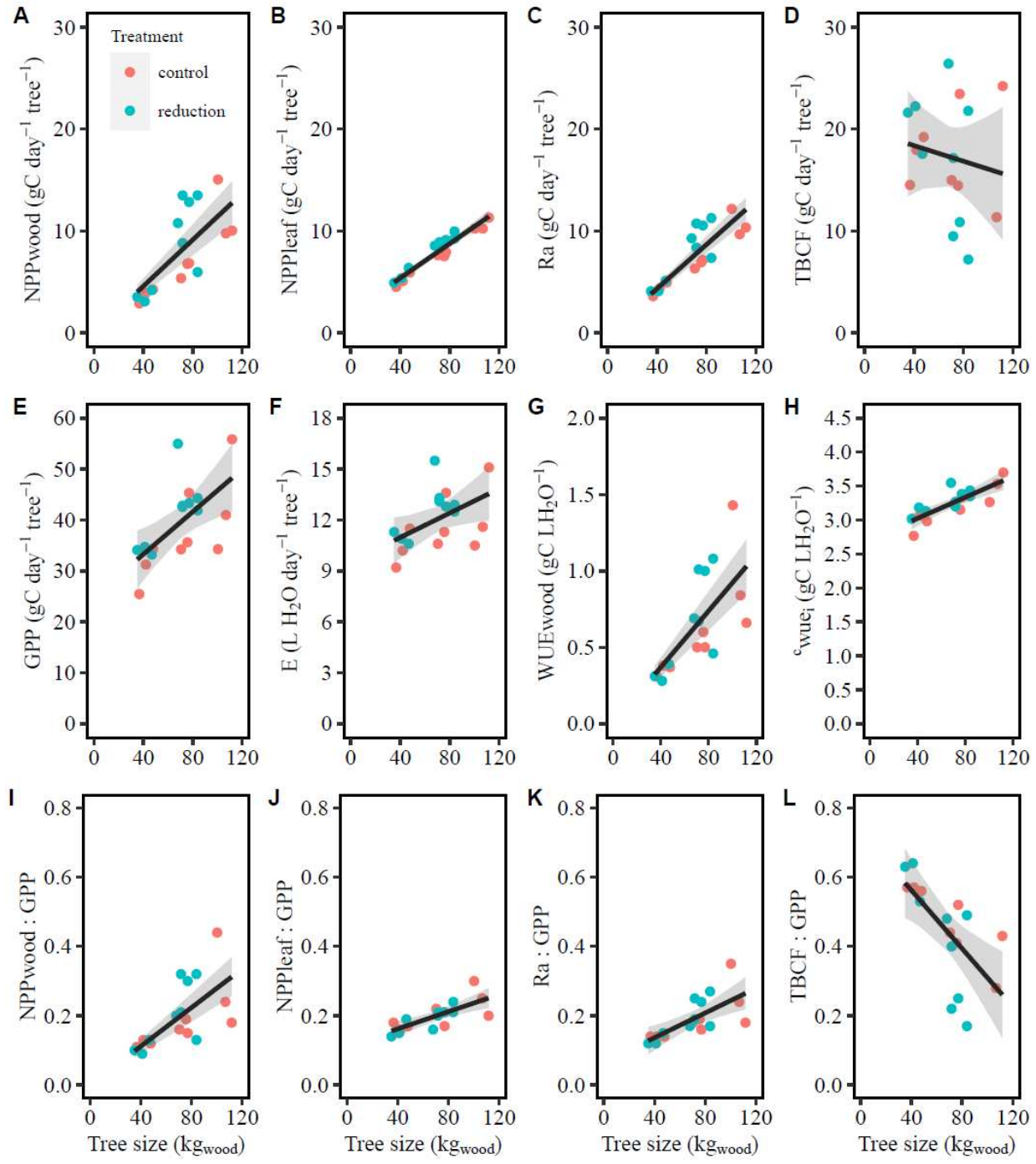

Figure 4.1. Aboveground fluxes (NPP_{wood}, NPP_{leaf} and Ra) increased with tree size and belowground fluxes (TBCF) were relatively similar between trees. Similarly, transpiration (E), water use efficiency (WUE_{wood} and $^{c}wue_i$) and aboveground carbon partitioning all increased with tree size. In contrast, belowground carbon partitioning decreased with tree size in eucalyptus experimental plots. Solid lines represent least squares regressions as described in Table 4.3. Grey shaded areas reflect 95% confidence interval.

Discussion

Production ecology and carbon partitioning

As observed in previous studies about the production ecology of eucalyptus trees, wood productivity of trees increased with tree size as the result of a greater transpiration and higher water use efficiency of large trees (Binkley et al. 2002, Otto et al. 2014). A similar pattern has been observed for light interception and light use efficiency in eucalyptus and pine plantations (Binkley et al. 2002, 2010, Campoe et al. 2013b). However, other studies showed no trend in light use efficiency with tree size in eucalyptus (Forrester et al. 2013, le Maire et al. 2013). Higher transpiration of large trees is explained by the positive correlation between leaf area of trees and transpiration (Hatton and Wu 1995, Vertessy et al. 1995). Changes in water use efficiency to produce wood can be explained by changes in the integrated water use efficiency of tree crowns (the amount of carbon fixed during photosynthesis per unit of water transpired) and by the amount of carbon partitioned to wood production by trees.

Water use efficiency to produce wood was strongly correlated with both the integrated water use efficiency of tree crowns and the carbon partitioned to wood production. However, the increasing integrated water use efficiency of tree crowns was likely too small to account for differences in wood production per unit of water use. Water use efficiency for wood production between dominant and suppressed trees was about 2.3-times that in suppressed trees, whereas integrated water use efficiency for dominant trees was only about 1.1-times. Results from *E. globulus* trees also suggested that photosynthetic efficiency might be relatively similar between trees (O'Grady et al. 2008).

The size of the change in carbon partitioning to wood production between dominant and suppressed trees was similar to that for water use efficiency for wood production. Dominant trees

partitioned 2.2-times more carbon to wood production that suppressed trees. Partitioning for dominant and suppressed trees were similar to the partitioning values in young *E. tereticornis* trees (Drake et al. 2019). Using whole tree chambers, Drake et al. (2019) found that trees partitioned between 0.4 and 0.5 of the carbon fixed during photosynthesis to aboveground net primary production. Dominant and suppressed eucalyptus trees partitioned around 0.5 and 0.3 of to the carbon fixed by photosynthesis to produce aboveground biomass.

In support of our hypothesis, we found that belowground carbon partitioning decreased with tree size. This pattern was the result of increasing gross primary production with tree size and a similar belowground carbon flux between trees. In contrast to our results, Drake et al. (2019) found that belowground carbon flux of trees increased with gross primary production. An analysis of the relationship between belowground carbon flux and gross primary production -Fig. 7.c in Drake et al. (2019)[3]- suggested that belowground carbon partitioning increased with tree gross primary production in ambient temperature treatment but was constant in warming treatment.

A similar belowground carbon flux between trees was an unexpected result. Total belowground carbon flux was estimated by subtracting aboveground production and aboveground respiration from gross primary production. Therefore, any bias in the estimation of gross primary production would affect the estimation of total belowground carbon flux and belowground partitioning.

Similar to Hu et al. (2010b), estimates of gross primary production relied strongly on transpiration. Dominant trees transpired 1.2-times more water than suppressed trees as the result of a slightly greater sap flux density in suppressed trees (6.6 vs. 5.9 g cm^{-2} h^{-1}) but a larger

[3] We used the R package metaDigitise (Pick et al. 2019) to extract and analyze the pattern of belowground carbon partitioning.

sapwood area of dominant trees compare to suppressed trees (91.4 vs. 67.7 cm^2). However, dominant trees had almost 2-times more leaf area (10.8 vs. 5.7 m^2 leaf area $tree^{-1}$), and consequently, dominant trees transpired 40% less water per unit of leaf area than suppressed trees (1.2 vs. 1.9 L H_2O m^{-2} leaf area day^{-1}). Since transpiration of individual trees is related to leaf area (Hatton and Wu 1995, Vertessy et al. 1995), the discrepancy between tree leaf area and tree transpiration might indicate that transpiration of dominant trees was underestimated.

Any underestimation of transpiration for large trees would be confounded with an underestimation of gross primary production for dominant trees. If gross primary production was underestimated for large trees total belowground carbon flux and belowground carbon partitioning would be underestimated. Therefore, underestimating transpiration of dominant trees would be confounded with the test of the hypothesis of this study, i.e., increasing water use efficiency for wood production and decreasing belowground carbon partitioning with tree size. A similar analysis would be true if transpiration of suppressed trees was overestimated.

Assuming that transpiration of dominant trees was underestimated, we explored how increasing transpiration of dominant trees would modify the water use efficiency for wood production and belowground carbon partitioning patterns. We simulated three scenarios where transpiration of dominant trees was increased 1.5-, 2- and 2.5- times relative to transpiration of suppressed trees, scenario A, B and C, respectively (Fig. 4.2).

Water use efficiency for wood production of dominant trees was greater than suppressed trees even when transpiration of dominant trees was simulated to be 2.5-times than the transpiration of suppressed trees (Fig. 4.2. A, B and C). Similar to water use efficiency for wood production, growth efficiency of trees (GE = NPP_{wood} / leaf area) increased linearly with tree size (GE = 0.379 + 0.007 x tree size, R^2 = 0.4). On averaged, dominant trees produced 1.6-more

wood per unit of leaf area compared with suppressed trees (1.1 vs 0.7 gC m^{-2} leaf area). In contrast, a simulated transpiration of dominant trees about 2-times greater than the transpiration of suppressed trees, was sufficient to equal belowground partitioning between trees (Fig. 4.2. B). The increase in the partitioning of carbon to belowground fluxes in dominant trees was matched with a decrease of carbon partitioning to leaf production and aboveground respiration.

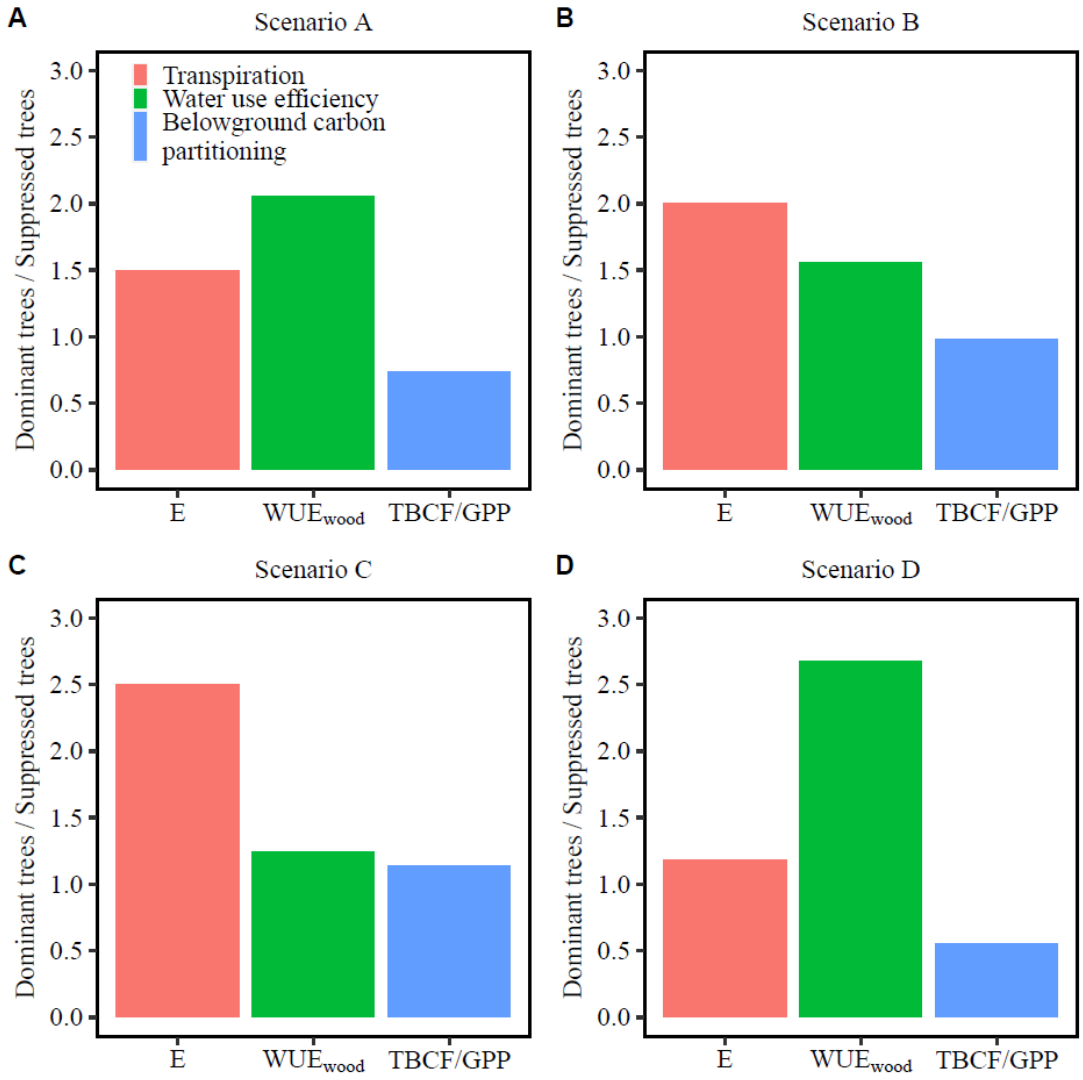

Figure 4.2. Effect of increasing the transpiration of dominant trees on the relative difference in water use efficiency for wood production and belowground carbon partitioning between dominant and suppressed trees. We simulated three different scenarios where transpiration of dominant trees was increased to be 1.5-times greater than the transpiration of suppressed trees

(Scenario A), transpiration of dominant trees was increased to be 2-times greater than the transpiration of suppressed trees (Scenario B), and transpiration of dominant trees was increased to be 2.5-times greater than the transpiration of suppressed trees (Scenario C). Scenario D were the calculations based on the original experimental data (see Fig. 4.1). Relative difference equal to 1 means that dominant and suppressed trees have the same absolute value for the variable.

Conclusion

We used a combination of transpiration and carbon isotopes of phloem sap contents to estimate gross primary production of trees. Together with aboveground net primary production measurements and estimates of respiration (estimated from wood productivity and leaf area), we assessed the hypothesis that greater water use efficiency for wood production in large trees was driven by an increasing partitioning of carbon to wood production and a decreasing partitioning to belowground fluxes with tree size. At the scale of individual trees, carbon partitioning to wood production was an important driver of the differences in water use efficiency for wood production between dominant and suppressed trees. Carbon partitioning to belowground fluxes showed the opposite pattern than partitioning to wood production; it decreased with tree size. However, estimates of belowground partitioning were uncertain because were conditioned to the uncertainty in the estimates of gross primary production and respiration. Gross primary production at the tree scale might have been underestimated in dominant trees as the result of underestimating the transpiration of dominant trees. Underestimating gross primary production had two consequences. First, because belowground fluxes were estimated subtracting aboveground fluxes (net productivity and respiration) from gross primary production, belowground fluxes might have been underestimated in dominant trees. Second, and as a consequence of the former, partitioning to belowground fluxes could have been underestimated for dominant trees. With a simple simulation exercise, we showed that if the relative difference

in transpiration between dominant and suppressed trees were similar to the relative difference in leaf area, belowground carbon partitioning would be similar between trees.

The ratio between photosynthesis and water use (integrated water use efficiency) was only slightly greater in dominant trees, and wood growth per unit leaf area (both well measured) was larger for the dominant trees. These two facts suggested that decreasing belowground partitioning with tree size as being an important driver explaining the greater wood production and higher resource use efficiency of wood production in dominant trees. The method used in this paper has the potential to estimate gross primary production and belowground fluxes at the scale of individual trees. Best results would likely be obtained with an accurate calibration for sap flux for a given site that includes trees of different sizes and social positions to estimate transpiration. We conclude that differences in water use efficiency for wood production between trees were explained by both the amount of carbon fixed per unit of water transpired by tree crowns and by the pattern of carbon partitioning to wood production. However, a robust test of the pattern of belowground carbon partitioning with tree size was not possible because the size effect of belowground partitioning was within the range of the uncertainty of the estimation of transpiration for individual trees.

CONCLUSION

In this dissertation I combined the pattern-focused approach of growth dominance with the process-focused approach of production ecology to test the link between growth dominance with competition and the variation in resource use efficiency between trees. I also explored a method to estimate belowground carbon partitioning of trees by subtracting aboveground productivity and respiration from gross primary production of trees. Gross primary production was estimated from tree transpiration and integrated water use efficiency of tree crowns. With this approach I analyzed whether the resource use efficiency variation observed between large and small trees was related to the variation in photosynthetic efficiency or to the variation in carbon partitioning patterns between trees.

The production ecology equation was a useful approach to decompose growth dominance into competition for resources between trees and into patterns of resource use efficiency with tree size. I proposed specific growth dominance – production ecology patterns that were tested.

Growth dominance reflected the patterns of competition for resources between trees and the patterns of light use efficiency. In a single ponderosa stand undergoing strong growth dominance, small trees showed higher light use efficiency for wood production than large trees. In addition, light interception was size-symmetric; light interception of individual trees increased with tree size but less than proportional. Also, across species growth dominance was positively related with the degree of symmetric-asymmetric competition for light and with the asymmetry in light use efficiency between trees. Growth dominance increased as large trees intercepted an increasingly disproportional amount of light and as larger trees increase their light use efficiency compare with small trees.

Growth dominance was a simple approach to quantify the growth distribution within stands and was an effective link between processes at the tree scale -competition and resource use efficiency- and processes at the stand scale -growth distribution.

At the scale of individual trees, carbon partitioning to wood production was an important driver of the relative differences in water use efficiency for wood production between dominant and suppressed trees. Differences in the amount of carbon fixed per unit of water transpired by tree crowns also explained the pattern in water use efficiency for wood production, but it had a smaller effect. Estimates of belowground partitioning were conditioned to the uncertainty of gross primary production estimation, therefore this pattern could not be tested with confidence.

The combination of transpiration and carbon isotopes of phloem sap contents to estimate gross primary production of trees has potential to calculate belowground fluxes at the scale of individual trees. However, it needs an accurate site- and possible tree class size-specific calibration at the tree level to estimate transpiration.

REFERENCES

Almeida, A. C., J. V Soares, J. J. Landsberg, and G. D. Rezende. 2007. Growth and water balance of Eucalyptus grandis hybrid plantations in Brazil during a rotation for pulp production. Forest Ecology and Management 251:10–21.

Asherin, L. A. 2016. Manitou Experimental Forest hourly meteorology data (2nd Edition). Fort Collins, CO: Forest Service Research Data Archive. Updated 09 February 2018. https://doi.org/10.2737/RDS-2011-0001-2. Fort Collins, CO: Forest Service Research Data Archive. Updated 09 February 2018.

Assmann, E. 1970. The Principles of Forest Yield Study. Pergamon, Oxford.

Attia, A., Y. Nouvellon, S. Cuadra, O. Cabral, J.-P. Laclau, J. Guillemot, O. Campoe, J.-L. Stape, M. Galdos, R. Lamparelli, and G. le Maire. 2019. Modelling carbon and water balance of Eucalyptus plantations at regional scale: Effect of climate, soil and genotypes. Forest Ecology and Management 449:117460.

Barnard, H. R., and M. G. Ryan. 2003. A test of the hydraulic limitation hypothesis in fast-growing Eucalyptus saligna. Plant, Cell & Environment 26:1235–1245.

Baskerville, G. L. 1972. Use of Logarithmic Regression in the Estimation of Plant Biomass. Canadian Journal of Forest Research 2:49–53.

Battie-Laclau, P., J. S. Delgado-Rojas, M. Christina, Y. Nouvellon, J.-P. Bouillet, M. de C. Piccolo, M. Z. Moreira, J. L. de M. Gonçalves, O. Roupsard, and J.-P. Laclau. 2016. Potassium fertilization increases water-use efficiency for stem biomass production without affecting intrinsic water-use efficiency in Eucalyptus grandis plantations. Forest Ecology and Management 364:77–89.

Bendel, R. B., S. S. Higgins, J. E. Teberg, and D. A. Pyke. 1989. Comparison of skewness coefficient, coefficient of variation, and Gini coefficient as inequality measures within populations. Oecologia 78:394–400.

Berntson, G. M., and P. M. Wayne. 2000. Characterizing the size dependence of resource acquisition within crowded plant populations. Ecology 81:1072–1085.

Binkley, D. 2004. A hypothesis about the interaction of tree dominance and stand production through stand development. Forest Ecology and Management 190:265–271.

Binkley, D., O. C. Campoe, C. A. Alvares, R. L. Carneiro, and J. L. Stape. 2020. Variation in whole-rotation yield among Eucalyptus genotypes in response to water and heat stresses: The TECHS project. Forest Ecology and Management 462:117953.

Binkley, D., O. C. Campoe, C. Alvares, R. L. Carneiro, Í. Cegatta, and J. L. Stape. 2017. The interactions of climate, spacing and genetics on clonal Eucalyptus plantations across Brazil and Uruguay. Forest Ecology and Management 405:271–283.

Binkley, D., O. C. Campoe, M. Gspaltl, and D. I. Forrester. 2013. Light absorption and use efficiency in forests: Why patterns differ for trees and stands. Forest Ecology and Management 288:5–13.

Binkley, D., and D. M. Kashian. 2015. Tree-level patterns of lodgepole pine growth and leaf area in Yellowstone National Park: explaining anomalous patterns of growth dominance within stands. Ecosystems 18:251–259.

Binkley, D., D. M. Kashian, S. Boyden, M. W. Kaye, J. B. Bradford, M. A. Arthur, P. J. Fornwalt, and M. G. Ryan. 2006. Patterns of growth dominance in forests of the Rocky Mountains, USA. Forest Ecology and Management 236:193–201.

Binkley, D., R. Senock, S. Bird, and T. G. Cole. 2003. Twenty years of stand development in

pure and mixed stands of *Eucalyptus saligna* and nitrogen-fixing *Facaltaria moluccana*. Forest Ecology and Management 182:93–102.

Binkley, D., J. L. Stape, W. L. Bauerle, and M. G. Ryan. 2010. Explaining growth of individual trees: Light interception and efficiency of light use by Eucalyptus at four sites in Brazil. Forest Ecology and Management 259:1704–1713.

Binkley, D., J. L. Stape, and M. G. Ryan. 2004. Thinking about efficiency of resource use in forests. Forest Ecology and Management 193:5–16.

Binkley, D., J. L. Stape, M. G. Ryan, H. R. Barnard, and J. Fownes. 2002. Age-related decline in forest ecosystem growth: an individual-tree, stand-structure hypothesis. Ecosystems 5:58–67.

Biondi, F. 1996. Decadal-scale dynamics at the Gus Pearson Natural Areas: evidence for inverse (a)symmetric competition? Canadian Journal of Forest Research 26:1397–1406.

Bosc, A., A. De Grandcourt, and D. Loustau. 2003. Variability of stem and branch maintenance respiration in a Pinus pinaster tree. Tree Physiology 23:227–236.

Boyden, S., and D. Binkley. 2016. The effects of soil fertility and scale on competition in ponderosa pine. European Journal of Forest Research 135:153–160.

Boyden, S., D. Binkley, and W. Shepperd. 2005. Spatial and temporal patterns in structure, regeneration, and mortality of an old-growth ponderosa pine forest in the Colorado Front Range. Forest Ecology and Management 219:43–55.

Bradford, J. B., A. W. D'Amato, B. J. Palik, and S. Fraver. 2010. A new method for evaluating forest thinning: growth dominance in managed *Pinus resinosa* stands. Canadian Journal of Forest Research 40:843–849.

Buck, A. L. 1981. New Equations for Computing Vapor Pressure and Enhancement Factor.

Journal of Applied Meteorology 20:1527–1532.

Burnham, K. P., and D. R. Anderson. 1998. Introduction. Page Model Selection and Inference: A Practical Information-Theoretical Approach. Springer-Verlag, New York.

Campoe, O. C., C. A. Alvares, R. L. Carneiro, D. Binkley, M. G. Ryan, R. M. Hubbard, J. Stahl, G. Moreira, L. F. Moraes, and J. L. Stape. 2020. Climate and genotype influences on carbon fluxes and partitioning in Eucalyptus plantations. Forest Ecology and Management 475:118445.

Campoe, O. C., J. L. Stape, T. J. Albaugh, H. Lee Allen, T. R. Fox, R. Rubilar, and D. Binkley. 2013a. Fertilization and irrigation effects on tree level aboveground net primary production, light interception and light use efficiency in a loblolly pine plantation. Forest Ecology and Management 288:43–48.

Campoe, O. C., J. L. Stape, J. P. Laclau, C. Marsden, and Y. Nouvellon. 2012. Stand-level patterns of carbon fluxes and partitioning in a Eucalyptus grandis plantation across a gradient of productivity, in São Paulo State, Brazil. Tree Physiology 32:696–706.

Campoe, O. C., J. L. Stape, Y. Nouvellon, J.-P. Laclau, W. L. Bauerle, D. Binkley, and G. Le Maire. 2013b. Stem production, light absorption and light use efficiency between dominant and non-dominant trees of *Eucalyptus grandis* across a productivity gradient in Brazil. Forest Ecology and Management 288:14–20.

Castagneri, D., P. Nola, P. Cherubini, and R. Motta. 2012. Temporal variability of size–growth relationships in a Norway spruce forest: the influences of stand structure, logging, and climate. Canadian Journal of Forest Research 42:550–560.

Ceriani, L., and P. Verme. 2012. The origins of the Gini index: extracts from Variabilità e Mutabilità (1912) by Corrado Gini. The Journal of Economic Inequality 10:421–443.

Cordonnier, T., and G. Kunstler. 2015. The Gini index brings asymmetric competition to light. Perspectives in Plant Ecology, Evolution and Systematics 17:107–115.

Damgaard, C., and J. Weiner. 2000. Describing inequality in plant size or fecundity. Ecology 81:1139–1142.

Devaux, M., J. Ghashghaie, D. Bert, C. Lambrot, A. Gessler, C. Bathellier, J. Ogee, and D. Loustau. 2009. Carbon stable isotope ratio of phloem sugars in mature pine trees throughout the growing season: comparison of two extraction methods. Rapid Communications in Mass Spectrometry 23:2511–2518.

Dlugokencky, E. J., J. W. Mund, A. M. Crotwell, M. J. Crotwell, and K. W. Thoning. 2019. Atmospheric Carbon Dioxide Dry Air MoleF ractions from the NOAA ESRL Carbon Cycle Cooperative Global Air Sampling Network, 1968-2018, Version: 2019-07. https://doi.org/10.15138/wkgj-f215.

Doi, B. T., D. Binkley, and J. L. Stape. 2010. Does reverse growth dominance develop in old plantations of *Eucalyptus saligna*? Forest Ecology and Management 259:1815–1818.

Drake, J. E., M. G. Tjoelker, M. J. Aspinwall, P. B. Reich, S. Pfautsch, and C. V. M. Barton. 2019. The partitioning of gross primary production for young Eucalyptus tereticornis trees under experimental warming and altered water availability. New Phytologist 222:1298–1312.

Ducey, M. J. 2010. Simplified inference about dominance in forest stands. Forest Ecology and Management 260:1282–1286.

Duursma, R. A., and B. E. Medlyn. 2012. MAESPA: a model to study interactions between water limitation, environmental drivers and vegetation function at tree and stand levels, with an example application to [CO_2] × drought interactions. Geosci. Model Dev. 5:919–940.

Dye, A., M. Ross Alexander, D. Bishop, D. Druckenbrod, N. Pederson, and A. Hessl. 2019. Size–growth asymmetry is not consistently related to productivity across an eastern US temperate forest network. Oecologia 189:515–528.

Edminster, C. B., R. T. Beeson, and G. E. Metcalf. 1980. Volume tables and point-sampling factors for ponderosa pine in the Front Range of Colorado. USDA Forest Service Research Paper 218:1–14.

Epron, D., J.-P. Laclau, J. C. R. Almeida, J. L. M. Gonçalves, S. Ponton, C. R. Sette, J. S. Delgado-Rojas, J.-P. Bouillet, and Y. Nouvellon. 2012. Do changes in carbon allocation account for the growth response to potassium and sodium applications in tropical Eucalyptus plantations? Tree Physiology 32:667–679.

Ex, S. A., and F. W. Smith. 2013. Wood production efficiency and growth dominance in multiaged and even-aged ponderosa pine stands. Forest Science 60:149–156.

Fan, H., M. A. McGuire, and R. O. Teskey. 2017. Effects of stem size on stem respiration and its flux components in yellow-poplar (Liriodendron tulipifera L.) trees. Tree Physiology 37:1536–1545.

Farquhar, G. D., M. C. Ball, S. von Caemmerer, and Z. Roksandic. 1982a. Effect of salinity and humidity on δ13C value of halophytes—Evidence for diffusional isotope fractionation determined by the ratio of intercellular/atmospheric partial pressure of CO2 under different environmental conditions. Oecologia 52:121–124.

Farquhar, G. D., J. R. Ehleringer, and K. T. Hubick. 1989. Carbon Isotope Discrimination and Photosynthesis. Annual Review of Plant Physiology and Plant Molecular Biology 40:503–537.

Farquhar, G. D., M. H. O'Leary, and J. A. Berry. 1982b. On the Relationship Between Carbon

Isotope Discrimination and the Intercellular Carbon Dioxide Concentration in Leaves. Functional Plant Biology 9:121–137.

Farquhar, G. D., and R. A. Richards. 1984. Isotopic Composition of Plant Carbon Correlates With Water-Use Efficiency of Wheat Genotypes. Functional Plant Biology 11:539–552.

Fernández-Tschieder, E., and D. Binkley. 2018. Linking competition with Growth Dominance and production ecology. Forest Ecology and Management 414:99–107.

Fernández-Tschieder, E., D. Binkley, and W. Bauerle. 2020. Production ecology and reverse growth dominance in an old-growth ponderosa pine forest. Forest Ecology and Management 460:117891.

Fernández, M. E., E. Fernández Tschieder, F. Letourneau, and J. E. Gyenge. 2011. Why do Pinus species have different growth dominance patterns than Eucalyptus species? A hypothesis based on differential physiological plasticity. Forest Ecology and Management 261:1061–1068.

Fernández, M. E., and J. Gyenge. 2009. Testing Binkley's hypothesis about the interaction of individual tree water use efficiency and growth efficiency with dominance patterns in open and close canopy stands. Forest Ecology and Management 257:1859–1865.

Fernández Tschieder, E., M. E. Fernández, T. M. Schlichter, M. A. Pinazo, and E. H. Crechi. 2012. Influence of growth dominance and individual tree growth efficiency on *Pinus taeda* stand growth. A contribution to the debate about why stands productivity declines. Forest Ecology and Management 277:116–123.

Field, C. 1983. Allocating leaf nitrogen for the maximization of carbon gain: Leaf age as a control on the allocation program. Oecologia 56:341–347.

Ford, E. D. 1975. Competition and Stand Structure in Some Even-Aged Plant Monocultures.

Journal of Ecology 63:311–333.

Forrester, D. I. 2019. Linking forest growth with stand structure: Tree size inequality, tree growth or resource partitioning and the asymmetry of competition. Forest Ecology and Management 447:139–157.

Forrester, D. I., J. J. Collopy, C. L. Beadle, and T. G. Baker. 2013. Effect of thinning, pruning and nitrogen fertiliser application on light interception and light-use efficiency in a young Eucalyptus nitens plantation. Forest Ecology and Management 288:21–30.

Gessler, A., H. Rennenberg, and C. Keitel. 2004. Stable Isotope Composition of Organic Compounds Transported in the Phloem of European Beech - Evaluation of Different Methods of Phloem Sap Collection and Assessment of Gradients in Carbon Isotope Composition during Leaf-to-Stem Transport. Plant Biology 6:721–729.

Giardina, C. P., M. G. Ryan, D. Binkley, and J. H. Fownes. 2003. Primary production and carbon allocation in relation to nutrient supply in a tropical experimental forest. Global Change Biology 9:1438–1450.

Gini, C. 1912. Variabilità e Mutuabilità. Contributo allo Studio delle Distribuzioni e delle Relazioni Statistiche. C. Cuppini. Bologna.

Gonçalves, J. L. de M., C. A. Alvares, A. R. Higa, L. D. Silva, A. C. Alfenas, J. Stahl, S. F. de B. Ferraz, W. de P. Lima, P. H. S. Brancalion, A. Hubner, J.-P. D. Bouillet, J.-P. Laclau, Y. Nouvellon, and D. Epron. 2013. Integrating genetic and silvicultural strategies to minimize abiotic and biotic constraints in Brazilian eucalypt plantations. Forest Ecology and Management 301:6–27.

Granier, A. 1987. Evaluation of transpiration in a Douglas-fir stand by means of sap flow measurements. Tree Physiology 3:309–320.

Gspaltl, M., W. Bauerle, D. Binkley, and H. Sterba. 2013. Leaf area and light use efficiency patterns of Norway spruce under different thinning regimes and age classes. Forest ecology and management 288:49–59.

Gyenge, J., and M. E. Fernández. 2014. Patterns of resource use efficiency in relation to intra-specific competition, size of the trees and resource availability in ponderosa pine. Forest Ecology and Management 312:231–238.

Han, J., J. Chen, Y. Miao, and S. Wan. 2016. Multiple Resource Use Efficiency (mRUE): A New Concept for Ecosystem Production. Scientific Reports 6:37453.

Hara, T. 1993. Mode of Competition and Size-structure Dynamics in Plant Communities. Plant Species Biology 8:75–84.

Hatton, T. J., and H.-I. Wu. 1995. Scaling theory to extrapolate individual tree water use to stand water use. Hydrological Processes 9:527–540.

Hu, J. I. A., D. J. P. Moore, and R. K. Monson. 2010a. Weather and climate controls over the seasonal carbon isotope dynamics of sugars from subalpine forest trees. Plant, Cell & Environment 33:35–47.

Hu, J., D. J. P. Moore, D. A. Riveros-Iregui, S. P. Burns, and R. K. Monson. 2010b. Modeling whole-tree carbon assimilation rate using observed transpiration rates and needle sugar carbon isotope ratios. New Phytologist 185:1000–1015.

Hubbard, R. M., B. J. Bond, and M. G. Ryan. 1999. Evidence that hydraulic conductance limits photosynthesis in old *Pinus ponderosa* trees. Tree Physiology 19:165–172.

Hubbard, R. M., R. L. Carneiro, O. Campoe, C. A. Alvares, M. A. Figura, and G. G. Moreira. 2020. Contrasting water use of two Eucalyptus clones across a precipitation and temperature gradient in Brazil. Forest Ecology and Management 475:118407.

Hubbard, R. M., J. Stape, M. G. Ryan, A. C. Almeida, and J. Rojas. 2010. Effects of irrigation on water use and water use efficiency in two fast growing Eucalyptus plantations. Forest Ecology and Management 259:1714–1721.

Kashian, D. M., M. G. Turner, W. H. Romme, and C. G. Lorimer. 2005. Variability and convergence in stand structural development on a fire-dominated subalpine landscape. Ecology 86:643–654.

Keitel, C., M. A. Adams, T. Holst, A. Matzarakis, H. Mayer, H. Rennenberg, and A. Gessler. 2003. Carbon and oxygen isotope composition of organic compounds in the phloem sap provides a short-term measure for stomatal conductance of European beech (Fagus sylvatica L.). Plant, Cell & Environment 26:1157–1168.

Keyser, T. L. 2012. Patterns of growth dominance in thinned yellow-poplar stands in the southern Appalachian Mountains, USA. Canadian Journal of Forest Research 42:406–412.

Kim, M. H., K. Nakane, J. T. Lee, H. S. Bang, and Y. E. Na. 2007. Stem/branch maintenance respiration of Japanese red pine stand. Forest Ecology and Management 243:283–290.

Landsberg, J. J., and R. H. Waring. 1997. A generalised model of forest productivity using simplified concepts ofradiation-use efficiency , carbon balance and partltlonlng. Forest Ecology and Management 95:209–228.

Liberloo, M., P. De Angelis, and R. Ceulemans. 2008. Stem CO2 efflux of a Populus nigra stand: effects of elevated CO2, fertilization, and shoot size. Biologia Plantarum 52:299–306.

Litton, C. M., J. W. Raich, and M. G. Ryan. 2007. Carbon allocation in forest ecosystems. Global Change Biology 13:2089–2109.

Lorenz, M. O. 1905. Methods of Measuring the Concentration of Wealth. Publications of the American Statistical Association 9:209–219.

Macinnis-Ng, C., S. V Wyse, T. Webb, D. Taylor, and L. Schwendenmann. 2017. Sustained carbon uptake in a mixed age southern conifer forest. Trees 31:967–980.

le Maire, G., J. Guillemot, O. C. Campoe, J.-L. Stape, J.-P. Laclau, and Y. Nouvellon. 2019. Light absorption, light use efficiency and productivity of 16 contrasted genotypes of several Eucalyptus species along a 6-year rotation in Brazil. Forest Ecology and Management 449:117443.

le Maire, G., Y. Nouvellon, M. Christina, F. J. Ponzoni, J. L. M. Gonçalves, J.-P. Bouillet, and J.-P. Laclau. 2013. Tree and stand light use efficiencies over a full rotation of single- and mixed-species *Eucalyptus grandis* and *Acacia mangium* plantations. Forest Ecology and Management 288:31–42.

Marshall, J. D., and R. A. Monserud. 2003. Foliage height influences specific leaf area of three conifer species. Canadian Journal of Forest Research 33:164–170.

Martin, T. A., and E. J. Jokela. 2004. Developmental patterns and nutrition impact radiation use efficiency components in southern pine stands. Ecological Applications 14:1839–1854.

de Mattos, E. M., D. Binkley, O. C. Campoe, C. A. Alvares, and J. L. Stape. 2020. Variation in canopy structure, leaf area, light interception and light use efficiency among Eucalyptus clones. Forest Ecology and Management 463:118038.

McGown, K. I., K. O'Hara, and A. Youngblood. 2016. Patterns of size variation over time in ponderosa pine stands established at different initial densities. Canadian Journal of Forest Research 46:101–113.

Medlyn, B. E. 2004. A MAESTRO retrospective. Pages 105--121 *in* M. Mencuccini, J. Grace, J. Moncrieff, and K. McNaughton, editors. Forest at the land-atmosphere interface. CABI Publishing, Wallingford, UK.

Metsaranta, J. M., and V. J. Lieffers. 2010. Patterns of inter-annual variation in the size asymmetry of growth in *Pinus banksiana*. Oecologia 163:737–745.

Monteith, J. L., and C. J. Moss. 1977. Climate and the efficiency of crop production in Britain [and Discussion]. Philosophical Transactions of the Royal Society of London. Series B, Biological Sciences 281:277–294.

Nelson, A. S., R. G. Wagner, M. E. Day, I. J. Fernandez, A. R. Weiskittel, and M. R. Saunders. 2016. Light absorption and light-use efficiency of juvenile white spruce trees in natural stands and plantations. Forest Ecology and Management 376:158–165.

O'Grady, A. P., D. Worledge, A. Wilkinson, and M. Battaglia. 2008. Photosynthesis and respiration decline with light intensity in dominant and suppressed Eucalyptus globulus canopies. Functional Plant Biology 35:439–447.

Oliver, C. D., and B. C. Larson. 1990. Forest stand dynamics. Wiley, New York.

Onoda, Y., J. B. Saluñga, K. Akutsu, S. Aiba, T. Yahara, and N. P. R. Anten. 2014. Trade-off between light interception efficiency and light use efficiency: implications for species coexistence in one-sided light competition. Journal of Ecology 102:167–175.

Otto, M. S. G., R. M. Hubbard, D. Binkley, and J. L. Stape. 2014. Dominant clonal Eucalyptus grandis×urophylla trees use water more efficiently. Forest Ecology and Management 328:117–121.

Pate, J., and D. Arthur. 1998. δ13C analysis of phloem sap carbon: novel means of evaluating seasonal water stress and interpreting carbon isotope signatures of foliage and trunk wood of Eucalyptus globulus. Oecologia 117:301–311.

Pick, J. L., S. Nakagawa, and D. W. A. Noble. 2019. Reproducible, flexible and high-throughput data extraction from primary literature: The metaDigitise r package. Methods in Ecology

and Evolution 10:426–431.

Pinheiro, J., D. Bates, S. DebRoy, D. Sarkar, and R Core Team. 2019. nlme: Linear and Nonlinear Mixed Effects Models. R package version 3.1-140. https://cran.r-project.org/package=nlme.

Pommerening, A., B. Brzeziecki, and D. Binkley. 2016. Are long-term changes in plant species composition related to asymmetric growth dominance in the pristine Białowieża Forest? Basic and Applied Ecology 17:408–417.

Pothier, D. 2017. Relationships between patterns of stand growth dominance and tree competition mode for species of various shade tolerances. Forest Ecology and Management 406:155–162.

Pretzsch, H., and P. Biber. 2010. Size-symmetric versus size-asymmetric competition and growth partitioning among trees in forest stands along an ecological gradient in central Europe. Canadian Journal of Forest Research 40:370–384.

Pretzsch, H., and J. Dieler. 2011. The dependency of the size-growth relationship of Norway spruce (*Picea abies* [L.] Karst.) and European beech (*Fagus sylvatica* [L.]) in forest stands on long-term site conditions, drought events, and ozone stress. Trees 25:355–369.

R Core Team. 2018. R: A language and environment for statistical computing. R Foundation for Statistical Computing, Vienna, Austria.

Rascher, K. G., C. Máguas, and C. Werner. 2010. On the use of phloem sap δ13C as an indicator of canopy carbon discrimination. Tree Physiology 30:1499–1514.

Rennenberg, H., S. Schneider, and P. Weber. 1996. Analysis of uptake and allocation of nitrogen and sulphur compounds by trees in the field. Journal of Experimental Botany 47:1491–1498.

Rowland, L., A. C. L. da Costa, A. A. R. Oliveira, R. S. Oliveira, P. L. Bittencourt, P. B. Costa, A. L. Giles, A. I. Sosa, I. Coughlin, J. L. Godlee, S. S. Vasconcelos, J. A. S. Junior, L. V Ferreira, M. Mencuccini, and P. Meir. 2018. Drought stress and tree size determine stem CO2 efflux in a tropical forest. New Phytologist 218:1393–1405.

Ryan, M. G. 1990. Growth and maintenance respiration in stems of Pinus contorta and Picea engelmannii. Canadian Journal of Forest Research 20:48–57.

Ryan, M. G. 1991. A simple method for estimating gross carbon budgets for vegetation in forest ecosystems. Tree physiology 9:255–266.

Ryan, M. G., D. Binkley, and J. H. Fownes. 1997. Age-Related Decline in Forest Productivity: Pattern and Process.

Ryan, M. G., D. Binkley, J. H. Fownes, C. P. Giardina, and R. S. Senock. 2004. An experimental test of the causes of forest growth decline with stand age. Ecological Monographs 74:393–414.

Ryan, M. G., M. A. Cavaleri, A. C. Almeida, R. Penchel, R. S. Senock, and J. Luiz Stape. 2009. Wood CO2 efflux and foliar respiration for Eucalyptus in Hawaii and Brazil. Tree Physiology 29:1213–1222.

Ryan, M. G., J. L. Stape, D. Binkley, S. Fonseca, R. A. Loos, E. N. Takahashi, C. R. Silva, S. R. Silva, R. E. Hakamada, J. M. Ferreira, A. M. N. Lima, J. L. Gava, F. P. Leite, H. B. Andrade, J. M. Alves, and G. G. C. Silva. 2010. Factors controlling Eucalyptus productivity: How water availability and stand structure alter production and carbon allocation. Forest Ecology and Management 259:1695–1703.

Ryan, M. G., and B. J. Yoder. 1997. Hydraulic limits to tree height and tree growth. BioScience 47:235–242.

Schneider, S., A. Gessler, P. Weber, D. Von Sengbusch, U. Hanemann, and H. Rennenberg. 1996. Soluble N compounds in trees exposed to high loads of N: a comparison of spruce (Picea abies) and beech (Fagus sylvatica) grown under field conditions. New Phytologist 134:103–114.

Schwinning, S., and J. Weiner. 1998. Mechanisms determining the degree of size asymmetry in competition among plants. Oecologia 113:447–455.

Soares, A. A. V, H. G. Leite, J. P. Cruz, and D. I. Forrester. 2017. Development of stand structural heterogeneity and growth dominance in thinned Eucalyptus stands in Brazil. Forest Ecology and Management 384:339–346.

Soares, A. A. V, H. F. Scolforo, D. I. Forrester, R. L. Carneiro, and O. C. Campoe. 2020. Exploring the relationship between stand growth, structure and growth dominance in Eucalyptus monoclonal plantations across a continent-wide environmental gradient in Brazil. Forest Ecology and Management 474:118340.

Stape, J. L., D. Binkley, and M. G. Ryan. 2008. Production and carbon allocation in a clonal Eucalyptus plantation with water and nutrient manipulations. Forest Ecology and Management 255:920–930.

Stephenson, N. L., A. J. Das, R. Condit, S. E. Russo, P. J. Baker, N. G. Beckman, D. A. Coomes, E. R. Lines, W. K. Morris, N. Ruger, E. Alvarez, C. Blundo, S. Bunyavejchewin, G. Chuyong, S. J. Davies, A. Duque, C. N. Ewango, O. Flores, J. F. Franklin, H. R. Grau, Z. Hao, M. E. Harmon, S. P. Hubbell, D. Kenfack, Y. Lin, J.-R. Makana, A. Malizia, L. R. Malizia, R. J. Pabst, N. Pongpattananurak, S.-H. Su, I.-F. Sun, S. Tan, D. Thomas, P. J. van Mantgem, X. Wang, S. K. Wiser, and M. A. Zavala. 2014. Rate of tree carbon accumulation increases continuously with tree size. Nature 507:90–93.

Stoll, P., J. Weiner, and B. Schmid. 1994. Growth Variation in a Naturally Established Population of Pinus Sylvestris. Ecology 75:660–670.

Trouvé, R., J.-D. Bontemps, C. Collet, I. Seynave, and F. Lebourgeois. 2014. Growth partitioning in forest stands is affected by stand density and summer drought in sessile oak and Douglas-fir. Forest Ecology and Management 334:358–368.

Ubierna, N., and J. D. Marshall. 2011. Estimation of canopy average mesophyll conductance using δ13C of phloem contents. Plant, Cell & Environment 34:1521–1535.

Vanninen, P., and A. Mäkelä. 2005. Carbon budget for Scots pine trees: effects of size, competition and site fertility on growth allocation and production. Tree Physiology 25:17–30.

Vertessy, R. A., R. G. Benyon, S. K. O'Sullivan, and P. R. Gribben. 1995. Relationships between stem diameter, sapwood area, leaf area and transpiration in a young mountain ash forest. Tree Physiology 15:559–567.

Wang, Y. P., and P. G. Jarvis. 1990. Description and validation of an array model — MAESTRO. Agricultural and Forest Meteorology 51:257–280.

Weiner, J. 1990. Asymmetric competition in plant populations. Trends in Ecology & Evolution 5:360–364.

Weiner, J., and C. Damgaard. 2006. Size-asymmetric competition and size-asymmetric growth in a spatially explicit zone-of-influence model of plant competition. Ecological Research 21:707–712.

Weiner, J., and O. T. Solbrig. 1984. The meaning and measurement of size hierarchies in plant populations. Oecologia 61:334–336.

Weiner, J., and S. C. Thomas. 1986. Size variability and competition in plant monocultures.

Oikos 47:211–222.

West, P. W. 2014. Calculation of a growth dominance statistic for forest stands. Forest Science 60:1021–1023.

Westoby, M. 1982. Frequency distributions of plant size during competitive growth of stands: the operation of distribution-modifying functions. Annals of Botany 50:733–735.

White, J. W. C., B. H. Vaughn, and S. E. Michel. 2015. University of Colorado, Institute of Arctic and Alpine Research (INSTAAR), Stable Isotopic Composition of Atmospheric Carbon Dioxide (13C and 18O) from the NOAA ESRL Carbon Cycle Cooperative Global Air Sampling Network, 1990-2014, Version: 2015-10-26. ftp://aftp.cmdl.noaa.gov/data/trace_gases/co2c13/flask/.

Zeileis, A. 2014. ineq: Measuring Inequality, Concentration, and Poverty. R package version 0.2-13.

Zhao, G., G. Liu, and W. Zhu. 2019. Estimating individual- and stand-level stem CO2 efflux in a subalpine forest: assessment of different extrapolation methods. Trees 33:1603–1613.

APPENDIX

Uncertainties of the estimates of gross primary production

Here we discussed the uncertainties of the estimates of gross primary production, transpiration, and respiration in Chapter 4, and how these uncertainties might affect our conclusions.

Originally, our data set included an *E. urophylla* × sp. clone. However, this clone was discarded from the analysis because we suspected that transpiration was largely underestimated. The underestimation of transpiration affected the estimation of gross primary production of trees. When the aboveground net primary production and aboveground respiration were subtracted from gross primary production to calculate total belowground carbon flux, we obtained negative values for almost 80% of the trees that were sampled.

The decision to remove this clone from our analysis was based on three points. First, the consumption of rainfall by trees was low compared to other eucalyptus plantations. Transpiration represented about 33% of rainfall (1193 mm $year^{-1}$). Other eucalyptus plantations with similar LAI than the plots of *E. urophylla* × sp. clone accounted for more than 60% of precipitation (Almeida et al. 2007, Stape et al. 2008, Hubbard et al. 2010, Battie-Laclau et al. 2016, Attia et al. 2019). Second, the transpiration rate per unit of leaf area (145 L H_2O $m^{-2}_{leaf\ area}$ $year^{-1}$) was about the half compared to other eucalyptus plantations (Stape et al. 2008, Hubbard et al. 2010, Attia et al. 2019). Third, gross primary production estimated scaling up individual tree estimations to the area level was around half than the gross primary production based on the carbon budget approach (1.5 vs. 3 kg C m^{-2} $year^{-1}$) (see below for details on the carbon budget estimates).

Gross primary production

We assessed the accuracy of gross primary production estimations at the tree level scaling up individual tree estimations and compared them with stand level estimations based on carbon budget approach. We scaled up the tree level gross primary production to the area level as $GPP_{area\text{-}scaled}$ (kg m^{-2} $year^{-1}$) = mean GPP_{tree} / average area per tree (9 m^2 $tree^{-1}$). The stand-level gross primary production was summed as:

GPP_{area} = WNPP + FNPP + Ra + TBCF,

where WNPP is wood net primary production (WNPP = NPP stem wood + branch litterfall + bark litterfall), FNPP is foliage net primary production (FNPP = NPP foliage + foliage litterfall, with NPP leaves estimated from change in LAI), Ra is above ground respiration (sum of wood respiration (Rw) and foliage respiration (Rf) estimated as Rw = (0.7163 - 0.0579 * age (month) / 12)*(WNPP))* temperature correction and Rf = leaf area x 0.66 μmol C $m^{-2}{}_{leaf\ area}$ s^{-1} x temperature correction (Ryan et al. 2009, 2010), TBCF is total below ground carbon flux (TBCF = ANPP x 0.66, where ANPP is above ground net primary production and 0.66 was obtained from Campoe et al. (2020) for based on younger ages at the same plots).

Stand level gross primary production based on $\delta^{13}C_{ph}$ and transpiration was similar than gross primary production based on the carbon budget approach (1.6 kg C m^{-2} $year^{-1}$ for both methods). Our estimation of gross primary production was low compared to other estimations for eucalyptus stands that were closer or above 4.0 kg C m^{-2} $year^{-1}$ (Stape et al. 2008, Ryan et al. 2010, Campoe et al. 2012, Epron et al. 2012). We speculate that the low gross primary production of these plots was related to the influence of pests. Hybrids between *E. camaldulensis* x *grandis* are susceptible to a number of pests (Gonçalves et al. 2013). In the site we analyzed trees were affected by several pests (Stape, personal communication) that might have affected

the wood productivity component of the carbon budget of trees. Potential evidence for this includes that analyzed clone displayed a similar leaf litterfall than other clones in the same site, despite carrying less than half the LAI. This implies a leaf lifespan for this clone of about half than leaf lifespan of other clones.

Transpiration

Because the estimated gross primary production of individual trees relies on the estimation of tree transpiration, any bias in the estimation of transpiration between small and large trees can influence our results and conclusions. Similarly, any underestimation of transpiration will be reflected in the estimation of gross primary productivity. We extrapolated tree transpiration to the stand level and compared this value with other published values from the bibliography.

Transpiration typically accounts for 60% to 90% of precipitation (Almeida et al. 2007, Stape et al. 2008, Hubbard et al. 2010, Battie-Laclau et al. 2016, Attia et al. 2019). Estimates of tree transpiration at the plot level showed that transpiration represented 41% of rainfall (1193 mm $year^{-1}$). However, LAI of the *E. grandis* × *E. camaldulensis* clone was about half of typical LAI found in highly productive eucalyptus plantations (LAI ≈ 3) (Table 4.1). Transpiration rate per unit leaf area was 375 L H_2O $m^{-2}_{leaf\ area}$ $year^{-1}$ for the studied clone. This rate was similar than others eucalyptus plantations (Stape et al. 2008, Hubbard et al. 2010, Attia et al. 2019).

Aboveground respiration

We did not directly measure wood and foliar respiration, instead we estimated these two fluxes from wood net primary production and leaf area of trees. Our results showed that aboveground respiration and carbon partitioning flux increased with tree, implying that aboveground respiration increased relatively more than GPP with tree size. Here we briefly

discussed how this pattern might be affected by the approach we used to estimate foliar and wood respiration.

Similar to our results O'Grady et al. (2008) found that leaf respiration rate was higher in dominant trees compared to suppressed trees, though for a similar crown height suppressed trees had a higher ratio of respiration:photosynthesis than dominant trees. We estimated leaf respiration from leaf area of trees and the rate of respiration per unit of leaf area (Ryan et al. 2009). Respiration of leaves is also correlated with nitrogen content of leaves (Ryan et al. 2004, 2009). As nitrogen concentration of leaves within the crown declines with tree height at a similar rate between dominant and suppressed trees (O'Grady et al. 2008), we would expect a similar respiration pattern using nitrogen content of leaves or leaf area of trees. We did not estimate construction respiration of leaves, we expected that construction respiration would increase with tree size. Construction respiration can be estimated as a proportion of leaf primary production (Ryan 1991), and our estimations of leaf primary production increase with tree size. This approach assumes a similar tissue composition and similar leaves lifespan between dominant and suppressed trees.

Other studies have found that that wood respiration increase with tree size. Wood respiration is comprised of CO_2 derived from construction of new tissue and CO_2 derived from maintenance of existing tissues (Ryan 1990). Growth respiration is related to the carbon concentration on tissues, the energy costs for the construction of wood and productivity (Ryan 1991). Assuming that wood composition is relatively similar between dominant and suppressed trees, is expected that construction respiration increases with tree size relatively proportional to wood productivity. Maintenance respiration of woody tissues is associated with phloem and xylem tissues in the sapwood. Their respective respiration rates appear to be strongly related to

temperature (Lavigne 1987, Bosc et al 2003) and nitrogen concentration (Ryan 1991). Total wood CO_2 efflux (construction and maintenance) (Liberloo et al. 2008, Fan et al. 2017, Zhao et al. 2019) and maintenance CO_2 efflux (Bosc et al. 2003, Kim et al. 2007) to the atmosphere from woody tissues calculated on a unit volume basis (μmol m^{-3} s^{-1}) decreased with stem and branch diameter. Usually, when CO_2 efflux is measured on an unit area basis (μmol m^{-2} s^{-1}) it shows an increase with tree size (see for e.g. Rowland et al. 2018). However, when CO_2 efflux is scaled up to the tree level, respiration increase with tree size regardless the scaling method (Kim et al. 2007, Zhao et al. 2019).

Overall, depending on the relative increase between gross primary production and aboveground respiration with tree size, it is expected that carbon partitioning to aboveground respiration might increase or be relatively similar across a sized-range of trees and would only explain any or a minor part of the decreasing carbon partitioning to wood production in small trees.